2011

Provenance signature of a forearc basin modified by spreading ridge subduction: Detrital zircon geochronology and detrital modes from the Paleogene Arkose Ridge Formation, southern Alaska

Cullen Kortyna
Bucknell University

Follow this and additional works at: https://digitalcommons.bucknell.edu/honors_theses

Part of the Geology Commons

Recommended Citation

PROVENANCE SIGNATURE OF A FOREARC BASIN MODIFIED BY SPREADING
RIDGE SUBDUCTION: DETRITAL ZIRCON GEOCHRONOLOGY AND
DETRITAL MODES FROM THE PALEOGENE ARKOSE RIDGE FORMATION,
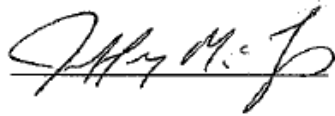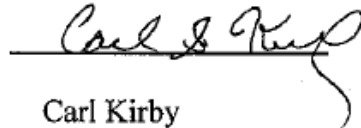SOUTHERN ALASKA

by

Cullen D. Kortyna

A Thesis

Presented to the Faculty of
Bucknell University
In Partial Fulfillment of the Requirements for the Degree of
Bachelor of Science with Honors in Geology
May, 2011

Approved: _____

Jeffrey M. Trop
Thesis Advisor, Department of Geology, Bucknell University

_____

Carl Kirby
Chair, Department of Geology, Bucknell University

ACKNOWLEDGEMENTS

preparation of samples and use of certain tools and machines. I want to thank fellow thesis student Rebekah Morris for her useful revisions, valuable discussion, and commiseration. Additionally, I would like to thank my fellow geology students from over the years who have inspired me, laughed with me, and made stressful days and weeks more bearable, namely Ed Bauer, Kaitlin Fleming, Eva Lipiec, Eric Lynch, Erin Donaghy, Lily Pfeifer, and Tyler Szwarc. David and Melissa Kortyna have given me all the love and support I could ask for from a father and mother. They fully support my academic and career interests, and even feign interest long enough for me to talk with them about my research, findings, and general geology-laden thought processes. My three younger sisters, Claire, Brighid, and Fiona Kortyna, have been very understanding of my dedication to my studies and research, especially since I have missed the past three family vacations to perform field work in Alaska. I want to thank Claire for her occasional phone calls and text messages, Brighid for her facebook messages, and Fiona for her handwritten letters and drawings. They all mean very much to me, and remind me that despite my absence, I am still loved. Finally, I would like to thank Kaitlin Fleming, whom without I am not sure how I would have survived. From making sure I was eating, constant words of kindness, and putting up with early morning phone calls to understanding when I was too tired to do anything on a Friday night but then staying in the O'Leary computer lab with me until late Saturday night, Kait has been there for me every step of the way. I will forever be in her debt for her support and unselfishness. Funding for this study was generously provided by the Geological Society of America – Northeast Section (to Cullen Kortyna), Bucknell Program for Undergraduate Research (to

TABLE OF CONTENTS

LIST OF TABLES

LIST OF FIGURES

ABSTRACT

Upper Paleocene–Eocene boulder conglomerate, cross-stratified sandstone, and laminated carbonaceous mudstone of the Arkose Ridge Formation exposed in the southern Talkeetna Mountains record fluvial-lacustrine deposition proximal to the volcanic arc in a forearc basin modified by Paleogene spreading ridge subduction beneath southern Alaska. U-Pb ages of detrital zircon grains and modal analyses were obtained from stratigraphic sections spanning the 2,000 m thick Arkose Ridge Formation in order to constrain the lithology, age, and location of sediment sources that provided detritus.

Detrital modes from 24 conglomerate beds and 54 sandstone thin sections are dominated by plutonic and volcanic clasts and plagioclase feldspar with minor quartz, schist, hornblende, argillite, and metabasalt. Westernmost sandstone and conglomerate strata contain <5% volcanic clasts whereas easternmost sandstone and conglomerate strata contain 40 to >80% volcanic clasts. Temporally, eastern sandstones and conglomerates exhibit an upsection increase in volcanic detritus from <40 to >80% volcanic clasts. U-Pb ages from >1400 detrital zircons in 15 sandstone samples reveal three main populations: late Paleocene–Eocene (60-48 Ma; 16% of all grains), Late Cretaceous–early Paleocene (85–60 Ma; 62%) and Jurassic–Early Cretaceous (200–100 Ma; 12%). A plot of U/Th vs U-Pb ages shows that >97% of zircons are <200 Ma and >99% of zircons have <10 U/Th ratios, consistent with mainly igneous source terranes. Strata show increased enrichment in late Paleocene–Eocene detrital zircons from <2% in the west to >25% in the east. In eastern sections, this younger age population increases temporally from 0% in the lower 50 m of the section to >40% in samples collected >740 m above the base.

Integration of the compositional and detrital geochronologic data suggests: (1) Detritus was eroded mainly from igneous sources exposed directly north of the Arkose Ridge Formation strata, mainly Jurassic–Paleocene plutons and Paleocene–Eocene volcanic centers. Subordinate metamorphic detritus was eroded from western Mesozoic low-grade metamorphic sources. Subordinate sedimentary detritus was eroded from eastern Mesozoic sedimentary sources. (2) Eastern deposystems received higher proportions of juvenile volcanic detritus through time, consistent with construction of adjacent slab-window volcanic centers during Arkose Ridge Formation deposition. (3) Western deposystems transported detritus from Jurassic–Paleocene arc plutons that flank the northwestern basin margin. (4) Metasedimentary strata of the Chugach accretionary prism, exposed 20-50 km south of the Arkose Ridge Formation, did not contribute abundant detritus.

Conventional provenance models predict reduced input of volcanic detritus to forearc basins during exhumation of the volcanic edifice and increasing exposure of subvolcanic plutons (Dickinson, 1995; Ingersoll and Eastmond, 2007). In the forearc strata of these conventional models, sandstone modal analyses record progressive increases upsection in quartz and feldspar concomitant with decreases in lithic grains, mainly volcanic lithics. Additionally, as the arc massif denudes through time, the youngest detrital U-Pb zircon age populations become significantly older than the age of forearc deposition as the arc migrates inboard or ceases magmatism. Westernmost strata of the Arkose Ridge Formation are consistent with this conventional model. However, easternmost strata of the Arkose Ridge Formation contain sandstone modes that record an upsection increase in lithic grains accompanied by a decrease in quartz and feldspar, and

detrital zircon age populations that closely match the age of deposition. This deviation from the conventional model is due to the proximity of the easternmost strata to adjacent juvenile volcanic rocks emplaced by slab-window volcanic processes. Provenance data from the Arkose Ridge Formation show that forearc basins modified by spreading ridge subduction may record upsection increases in non-arc, syndepositional volcanic detritus due to contemporaneous accumulation of thick volcanic sequences at slab-window volcanic centers. This change may occur locally at the same time that other regions of the forearc continue to receive increasing amounts of plutonic detritus as the remnant arc denudes, resulting in complex lateral variations in forearc basin petrofacies and chronofacies.

INTRODUCTION

Throughout its geologic history, southern Alaska has experienced several dynamic tectonic processes considered to be fundamental to the collisional growth of continental margins (Trop and Ridgway, 2007). Some of these processes include subduction of oceanic crust and arc magmatism, accretion of allochthonous terranes, and exhumation along regional strike-slip faults (Trop, 2008). For example, the Mesozoic collision of the Wrangellia composite terrane represents the largest addition of juvenile crust to western North America in the past 100 million years (Coney, 1980; Plafker and Berg, 1994). Volcanic arcs have been established, terminated, and re-established throughout southern Alaska's history. The Cenozoic collision of the Yakutat terrane and recent activity on some of Alaska's most prominent faults are reminders that collisional tectonic processes are still very much active in southern Alaska. Despite Alaska's

tectonic significance, many of the dynamic processes that have occurred in Alaska's geologic history remain poorly understood. One such process that modified southern Alaska during Paleogene time was the west-to-east oblique subduction of an oceanic spreading center (Bradley et al., 2003). Geologic evidence of this event is currently restricted to near-trench plutons in the accretionary prism with associated ages of 62 Ma in the west to 50 Ma in the east and an Eocene volcanic field that crops out in the central Talkeetna Mountains (Fig. 1). Both the plutons and the volcanic field have a depleted-mantle geochemical signature and are inferred to be associated with subduction of an oceanic spreading center (Cole et al., 2006). Recent studies deduce that deposition in the Matanuska Valley-Talkeetna Mountains forearc basin overlaps with slab-window formation, near-trench plutonism to the south, and formation of the Eocene volcanic field (Trop and Ridgway, 2007; Cole et al., 2006). These forearc strata record a detailed history of basin evolution modified directly by the subduction of an oceanic spreading center.

The Arkose Ridge Formation (ARF) consists of a >2000-m-thick sequence of upper Paleocene-Eocene fluvial-lacustrine sedimentary and volcanic strata deposited along the arcward (northern) margin of the remnant Matanuska Valley-Talkeetna Mountains forearc basin in southern Alaska (Fig. 2, 3; Trop et al., 2003; Trop and Ridgway, 2007). Exceptionally well-exposed in a 50-km-long and 2.5-10-km-wide outcrop belt in the southern Talkeetna Mountains (Winkler, 1992), these strata are broadly interpreted as recording exhumation of remnant Jurassic-Cretaceous magmatic arc plutons as well as Eocene volcanic centers attributed to slab-window magmatism during spreading ridge subduction (Trop and Ridgway, 2000; Cole et al., 2006; Trop and

Figure 1. Tectonic framework of southern Alaska and Canada, including major faults, Holocene volcanoes (yellow triangles), present-day plate motion vectors (from Leonard et al., 2007), exposed (light yellow) and interpreted subducted (translucent white region within dashed line) extent of the Yakutat microplate. From Ridgway et al. (in press). Edges of the subducted Yakutat microplate are loosely constrained (modified from Eberhart-Phillips et al., 2006 and Fuis et al., 2008). Near-trench plutons (red diamonds) intrude accretionary prism rocks and are interpreted as the product of slab window magmatism associated with subduction of a spreading ridge oriented subparallel to the plate margin from 62 Ma near present-day Sanak Island (lower left corner of the map) to 50 Ma at present-day Baranof Island (lower right corner of map) (Bradley et al., 2003). The eastward younging of ages in the near-trench plutons, together with supporting geologic studies, is interpreted to represent the eastward migration of spreading ridge subduction. Active sedimentary basins: TB-Tanana; CI-Cook Inlet. Exhumed Cenozoic sedimentary basins: CCB-Colorado Creek; MB-Matanuska. Major Cenozoic volcanic belts: AVA-Alaska Peninsula-Aleutian volcanic arc; CB-Cantwell basin volcanic belts: CTV-Central Talkeetna Mountains volcanics; CV-Caribou Creek volcanic field; JV-Jack River volcanics; WVB-Wrangell volcanic belt. Major faults: CMF-Castle Mountain fault; CSEF-Chugach-St. Elias fault; BRF-Border Ranges fault; DRF-Duke River fault; QC-F F-Queen Charlotte-Fairweather fault; TF-Totschunda fault; A-city of Anchorage; F-city of Fairbanks.

6
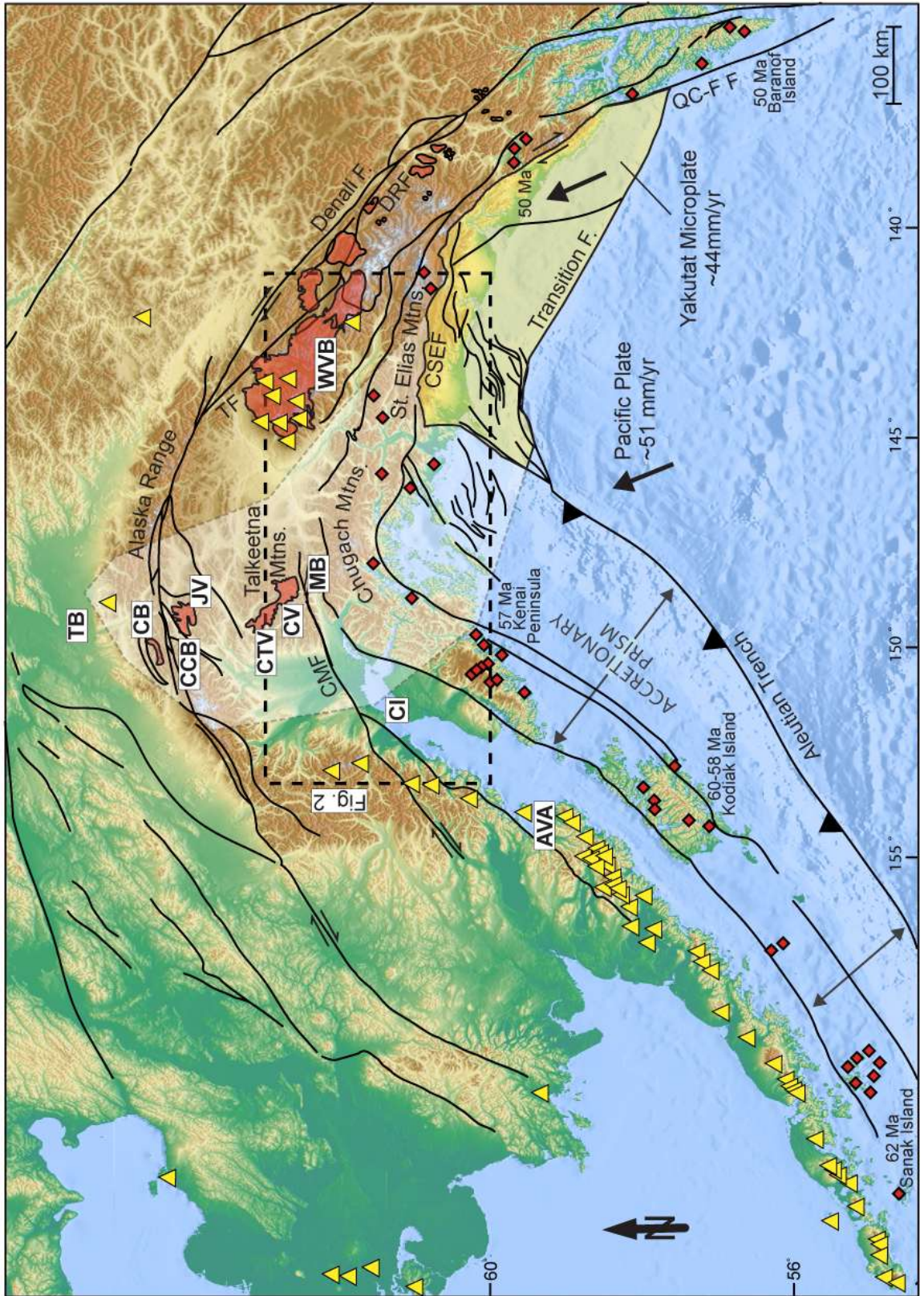
Figure 2. Generalized geologic map of south-central Alaska showing features attributable to latest Cretaceous "normal" subduction, Paleocene and Eocene flat-slab subduction of a spreading ridge, and Oligocene-Holocene subduction of the Yakutat microplate. From Ridgway et al. (in press). Dashed black line on Figure 1 shows map location. Abbreviations: A-Anchorage; BRF-Border Ranges fault; CV-Caribou Creek volcanic field; CTV-Central Talkeetna Mountains volcanics; FB-Frederika basin; MB-Matanuska basin; and WB-Wrangell Mountains basin. Black circles denote exploration wells. Thin black lines define 1:250,000 quadrangles.
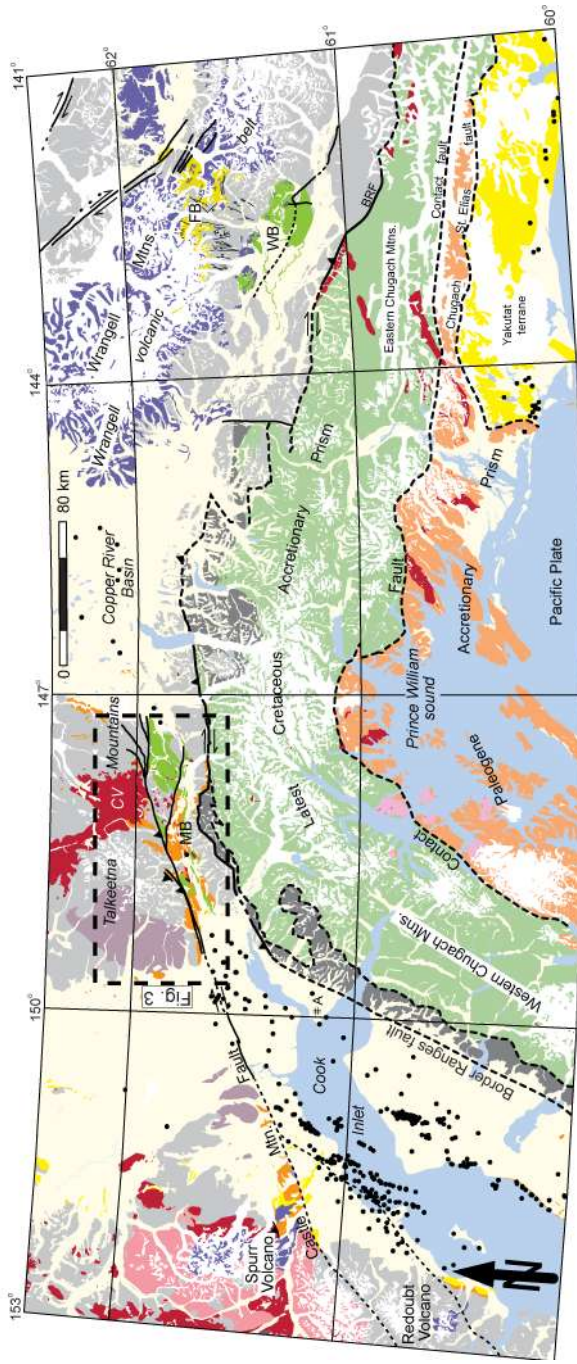
Quaternary
- Ice
- Lake/Ocean
- Quaternary surficial deposits
- Faults
- Exploratory Wells

Neogene Flat Slab Subduction
- Middle Miocene-Quaternary volcanic-intrusive rocks (Wrangell volcanic belt, Redoubt Volcano, Spurr Volcano)
- Oligocene-Pliocene alluvial-fluvial-lacustrine strata in Frederika transtensional basin (FB) and Cook Inlet forearc basin.
- Latest Eocene, Oligocene, and early Miocene igneous rocks (includes arc plutons and volcanic rocks)

Paleogene Spreading Ridge Subduction
- Paleocene-Eocene alluvial-fluvial-lacustrine strata in remnant forearc basin (MB) and Cook Inlet forearc basin.
- Paleocene-Eocene slab-window volcanics (CV, Caribou Creek volcanics), near-trench plutons in accretionary prism, and arc plutons (CP)
- Paleocene-Eocene accretionary prism (Orca Group) and ophiolites

Latest Cretaceous Subduction
- Latest Cretaceous marine sedimentary strata in Matanuska (MB) and Wrangell Mountains (WB) forearc basins
- Latest Cretaceous calc-alkaline magmatic arc plutons
- Latest Cretaceous accretionary prism (Valdez Group)

Pre- Latest Cretaceous Collisional Tectonics
- Permian-Jurassic accreted oceanic crust (Wrangellia composite terrane) and Jurassic-Cretaceous sedimentary and igneous rocks
- Permian-Upper Cretaceous accretionary prism (McHugh Complex)

Figure 3. Enlarged generalized geologic map of the southern Talkeetna Mountains, Matanuska Valley, and northern Chugach Mountains. Adapted from Wilson et al. (1998). On this map, the Talkeetna Mountains represent the exhumed arc-dominated part of the forearc region, the southernmost Talkeetna Mountains and Matanuska Valley represent exhumed forearc basin strata, and the Chugach Mountains represent exhumed accretionary prism (Ridgway et al., in press). TKg (dark pink-salmon) and Jpu (light gray) north of the Castle Mountain fault represent latest Cretaceous and Jurassic magmatic arcs. Paleogene volcanic (red-Tv) and intrusive (pink-Ti) igneous rocks are attributed to slab window magmatism. This study focuses on Paleogene fluvial-lacustrine strata exposed north (orange-Tar) of the Castle Mountain fault. See Fig. 2 for map location.
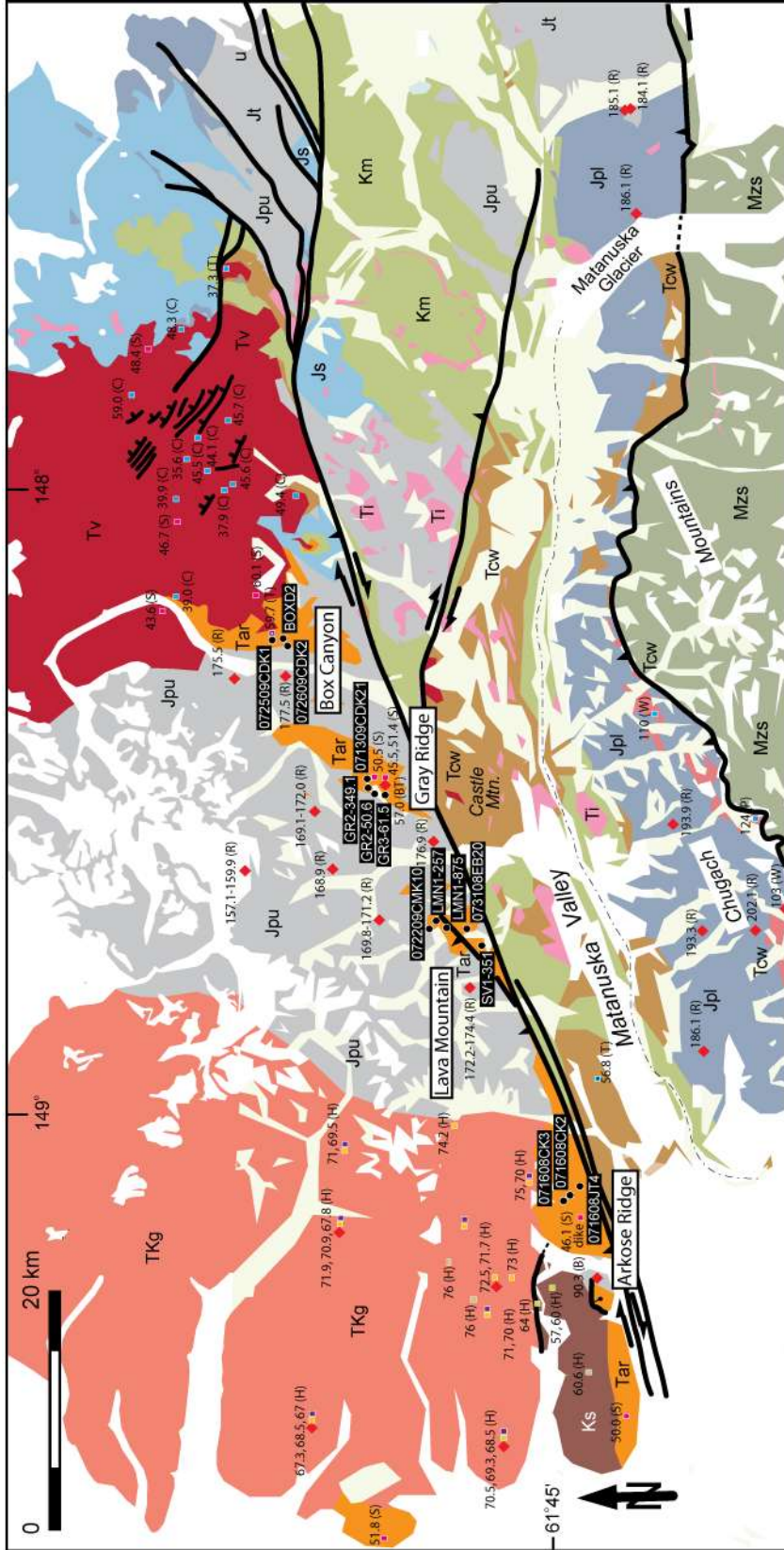
Cretaceous-Eocene Sedimentary Strata

- Tar — Paleocene-Eocene Arkose Ridge Fm. ~1800m sandstone, mudstone, conglomerate, lava, tuff.
- Tcw — Paleocene-Eocene Wishbone and Chickaloon Fms. ~1500m sandstone, mudstone, conglomerate, coal, tuff.
- Km — Cretaceous Matanuska Fm. ~2,500m mudstone, sandstone, conglomerate, coal, limestone, and tuff.

Cretaceous-Eocene Igneous and Metamorphic Rocks

- Tv — Eocene lava, tuff, volcaniclastic sandstone, and breccia.
- Ti — Eocene intrusive rocks.
- TKg — Latest Cretaceous-Paleocene pluton.
- Ks — Latest Cretaceous-Paleocene schist.
- Ki — Mid-Cretaceous felsic intrusive rocks.

Jurassic Accreted Oceanic Arc Rocks

- Js — Jurassic Middle to Upper Jurassic - 1150m conglomerate, sandstone, mudstone, tuff (Tuxedni, Chinitna, Naknek Fms.).
- Jpu — Middle to Late Jurassic plutons and subordinate volcanic rocks.
- Jpl — Lower to Middle Jurassic plutons and subordinate volcanic rocks.

Mesozoic Accretionary Prism Deposits

- Mzs — Triassic(?)-Cretaceous metasedimentary and volcanic rocks.

Symbols

- High-angle fault (u-upthrown block)
- Dextral-reverse fault
- River

Detrital zircon samples (this study) • 071608JT4

Published isotopic Ages

- ■ Ar/Ar biotite (300°C)
- □ Ar/Ar biotite (300°C) clast
- K/Ar muscovite (400°C)
- K/Ar whole rock (500°C)
- Ar/Ar whole rock (500°C)
- • Ar/Ar whole rock (500°C) clast
- Ar/Ar hornblende (550°C)
- ◆ U/Pb zircon (800°C)
- • Detrital zircon (800°C)

Sources of isotopic ages

(B) = Bleick et al. (2009)
(C) = Cole et al. (2006)
(H) = Harlan et al. (2003)
(P) = Pavlis et al. (1988)
(R) = Rioux et al. (2007)
(S) = Silberman and Grantz (1984)
(T) = Trop et al. (2003)
(W) = Winkler (1992)

Ridgway, 2007). However, sediment provenance data from these basinal strata are limited to sparse conventional modal analyses and paleocurrent data that suggest sediment was eroded from northern source terranes. These previously reported data cannot give the specific locations, ages, or lithologies of the sediment sources. Clast count and sandstone modal analyses reported by Trop and Ridgway (2000) do offer some insight on the lithologies of source terranes, but these data are limited to the westernmost portion of the outcrop belt. The purpose of this study is to integrate detrital zircon geochronologic analyses and conventional modal analyses from the entire Arkose Ridge Formation outcrop belt to better resolve the age, location, and lithology of sediment sources that contributed clastic detritus. In ancient active-margin settings characterized by abundant first-cycle detritus, the forearc strata can provide a more complete history of arc magmatism, topography, and, in this case, slab-window formation than the present exposure of the arc or volcanic center itself (DeGraaff-Surpless et al., 2002). A refined provenance analysis of the Arkose Ridge Formation offers improved constraints on processes that shaped the southern Alaska convergent margin, including the evolution of paleotopography, magmatic histories of volcanic-plutonic belts, sediment dispersal into sedimentary basins, and the effect of ridge subduction on basin evolution.

GEOLOGIC SETTING

The following section will summarize the geology surrounding the Arkose Ridge Formation and introduce the ages, lithologies, and locations of possible source terranes for the formation. The Matanuska Valley-Talkeetna Mountains forearc basin consists of a 90-km-long and 20-70-km-wide belt of Mesozoic-Cenozoic sedimentary strata that crop

11

out in the Matanuska Valley, southern Talkeetna Mountains, and northern Chugach Mountains (Fig. 1; Trop and Plawman, 2006). The forearc basin is bounded to the north by two remnant magmatic arcs (a Jurassic oceanic island arc and a late Cretaceous-Paleocene continental magmatic arc) as well as the Eocene depleted mantle volcanic field related to ridge subduction (Fig. 2; Rioux et al., 2007; Cole et al., 2006). To the southeast, the forearc strata are bounded by Mesozoic meta-sedimentary rocks of the Chugach subduction complex (Trop and Ridgway, 2000). The Border Ranges fault system separates the southern margin of the forearc basin from the Chugach subduction complex (Pavlis and Roeske, 2007). The east-west striking Castle Mountain fault bisects the forearc basin and bounds the Arkose Ridge Formation to the south. The fault experienced Eocene-Oligocene dextral strike-slip displacement and Neogene dip-slip displacement (Trop and Ridgway, 2000; Grantz, 1966; Fuchs, 1980; Little, 1990). However, the displacement history of the Castle Mountain fault is still poorly understood. Late Cretaceous-Tertiary piercing points record 20-40 km of dextral offset, but do not constrain timing of displacement (Grantz, 1966; Clardy, 1974; Detterman et al., 1976; Fuchs, 1980; Trop et al., 2003). Trop et al. (2005) infer ~130 km of displacement through the correlation of the Bruin Bay and Little Oshetna fault systems which Pavlis and Roeske (2007) hypothesize to be strike slip displacement transferred from the Border Ranges fault system northward to the Castle Mountain fault system.

Studies from the Upper Cretaceous-Paleogene volcanic rocks in the Talkeetna Mountains document three distinct phases of volcanism: 180 to 145 Ma arc plutons in the south-central Talkeetna Mountains attributed to the accreted Talkeetna oceanic magmatic arc, 80 to 60 Ma arc plutons in the southwestern Talkeetna Mountains attributed to

continental arc magmatism, and 59–36 Ma volcanic rocks and associated intrusions in the southeastern Talkeetna Mountains related to subduction of an oceanic spreading center (Fig. 3; Madsen et al., 2006; Cole et al., 2006; Rioux et al., 2007). The Arkose Ridge Formation unconformably overlies Upper Cretaceous-Paleocene arc plutons in the west (TKg on Fig. 3), Jurassic plutons in the center (Jpu on Fig. 3), and interfingers with and unconformably underlies Eocene volcanic rocks of the Caribou Creek volcanic field in the east (Tv on Fig. 3; Winkler, 1992; Cole et al., 2006).

Both the Upper Cretaceous-Paleocene plutons in the west and the Jurassic plutons in the center are subvolcanic plutons of two separate magmatic arcs. They are both composed primarily of diorite, quartz diorite, granodiorite, and tonalite plutons and some minor mica shist (TKg, Jpu, Ks on Fig. 3; Winkler, 1992). The Talkeetna magmatic arc is an allochthonous Jurassic andesitic oceanic island arc that accreted onto southern Alaska in late Mesozoic time (Plafker and Berg, 1994). K-Ar ages on related local granitoids (Jpu on Fig. 3) yield middle Jurassic biotite ages of 168-169 Ma and two hornblende ages of 154 and 173 Ma (Winkler, 1992; Csejtey et al., 1978). High precision U-Pb ages were calculated on Jurassic granitoids and metamorphic rocks (Jpu on Fig. 3) in both the Eastern and Western Talkeetna Mountains. Samples in the Eastern Talkeetna Mountains yield ages of 178-169 Ma. Samples in the Western Talkeetna Mountains yield ages of 153-157 Ma and 190-192 Ma (Rioux et al., 2007).

The late Cretaceous-Paleocene continental magmatic arc, due to north-northwest subduction (present coordinates) of oceanic plates, intrudes the accreted Talkeetna magmatic arc (Trop, 2008). Multiple K-Ar ages on the Upper Cretaceous granitoids (TKg on Fig. 3) from the southern Talkeetna Mountains document a range from 65 to 74

Ma (± 2 Ma on average) (Winkler, 1992; Csejtey et al., 1978). Harlan et al. (2003) performed thermochronologic analyses on the Willow Creek pluton of the Cretaceous granitoids. U-Pb ages were used to calculate crystallization ages and Ar-Ar thermochronologic ages were used to calculate cooling ages. They determined the Willow Creek pluton was emplaced between 73-63 Ma based on U-Pb data (Harlan et al., 2003; Trop et al., 2003). Hornblende Ar-Ar ages yield 72.8 to 70.5 Ma and biotite Ar-Ar ages yield 70-67.9 Ma, which led to calculated cooling rates indicating the pluton was below 280 °C by 68.8 Ma and below 200 °C by 66 Ma. Bleick et al., (2009) recorded more diverse U-Pb zircon ages on the Cretaceous granitoids ranging from 90.3 ± 0.3 to 67.3 ± 0.2 Ma. Zircon fission track dating (~225°C closure) led to similar calculated cooling ages of 77 to 66 Ma.

The Eocene Caribou Creek volcanic field, located to the northeast of the ARF, records the geochemical signature of depleted mantle volcanics related to slab window volcanism during ridge subduction. The Caribou Creek volcanic field is primarily composed of thick bedded basalt and andesite lavas (Tv on Fig. 3; Winkler, 1992). The Eocene Caribou Creek volcanics (Tv on Fig. 3) that locally unconformably overlie the ARF in the northeast have been dated using $^{40}Ar/^{39}Ar$, yielding ages that range from 49.4 ± 2.2 to 35.6 ± 0.2 Ma. An adakite-like tuff beneath the other volcanic rocks yields an age of 59.0 ± 0.4 Ma (Cole et al. 2006). Based on limited age data, deposition of the Arkose Ridge Formation apparently overlapped with both late Cretaceous-Paleocene and Eocene phases of volcanism (Fig. 4; Cole et al., 2006; Winkler, 1992). However, prior to this study the relationship between volcanism and sedimentation was not well

Figure 4. Age-event diagram showing isotopic ages from igneous rocks and igneous clasts in the Matanuska Valley and Talkeetna Mountains. Note that onset of deposition of the Arkose Ridge Formation was coeval with timing of slab window formation in south-central Alaska. Slab window formation is attributed to subduction of a spreading ridge (Bradley et al., 2003). Also note that the formation of the Caribou Creek volcanic field, Matanuska Valley intrusives, and near-trench plutons in the accretionary prism overlap with slab window formation and deposition of the Arkose Ridge Formation. CTM-Central Talkeetna Mountains volcanics; CCV-Caribou Creek volcanic field. Sources for age data are as follows: 1-Cjestey et al. (1978), Adams et al. (1985), Little (1988), and R.B. Cole and P.W. Layer (2002, person commun.); 2-Cole et al. (2006), Silberman and Grantz (1984), Panuska et al. (1990), and Trop et al. (2003); 3-Silberman and Grantz (1984), Little (1988), and Little and Naeser (1989); 4-Triplehorn et al. (1984); 5-Silberman and Grantz (1984); 6-Trop (2008). Adapted from Cole et al. (2006).
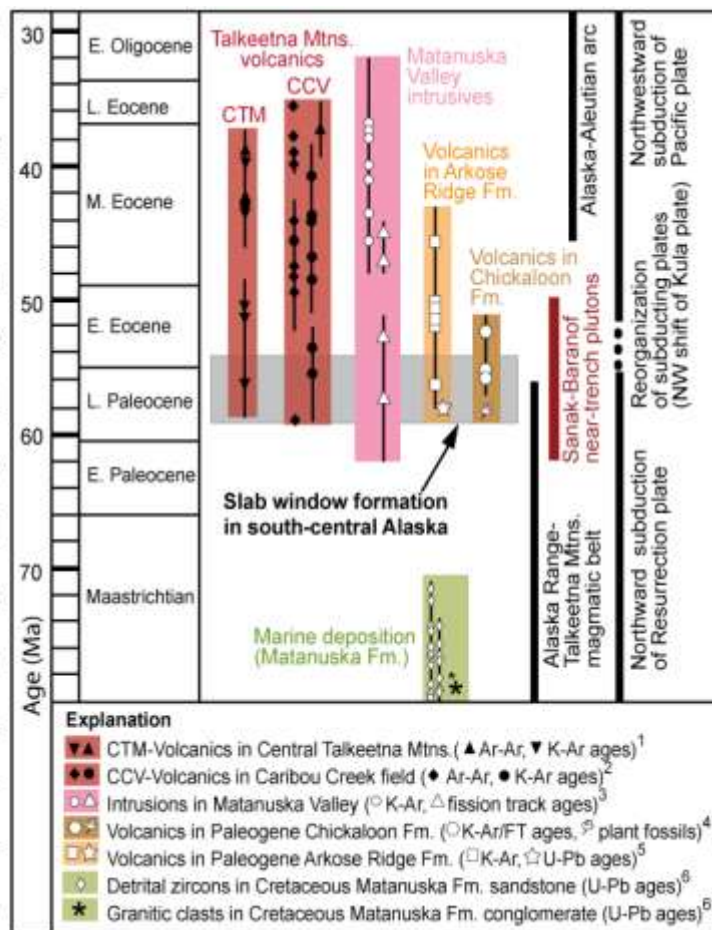
15

documented, including whether volcanic centers contributed detritus to the Arkose Ridge Formation.

The Chugach subduction complex is exposed ~20-50 km south of the ARF and consists of Jurassic-Paleocene marine metasedimentary and metavolcanic rocks interpreted as offscraped oceanic strata (Fig. 2). The Border Ranges fault juxtaposes subduction complex rocks to the south against Paleogene forearc strata (Chickaloon Formation) that are age equivalent to the Arkose Ridge Formation to the north (BRF on Fig. 2). A systemic decrease southward in age of strata, deformation and metamorphic grade across the subduction complex suggests long-lived northward subduction (present coordinates). The subduction complex includes three distinct belts from north to south: (1) the McHugh Complex, comprised of spatially limited late Triassic-early Jurassic blueschist and Triassic to late Cretaceous mélange; (2) the Valdez Group, consisting mainly of latest Cretaceous marine metasedimentary and minor metavolcanic rocks; and southernmost, (3) the Orca Group, consisting of offscraped Paleocene-Eocene marine sedimentary and volcanic rocks (Plafker et al., 1994). Amato and Pavlis (2010) reported two main detrital zircon age populations for the McHugh Complex of 91-84 Ma and 157-146 Ma.

Northern source terranes exposed >100 km north of the ARF outcrop belt include, from north to south, the Yukon-Tanana terrane, the Kahiltna assemblage, and the Wrangellia composite terrane. The Yukon-Tanana terrane consists of ductilely and structurally dismembered and dislocated Proterozoic-Paleozoic metamorphic rocks and arc-related rocks (Mortensen, 1992; Foster et al., 1994; Hansen and Dusel-Bacon, 1998). U-Pb zircon ages on mafic and felsic metaigneous rocks of the Yukon-Tanana terrane

yield late Devonian to early Mississippian crystallization ages, ranging from 378-346 Ma (Dusel-Bacon et al., 2004). Metamorphic rocks of the Yukon-Tanana terrane are faulted between autochthonous North American crust and outboard allochthonous accreted terranes (Mortensen, 1992; Foster et al., 1994; Hansen and Dusel-Bacon, 1998). One of these is the allochthonous Wrangellia composite terrane, one of the largest accreted terranes in the North American Cordillera. It consists primarily of volcanic and sedimentary strata of the Peninsular terrane, the Wrangellia terrane, and the Alexander terrane (Jones et al., 1977; Gehrels and Saleeby, 1987; Plafker and Berg, 1994). The Paleozoic-Triassic Wrangellia composite terrane accreted during Mesozoic time (Trop and Ridgway, 2007), and is juxtaposed along the southern margin of the Yukon-Tanana terrane. Potential source terranes associated with the Wrangellia composite terrane include the Skolai arc ranging from 320-285 Ma (Hampton et al., 2007). The suture zone between these two terranes is characterized by complexly deformed rocks and is bisected by the Denali Fault.

The Kahiltna assemblage is exposed in a 100 by 300 km outcrop in the Alaska Range and a 60 by 150 km outcrop in the northern Talkeetna Mountains. The Kahiltna assemblage records mudstone, sandstone and limestone deposition in a remnant ocean basin from late Jurassic to middle Cretaceous time (Hampton et al., 2007). In the northeastern Talkeetna Mountains, the Kahiltna assemblage has been locally metamorphosed to kyanite-garnet-schist and gneiss. In the northwestern Talkeetna Mountains, the nonmarine, middle Cretaceous Caribou Pass Formation overlies the Kahiltna assemblage. The Caribou Pass Formation records deposition of sandstone, mudstone and conglomerate (Hampton et al., 2007). Upper Cretaceous arc plutons

17

intrude the Kahiltna Formation. U-Pb zircon ages from these plutons yield 68.3 to 62.6 Ma ages (Davidson and McPhillips, 2007). Another potential northern source terrane is the Jack River suite, which consists of volcanic and granitic rocks that were erupted and emplaced along the suture zone between the Wrangellia composite terrane and southern Alaska. They unconformably overlie the Jurassic-Cretaceous Kahiltna Formation. $^{40}Ar/^{39}Ar$ ages on the volcanics yielded ages ranging from 56.0 ± 0.3 to 49.5 ± 0.3 Ma. $^{40}Ar/^{39}Ar$ ages on the plutons yielded two ages of 54.6 ± 0.4 and 62.7 ± 0.4 Ma. The Jack River volcanic and granitic rocks record the magmatic response to terrane accretion and margin-parallel transport of an accreted terrane after sutured to the margin (Cole et al., 2007).

U-Pb detrital zircon ages and sandstone modal composition indicate that the Jurassic-Cretaceous Kahiltna Formation in the central Talkeetna Mountains received igneous detritus primarily from the Chisana arc (early Cretaceous arc located east of the Talkeetna arc), the remnant Talkeetna and Chitina (late Jurassic arc located east of the Talkeetna arc) arcs and Permian-Triassic plutons of the Wrangellia composite terrane. Minor populations of detrital zircon ages indicate other sources of detritus from the Devonian-Mississippian plutons of the Yukon-Tanana terrane and the late Triassic-early Jurassic Taylor Mountains batholith located in the Yukon-Tanana terrane (Hampton et al., 2007).

The Upper Cretaceous Matanuska Formation (Km on Fig. 3) consists of submarine ramp/slope lithofacies, characterized by sandstone, conglomerate, and mudstone deposited by mass slumps, slides, debris flows, and turbidity currents into the forearc basin of the late Cretaceous-early Paleocene magmatic arc (Trop, 2008).

Stratigraphically, it precedes deposition of the Arkose Ridge Formation in the forearc basin. Additionally, there is a regional angular unconformity between the Matanuska and Arkose Ridge Formations. Inferred base-level changes across the unconformity exceeded fluctuations in eustatic sea-level (<100 m; Haq et al., 1988), requiring tectonically driven uplift (Trop, 2008). Deposition of the Matanuska Formation was prior to forearc uplift related to the subduction of progressively younger oceanic lithosphere inboard of an oceanic spreading center. This forearc uplift is posited to accommodate the upsection change from submarine ramp/slope to alluvial-fluvial facies between the Matanuska Formation and the Arkose Ridge Formation (Trop, 2008). U-Pb detrital zircon data in sandstones and U-Pb ages of granitoids clasts from the Matanuska Formation suggest that the Jurassic-Cretaceous arc plutons of both the Talkeetna and late-Cretaceous-early Paleocene arcs were important sediment sources. Sparse Paleozoic-Triassic detrital zircons indicate minor sediment contribution from more northerly sources in the Yukon-Tanana and Kahiltna terranes (Trop, 2008). The presence of 77-71 Ma detrital zircons in sandstone and 79-77 Ma granitic clasts in conglomerate, along with Maastrichtian (71-65 Ma) ammonite and foraminifera fossils, imply that the coeval Cretaceous-Paleocene magmatic arc plutons were unroofed relatively quickly. Trop (2008) reports a maximum of 6-7 m.y. passed between zircon crystallization, pluton exhumation, and detrital zircon deposition. Assuming pluton emplacement depths of ~6-12 km, typical of silicic continental-arc plutons (Martel et al., 1998; Scaillet and Evans, 1999; Scaillet et al., 2001), estimated latest Cretaceous unroofing rates range from 0.75 to ~1.00 mm/yr (Trop, 2008).

STRATIGRAPHY, AGE, AND STRUCTURAL FRAMEWORK OF THE ARKOSE RIDGE FORMATION

Published geologic studies provide a general framework on the sedimentology, geochronology, paleoclimate, and structural framework of the ARF. The western part of the ARF outcrop belt consists of siliciclastic and minor volcanic strata with preserved thicknesses >2000 m (Trop and Ridgway, 2000; Kortyna et al., 2009). Geologic mapping and measured stratigraphic sections show that four lithofacies associations dominate the stratigraphy. Boulder conglomerate and subordinate sandstone occur in paleovalleys incised into underlying Jurassic-Cretaceous granitic plutons. Cross-stratified sandstone, conglomerate, and carbonaceous mudstone record anastomosing and braided fluvial systems with bifurcating channels and vegetated floodplains. Laminated carbonaceous mudstone, shale, and tuff represent small floodplain lakes. Cross-stratified sandstone, heterolithic sandstone/mudstone, *in situ* coalified tree trunks, and minor lavas record deposition and minor effusive volcanism in tidally influenced fluvial-estuarine deposystems. Eastern ARF strata consist of siliciclastic and volcanic strata with preserved thicknesses >900m (Kassab et al., 2009). Strata consist of conglomerate with pumice/tuff clasts, cross-stratified sandstone, carbonaceous siltstone, and coal that represent fluvial-lacustrine environments routinely influenced by pyroclastic eruptions. Volcanic interbeds include welded tuff-breccia with bombs, welded lapilli tuff, crystalline tuff, pyroclastic flows, and sparse lavas. To the southwest, sections between the Kings and Chickaloon Rivers are dominated by carbonaceous mudstone and cross-stratified sandstone that represent fluvial-lacustrine environments. Volcanic interbeds include pumice-rich lapilli tuff, laminated crystalline tuff, pyroclastic flows, and rare

lavas. Southwestward lithofacies transitions and paleocurrent data indicate that volcanogenic strata were partly derived from the Caribou Creek volcanic field (Kassab et al. 2009), but provenance data have not been reported. Overall, sediment provenance data from these basinal strata are limited to sparse conventional modal analyses and paleocurrent data that suggest sediment sourced from northern source terranes (Fig. 5).

Age constraints from ARF strata are limited to a handful of conventional radiometric ages from volcanic interbeds and biostratigraphic ages from plant fossils. K-Ar radiometric ages from volcanic interbeds demonstrate a late Paleocene to early Eocene depositional age. Whole rock ages from two rhyolite tuffs yield ages of 50.5 ± 1.5 Ma and 45.5 ± 1.8 Ma (Silberman and Grantz, 1984). Alkali feldspar from a rhyolite ash-flow tuff yielded a 51.4 ± 1 Ma K-Ar age (Silberman and Grantz, 1984). A basaltic dike cross-cutting the ARF yielded a 46.1 ± 2.8 Ma whole-rock K-Ar age (Silberman and Grantz, 1984; Winkler, 1992). Plant fossils from ARF strata include diverse leaf, seed, and axis (stem/shoot) fossils delicately preserved in laminated siltstone and sandstone (Lecomte et al., 2010; Sunderlin et al., 2011). Age-diagnostic taxa support a Paleocene-Eocene depositional age for the ARF (J. Wolfe cited in Winkler, 1992). Foliage types include several species of conifer and broadleaf, as well as examples of *Equisetites*, cycad fronds and a palm frond. The fine preservation of all elements suggests that these plant assemblages were minimally transported out of habitat. Habitats of living relatives and fluvial-lacustrine sedimentary strata indicate that this flora represents a moderately diverse floodplain forest community. This assemblage suggests warm to cool temperate paleotemperatures during the deposition of the ARF (Lecomte et al., 2010; Sunderlin et al., 2011).
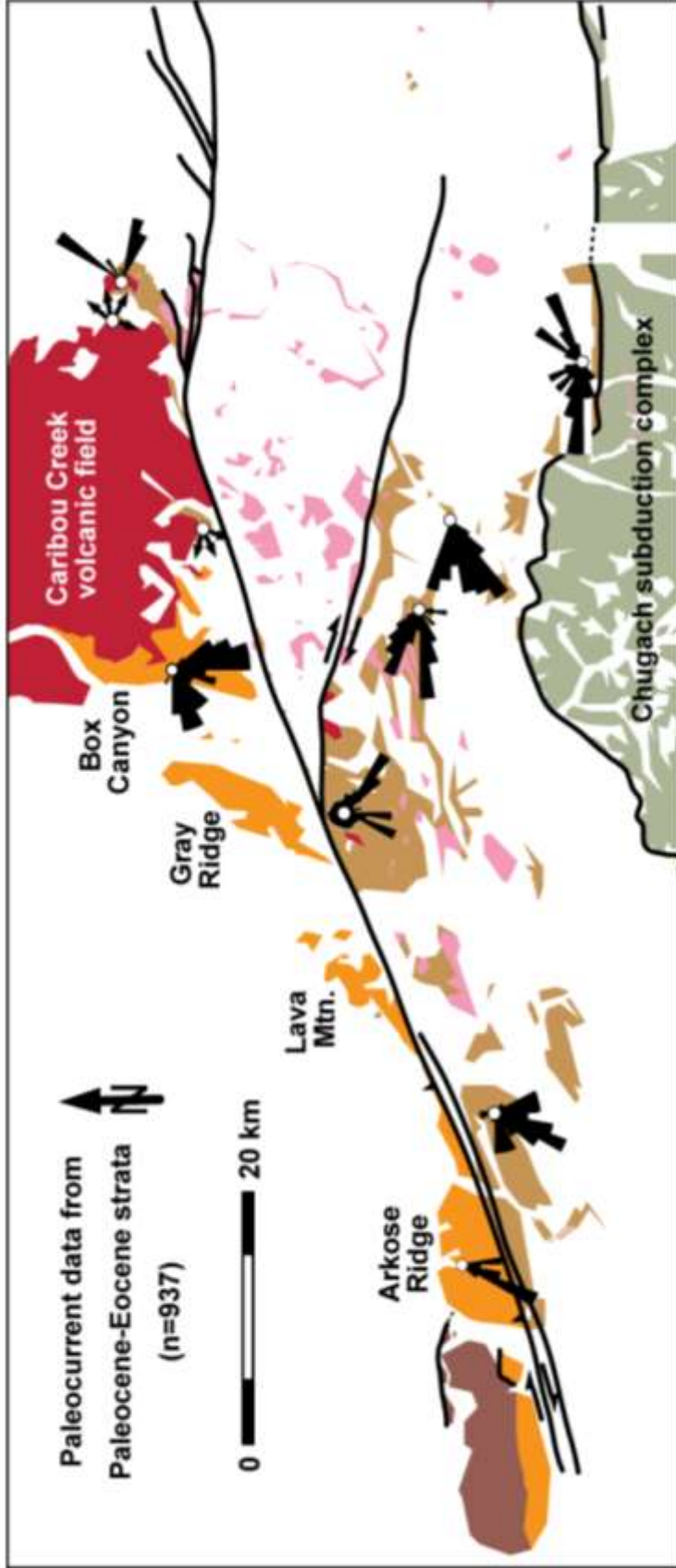
Figure 5. Map showing sediment transport directions measured in Paleocene-Eocene strata, including Arkose Ridge Formation (ARF) strata exposed north of the Castle Mountain fault. n = total number of paleocurrent measurements. All measurements were corrected for structural tilt if necessary. Note southeastward- to southwestward-directed paleoflow along the northern basin margin, westward-directed paleoflow along the axis of the basin, and northeastward- to northwest-directed paleoflow along the southern basin margin. Adapted from Trop et al. (2003) and Cole et al. (2006).

Northwest-dipping reverse faults, southeast-verging folds and northwest-striking normal faults deform Arkose Ridge Formation strata along the entire width of the outcrop belt (Winkler, 1992; Kortyna et al., 2009; Kassab et al., 2009). The orientation of these structures is consistent with the dextral transpressive shortening along the adjacent Castle Mountain Fault, a regional northeast-striking strike-slip fault. The reverse faults along with available age data from the Arkose Ridge Formation indicate contractile deformation during early Eocene or younger time.

METHODS

Field Sampling

Sandstone samples were collected within the context of measured stratigraphic sections for petrographic and detrital geochronological analyses. Fist-sized samples of medium-to coarse-grained sandstone were collected for petrography. Care was taken to locate samples with the least visible diagenetic alteration and organic content. For detrital geochronology, 10-15 kilograms of fist-sized medium-to coarse-grained sandstone samples were collected from outcrop faces. During sampling, special care was taken to attempt to avoid sampling veins and faults and contamination from soil and other rocks.

Conglomerate Clast Counts

A total of 24 conglomerate clast counts were obtained in the field within the context of measured stratigraphic section where conglomerate was present in the section. Each count was performed on a randomly selected 1 by 1 meter surface of a single conglomerate bed. The lithologies of 100 conglomerate clasts were identified per

conglomerate bed. See Tables 2, 3, 4, and 5 for raw clast count data and recalculated detrital modes for each stratigraphic section.

Sandstone Modal Analyses

Standard petrographic thin sections were made from 54 medium- to coarse-grained sandstones that were obtained within the context of measured stratigraphic sections. One half of each thin section was stained for plagioclase and potassium feldspar. All thin sections were examined to determine common framework grains and proper counting grid. Thin sections were point counted using an automated modal analysis system and polarizing microscope. 400 framework grains were counted per section to ensure a 2-σ confidence range of 5% or less for any calculated modal composition (Van Der Plas and Tobi, 1965). Sandstones were point counted using both the Gazzi-Dickinson and "traditional" methods (Dickinson, 1970; Ingersoll et al., 1984), so that granitic rock fragments could be noted independently. Matrix and cement were not counted. See Tables 6, 7, and 8 for petrographic point-counting parameters, raw point-count data, and recalculated detrital modes, respectively.

Detrital Geochronology

Care was taken throughout sample processing to avoid biasing the final separate of detrital zircon grains by size, shape, or color. Fist-sized sandstone samples were crushed to granule and finer grained particles using a jaw crusher. All remaining material was then pulverized to sand and finer grained particles using a disc mill. Material was pulverized through multiple steps with the discs spaced progressively closer together.

24

The sample was sieved between each pulverizing run to avoid pulverizing monocrystalline zircon grains. Most samples yielded 6-8 kilograms of pulverized sand and silt. Samples were then shipped to the University of Arizona or Lehigh University where zircon grains were separated in a clean lab using conventional density and magnetic techniques, including a Wilfley table, methylene iodide, and a Franz magnetic separator. Every sample yielded hundreds or thousands of detrital zircon grains. For each sample, all detrital zircons were mounted in a 1" diameter round epoxy plug and polished to half thickness. Photomicrographs were taken of all mounted zircons using a light microscope to guide spot analyses.

Isotopic analyses were conducted using a laser-ablation-inductively-coupled-plasma-mass-spectrometer (LA-ICP-MS) at the Arizona LaserChron Center utilizing methods described by Gehrels et al. (2006, 2008). At minimum, 100 zircon crystals from each sandstone sample were randomly selected for analysis. Individual zircons were ablated using a New Wave DUV193 Excimer laser using a spot diameter of 10-35 microns and a pit depth ranging from 4-15 microns. Ablated material was carried with helium gas into a plasma source of an isoprobe equipped with a flight tube of sufficient width such that U, Th and Pb isotopes were measured simultaneously (Gehrels et al., 2006). After every fourth or fifth measurement of an unknown detrital zircon, analyses were calibrated against a measurement of a Sri Lanka zircon standard (563 ± 3.2 Ma; Gehrels et al., 2008). For each spot analysis, $^{207}Pb/^{235}U$ and $^{206}Pb/^{238}U$ ratios and apparent ages were calculated using the Isoplot software program (Ludwig, 2003). Raw data are presented in Appendix 1. The systematic error, which includes contributions from the standard calibration, the age of the calibration standard, the composition of

common Pb and the ^{238}U decay constant, is 1-2% based on similar analyses (Gehrels et al., 2008). The data were filtered according to precision (10% cutoff) and discordance (30%) and then plotted on Pb/U Concordia diagrams and age probability plots (Ludwig, 2003). Age probability curves were then constructed by calculating a normal distribution for each analysis based on the reported age and uncertainty, then summing the probability distributions of all acceptable analyses into a single curve. Interpretations derived from the detrital age spectra focus on clusters of ages because single age determinations may be compromised by Pb loss and/or inheritance. However, it is highly unlikely that three or more grains will experience Pb loss and/or inheritance and still yield the same age. U/Th ratios are plotted to evaluate the degree to which metamorphic fluids were present during crystal growth (Rubatto, 2002; Gehrels et al., 2008; Johnston et al., 2009), aiding in discriminating detrital grains derived from metamorphic versus igneous/sedimentary sources.

PROVENANCE DATA

Modal analyses of conglomerate clast counts and sandstone thin sections and detrital zircon age determinations help resolve sediment provenance and determine the erosional history of bedrock sources, including the lithologies and locations of these source terranes (Fig. 6). These data allow for the reconstruction of basin drainage pathways, and the development of the first depositional model of the Arkose Ridge Formation.

Published compositional data from the Arkose Ridge Formation are limited to reconnaissance studies by Trop and Ridgway (2000) and Winkler (1978). Those workers
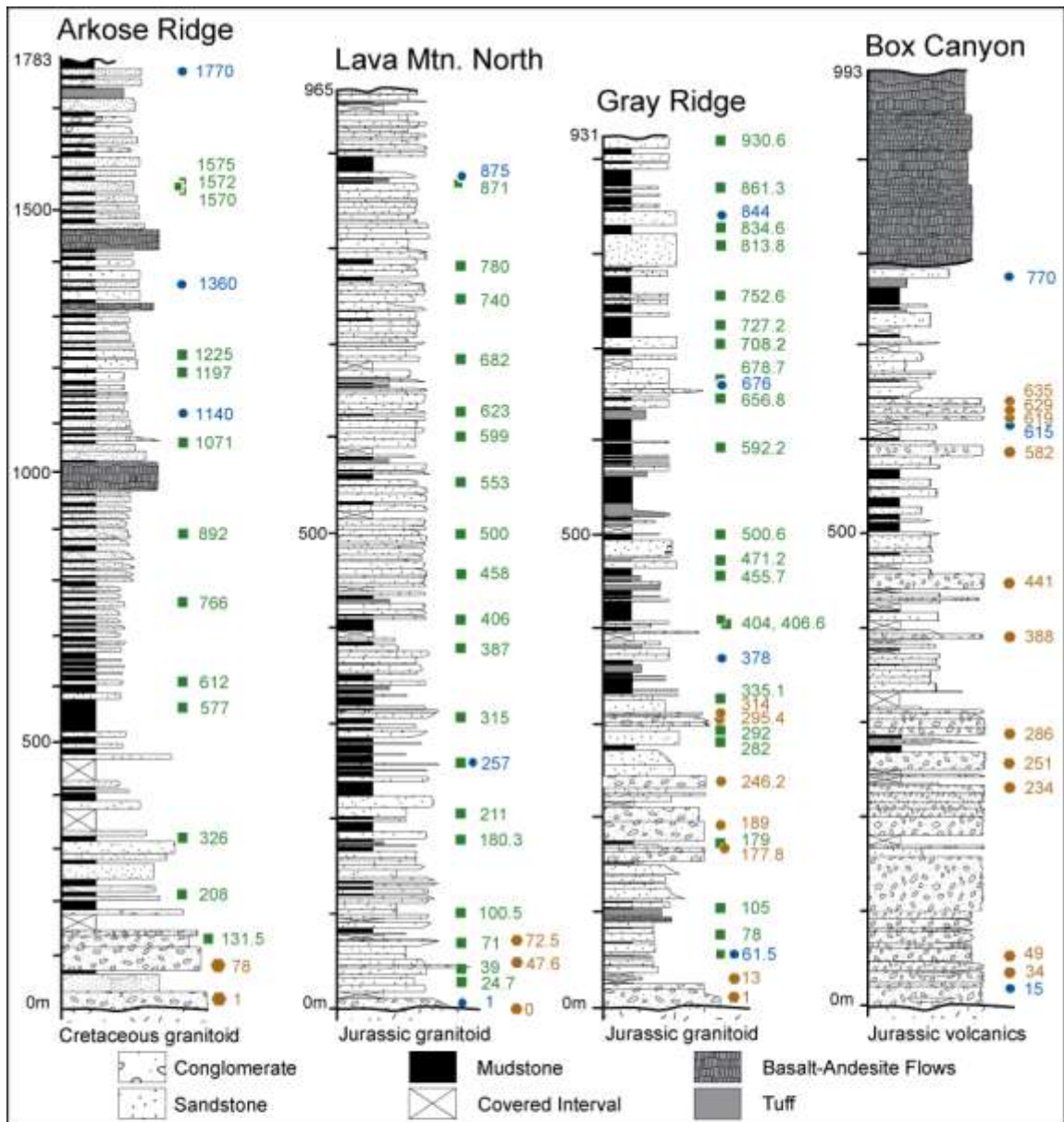
Figure 6. Generalized stratigraphic sections measured through Arkose Ridge, Lava Mountain, Gray Ridge, and Box Canyon. A total of 23 clast counts (brown hexagons) were collected from conglomerate beds. A total of 54 sandstone petrography samples (green squares) were collected for modal analyses. A total of 15 sandstone samples (blue circles) were collected for U-Pb detrital zircon analyses. Lithofacies and paleobotanical analyses demonstrate that these strata were deposited in alluvial paleovalleys, anastomosing to braided fluvial systems, floodplain ponds and lakes, and tidally influenced streams. Measured sections adapted from Trop et al. (2003), Kortyna et al. (2009), and Kassab et al. (2009).

Table 1. - Possible Source Rocks for the Arkose Ridge Formation

Terrane	Abbrev. in Fig. 3	Age	Lithologies
Rocks Located >50 Km North of ARF in the Northern Talkeetna Mountains/Alaska Range			
Yukon-Tanana Tn.	NS	Precambrian-Paleozoic	Pelitic and quartzose schist
Wrangellia Composite Tn.	NS	Late Jurassic-	Mudstone, sandstone
Kahiltna Assemblage	NS	Late Jurassic-Middle Cretaceous	Mudstone, sandstone, and limestone
Caribou Pass Fm.	NS	Middle Cretaceous	Sandstone, mudstone, and conglomerate
Rocks Located <50 Km North of the Arkose Ridge Formation in the Southern Talkeetna Mountains			
Talkeetna Magmatic Arc	Jpu	Middle-Late Jurassic	Granodiorite, Diorite, Quartz Diorite, Tonalite, Trondhjemite
Jurassic Metamorphic Assemblage	NS	Early-Middle Jurassic	Amphibolite, Foliated Quartz Diorite, Trondhjemite
Alaska Range-Talkeetna Mtn. Magmatic Arc	TKg	Late Cretaceous-Early Paleocene	Granite, Granodiorite, Diorite Quartz Diorite, Tonalite
Hatcher Pass Schist	Ks	Late Cretaceous-Paleocene	Greenschist
Caribou Creek Volcanic Center	Tv	Late Paleocene-Eocene	Basalt, Andesite
Rocks Located South of the Arkose Ridge Formation/Castle Mountain Fault			
Matanuska Formation	Km	Middle-Late Cretaceous	Sandstone, mudstone, and conglomerate
Rocks Located South of the Border Ranges Fault in Chugach Accretionary Prism			
McHugh Complex	Mzs	Late Triassic-Early Jurassic	Blueschist
Valdez Group	NS	Late Cretaceous	Metasedimentary, metavolcanic rocks
Orca Group	NS	Paleocene-Eocene	Sedimentary, volcanic rocks

Notes: NS = Not Shown; See Fig. 3 for age sources; Lithologies from Winkler (1992).

performed sandstone modal analyses on samples obtained from the westernmost part of the outcrop belt (Arkose Ridge on Fig. 1). These prior studies show that sampled sandstones from the Arkose Ridge have average framework grain modes of Q:F:L = 23:67:10 and Qm:F:Lt = 21:68:11 and average framework mineral modes of Qm:P:K = 23:76:1. Sandstones classify as feldspathic arenites and plot mostly in the "continental block-basement uplift" provenance field. Subangular plagioclase feldspars dominate the feldspar population (Qm:P:K = 23:76:1) with minor plagioclase feldspars contained within plutonic fragments. The quartz population is dominated by monocrystalline quartz, subordinate quartz within plutonic fragments, minor polycrystalline quartz, and rare chert grains. Lithic fragments include abundant metamorphic grains with subordinate volcanic grains and rare mudstone grains (Lm:Lv:Ls = 79:21:0). Lathwork grains composed of plagioclase phenocrysts in dark glassy matrix dominate the volcanic population. Metamorphic lithic grains are dominated by mica schist and minor quartz tectonite. Plutonic fragments are common and consist mainly of plagioclase feldspar, monocrystalline quartz, biotite, and muscovite. Clinopyroxene and amphiboles make up rare accessory minerals. Trop and Ridgway (2000) do not report detrital geochronologic ages, and their sandstone modal analyses are limited to the westernmost (Arkose Ridge on Fig. 3) extent of the Arkose Ridge Formation.

Conglomerate Clast Counts

The conglomerate clast counts document two main petrofacies, a western petrofacies characterized by enrichment of plutonic clasts and an eastern petrofacies

characterized by enrichment of volcanic lithologies. See Tables 2, 3, 4, and 5 for raw and recalculated conglomerate clast count data.

Plutonic Petrofacies

The plutonic petrofacies comprise conglomerate clast compositions from the Arkose Ridge and Lava Mountain stratigraphic sections. This petrofacies is characterized predominantly by felsic plutonic clasts. Conglomerates from the Arkose Ridge section contain, in summary, an average of 85% felsic plutonic clasts, 4% siliceous tuff clasts, 2% amphibolite clasts and 9% vein quartz and minor chert. Felsic plutonic clasts are primarily granite with minor granodiorite. Conglomerates exposed 22-km east of Arkose Ridge at Lava Mountain are similarly dominated by felsic plutonic clasts and subordinate volcanic lithologies. Lava Mountain conglomerates have an average clast composition of 80% felsic plutonic clasts, <1% mafic-intermediate volcanic, <1% felsic volcanic, <1% metamorphic clasts, and 19% gabbro, quartz, and chert clasts. At Lava Mountain, the felsic plutonic clasts are predominantly unclassified granitoids (probable granodiorite), diorite, and quartz diorite.

Volcanic Petrofacies

The volcanic petrofacies comprise conglomerate clast compositions from the eastern stratigraphic sections at Gray Ridge and Box Canyon. This petrofacies is characterized by conglomerates enriched in volcanic lithologies that increase in abundance upsection. Conglomerates from the Gray Ridge section contain an average of 66% volcanic clasts, 25% unclassified felsic granitoid clasts, and 9% greenstone/metabasalt clasts. Mafic-intermediate volcanic lithologies make up 61% of the clast composition and include basaltic, basaltic-andesitic, and andesitic compositions.

Table 2. Clast count data for conglomerate of the Arkose Ridge Formation at Arkose Ridge

Clast Type (lithology)			
Raw	1 m	78 m	Summary
Felsic Plutonic			
granodiorite	8	0	8
granite	80	88	168
Mafic-Intermediate Volcanic			
none reported			
Felsic Volcanic			
tuff, siliceous	9	0	9
Metamorphic			
amphibolite	2	3	5
Other			
chert, tan to gray	1	1	2
vein quartz	1	15	16
Total number of clasts counted	**101**	**107**	**208**
Recalculated			
% Felsic Plutonic	87.13	82.24	**84.62**
% Mafic-Intermediate Volcanic	0.00	0.00	**0.00**
% Felsic Volcanic	8.91	0.00	**4.33**
% Metamorphic	1.98	2.80	**2.40**
% Other	1.98	14.95	8.65

Table 3. Clast count data for conglomerate of the Arkose Ridge Formation at Lava Mountain

Clast Type (lithology, color, grain size, foliation)

Raw	0* m	0** m	47.6 m	72.5 m	Summary
Felsic Plutonic					
unclassified granitoid, green/gray, coarse	104	96	0	0	200
unclassified granitoid, medium	1	0	0	0	1
unclassified quartz rich granitoid, fine	0	0	1	0	1
diorite, coarse	0	0	29	0	29
quartz diorite, white, coarse	0	0	9	64	73
quartz diorite, coarse, foliated	0	0	2	3	5
trondhjemite, white, coarse	0	0	16	11	27
Mafic-Intermediate Volcanic					
basaltic andesite(?), dark gray	0	0	0	1	1
Felsic Volcanic					
unclassifed siliceous volcanic, green, fine	0	0	2	0	2
Metamorphic					
gneissic gabbro	0	0	1	0	1
Other					
gabbro, green, medium to coarse	1	10	36	17	64
gabbroic diorite, coarse	0	0	1	0	1
vein quartz	2	4	0	0	6
quartz	0	0	4	5	9
chert, black	0	0	0	1	1
Total number of clasts counted	**108**	**110**	**101**	**102**	**421**
Recalculated					
% Felsic Plutonic	97.22	87.27	56.44	76.47	**79.81**
% Mafic-Intermediate Volcanic	0.00	0.00	0.00	0.98	**0.24**
% Felsic Volcanic	0.00	0.00	1.98	0.00	**0.48**
% Metamorphic	0.00	0.00	0.99	0.00	**0.24**
% Other	2.78	12.73	40.59	22.55	**19.24**

*Notes: 0*m = mapping station 072209CMK09; 0**m = mapping station 072109JMT12*

Table 4. Clast count data for conglomerate of the Arkose Ridge Formation at Gray Ridge

Clast Type (lithology, color, grain size, foliation)	1 m	13 m	177.8 m	189 m	246.2 m	295.4 m	314 m	Summary
Raw								
Felsic Plutonic								
unclassified felsic granitoid	72	38	15	12	10	28	22	197
Mafic-Intermediate Volcanic								
basalt, black	0	0	48	12	7	17	24	108
basaltic-andesite, dark gray to brown	31	78	0	0	0	0	0	109
andesite, brown/tan	0	0	0	0	0	0	31	31
andesite, tan to brown	0	0	26	88	65	47	0	226
Felsic Volcanic								
tuff	0	0	5	7	0	0	10	22
tuff, gray/tan	0	0	0	0	9	0	0	9
tuff, tan/white	0	0	0	0	0	10	0	10
Metamorphic								
greenstone/metabasalt	0	0	9	8	14	20	16	67
Other								
quartz	0	0	0	0	0	0	1	1
Total number of clasts counted	103	116	103	127	105	122	104	780
Recalculated								
% Felsic Plutonic	69.90	32.76	14.56	9.45	9.52	22.95	21.15	25.26
% Mafic-Intermediate Volcanic	30.10	67.24	71.84	78.74	68.57	52.46	52.88	60.77
% Felsic Volcanic	0.00	0.00	4.85	5.51	8.57	8.20	9.62	5.26
% Metamorphic	0.00	0.00	8.74	6.30	13.33	16.39	15.38	8.59
% Other	0.00	0.00	0.00	0.00	0.00	0.00	0.96	0.13

33

Table 5. Clast count data for conglomerate of the Arkose Ridge Formation at Box Canyon

Clast Type (lithology, color, grain size, foliation)

Row	34 m	49 m	234 m	251 m	286 m	388 m	441 m	582 m	619 m	629 m	635 m	Summary
Felsic Plutonic												
unclassified granitoid, green, medium-coarse	15	12	0	0	0	0	0	0	0	0	0	27
diorite	5	1	7	11	20	10	24	9	16	15	10	128
diorite, weakly foliated	0	0	1	0	0	0	0	0	0	1	0	2
quartz diorite	20	17	13	9	4	8	1	0	0	3	0	75
granodiorite, coarse	5	1	4	16	5	2	10	1	3	2	0	49
granite, pink	1	0	1	0	0	1	2	0	0	0	0	5
Mafic-Intermediate Volcanic												
basalt, black, aphanitic to plagpheric, siliceous locally	7	10	13	11	17	16	20	5	12	8	10	129
basaltic-andesite, aphanitic to plagpheric, siliceous locally	26	27	19	11	20	21	22	12	12	29	16	215
andesite, tan, brown, green, gray	9	12	1	1	6	24	4	12	7	3	6	85
unclassified volcanic, green, coarse, siliceous	1	1	0	0	0	0	0	0	0	0	0	2
Felsic Volcanic												
tuff, white, tan, green, gray, siliceous, massive to laminated	7	4	8	20	21	11	20	61	45	39	58	294
tuff, reddish gray	0	0	0	0	0	2	0	0	0	0	0	2
tuff, tan, pumice rich	0	1	0	1	0	0	0	0	0	0	0	2
tuff, white, gray, lapilli, siliceous	0	0	1	1	0	0	0	0	1	1	1	5
tuff breccia, green	1	1	2	0	0	0	0	0	0	0	0	4
pumice, white, tan	1	2	1	0	0	0	0	2	3	0	1	10
Metamorphic												
greenstone, fine, medium, coarse	10	16	26	14	9	5	1	2	0	4	0	87
Other												
gabbro, green, medium	2	1	0	0	0	0	0	0	0	0	0	3
quartzite, medium	1	2	0	0	0	0	0	0	0	0	0	3
chert, gray	0	0	1	0	0	0	0	0	1	0	1	3
quartz	2	3	2	0	0	0	0	0	0	0	0	7
vein quartz	0	0	0	1	0	0	2	0	0	0	0	3

Table 5. Clast count data for conglomerate of the Arkose Ridge Formation at Box Canyon

Clast Type (lithology; color; grain size, foliation)													
Raw cont'd	34 m	49 m	234 m	251 m	286 m	388 m	441 m	582 m	619 m	629 m	635 m	Summary
Total number of clasts counted	113	111	100	96	102	100	106	104	100	105	103	1140
Recalculated												
% Felsic Plutonic	40.71	27.93	26.00	37.50	28.43	21.00	34.91	9.62	19.00	20.00	9.71	25.09
% Mafic-Intermediate Volcanic	38.05	45.05	33.00	23.96	42.16	61.00	43.40	27.88	31.00	38.10	31.07	37.81
% Felsic Volcanic	7.96	7.21	12.00	22.92	20.59	13.00	18.87	60.58	49.00	38.10	58.25	27.81
% Metamorphic	8.85	14.41	26.00	14.58	8.82	5.00	0.94	1.92	0.00	3.81	0.00	7.63
% Other	4.42	5.41	3.00	1.04	0.00	0.00	1.89	0.00	1.00	0.00	0.97	1.67

Felsic volcanic lithologies, mainly tuff, comprise 5% of the clast composition. In addition, conglomerates display an upsection increase in volcanic clasts from ~30% of counts at the bottom of the section to as much as 85% of counts higher in the section. There is also an upsection increase in greenstone/basalts from 0% at the bottom of the section to as much as 16% higher in the section. Overall, Box Canyon 15 km to the east of Gray Ridge contains a similar concentration of volcanic clasts. Conglomerates from the Box Canyon section have an average composition of 66% volcanic clasts, 25% felsic plutonic clasts, 8% greenstone clasts, and 2% gabbro, quartzite, chert, and quartz clasts. Mafic-intermediate volcanic lithologies make up 38% of the clast composition and include basaltic, basaltic-andesitic, and andesitic compositions. Felsic volcanic lithologies, mainly tuff, tuff breccia, and pumice, comprise 28% of the clast composition. The Box Canyon section displays a distinct upsection increase in volcanic clasts, from ~40% at the bottom of the section to ~90% near the top of the section (Fig. 7).

Sandstone Modal Analyses

Sandstone samples for modal analyses were collected from three stratigraphic sections; Arkose Ridge (published in Trop and Ridgway, 2000) and Lava Mountain in the west, and Gray Ridge in the east. These sections divide into two main petrofacies based on modal composition. Overall, these two facies mirror the conglomerate clast count data, essentially splitting the formation into a western petrofacies characterized by enrichment of quartzofeldspathic mineral grains and plutonic lithic fragments and an eastern petrofacies characterized by an enrichment in volcanic lithic grains. See Tables

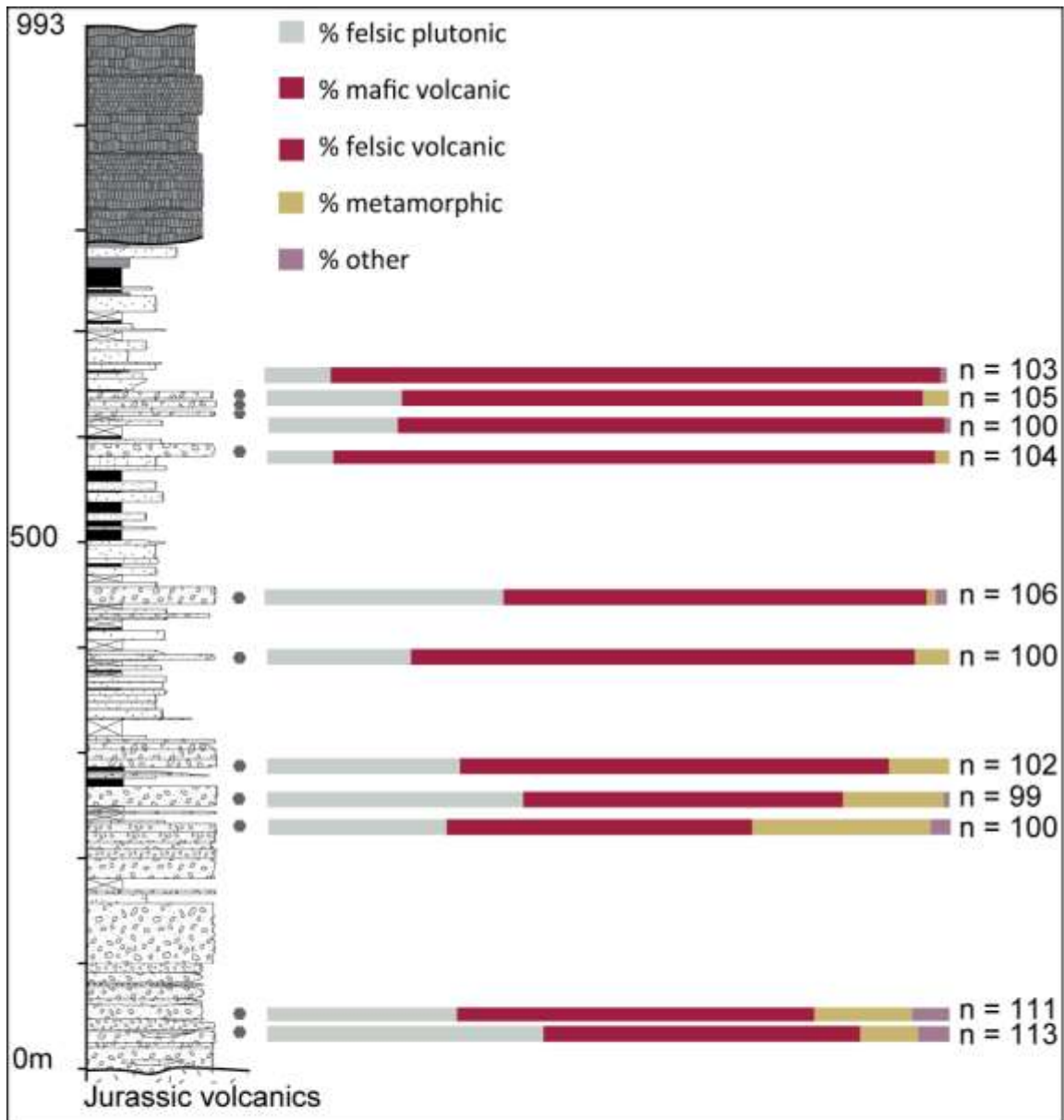Figure 7. Clast counts of conglomerate from Box Canyon plotted in stratigraphic order next to the generalized stratigraphic section. n = number of individual clasts counted per conglomerate bed. Each histogram summarizes a single clast count. Note the upsection increase in volcanic clasts (red) from ~40% at the base of the section to ~90% near the top of the section. See Tables 2, 3, 4, and 5 for details.

6, 7, and 8 for point-counting parameters and raw and recalculated point-count data, respectively.

Quartzofeldspathic Petrofacies

The quartzofeldspathic petrofacies comprise sandstone modal compositions from the western sections at Arkose Ridge and Lava Mountain. Point-counted sandstones are moderately to poorly sorted, with angular to subrounded framework grains. Most samples are very closely packed and contain sparse visible matrix and minor calcite cement. Overall, modal percentages for these western sandstones are dominated by plagioclase feldspar, monocrystalline quartz, and plutonic fragments, with minor schist fragments and accessory minerals (Fig. 8). Mean modal compositions for the Lava Mountain section are Q:F:L = 36:54:10 and Qm:F:Lt = 26:54:19. Sandstones classify as feldspathic arenites and plot mostly in the "continental block-basement uplift" provenance field (Fig. 9, 10). Subangular plagioclase feldspars dominate the feldspar population (Qm:P:K = 33:67:0) with subordinate plagioclase feldspars contained in plutonic fragments (Fig. 11). The quartz population is dominated by monocrystalline quartz, polycrystalline quartz, and quartz contained in plutonic fragments. Rare chert grains are also present. Lithic fragments include abundant mica schist grains with minor mudstone grains (Lm:Lv:Ls = 94:0:6, Fig. 12). Plutonic fragments are common and consist mainly of plagioclase feldspar, monocrystalline quartz, biotite, and muscovite (Fig. 13). Abundant amphiboles and subordinate sphene, muscovite and biotite make up minor accessory minerals.

Table 6. Categories used for point-count data for sandstone samples of the Arkose Ridge Formation

Raw

Qm	Monocrystalline quartz (single crystals)
Qm/Pl	Quartz in plutonic fragments
Qpq	Polycrystalline quartz
Qe	Embayed monocrystalline quartz
C	Impure chert
Cm	Impure muddy chert
P	Plagioclase feldspar (single crystals)
P/Pl	Plagioclase feldspar in plutonic fragments
K	Potassium feldspar (single crystals)
K/Pl	Potassium feldspar in plutonic fragments
Lvl	Volcanic lithic fragments (lathwork textures)
Lvu	Undifferentiated volcanic lithic fragments (primarily lathwork textures)
Lvf	Volcanic lithic fragments (felsitic to microlitic textures)
Lva	Volcanic lithic fragments (highly altered)
Lss	Sedimentary lithic fragments (quartzose to quartzofeldspathic siltstone)
Lsm	Sedimentary lithic fragments (shale)
Lsa	Argillaceous metasedimentary lithic fragments, weakly foliated
Lmm	Mica schist and subordinate chlorite schist lithic fragments, foliated
Lmt	Quartz-mica tectonite and subordinate quartz-mica-feldspar tectonite, foliated
Lmc	Metachert, foliated
Cp	Clinopyroxene
Ol	Olivine
Am	Amphibole
Mu	Muscovite (single crystals)
Bi	Biotite
M/Pl	Mica grains (muscovite and biotite) in plutonic fragments
Sp	Sphene
Zr	Zircon

Recalculated

Q	Total quartzose grains (=Qm+Qm/Pl+Qpq+Qe+C+Cm)
F	Total feldspar grains (=P+P/Pl+K+K/Pl)
L	Total unstable lithic grains (=Lvl+Lvu+Lvf+Lva+Lss+Lsm+Lsa+Lmm+Lmt+Lmc)
Pl	Total plutonic fragments (=Qm/Pl+P/Pl+K/Pl+M/Pl)
Lv	Total volcanic lithic fragments (=Lvl+Lvu+Lvf+Lva)
Ls	Total sedimentary lithic fragments (=Lss+Lsm+Lsa)
Lm	Total metamorphic lithic fragments (=Lmm+Lmt+Lmc)
Lt	Total lithic grains (=Qpq+C+Cm+Lv+Ls+Lm)

Notes: See Tables 7 and 8 for raw and recalculated data, respectively.

Table 7. Raw point-count data for sandstone samples of the Arkose Ridge Formation

Sample	Qm	Qm/Pl	Qpq	Qe	C	Cm	P	P/Pl	K	K/Pl	Lvl	Lvu	Lvf	Lva	Lss	Lsm	Lsa	Lmm	Lmt	Lmc	Cp	Ol	Am	Mu	Bi	M/Pl	Sp	Zr	n
LONE (Arkose Ridge) N=13																													
LONE1-131.5	101	9	10	0	0	0	245	16	7	0	3	0	0	0	0	1	0	34	0	0	0	0	0	0	0	0	0	0	426
LONE1-208	78	4	7	0	0	0	250	16	8	0	2	0	0	0	0	0	0	35	0	0	0	0	0	0	0	0	0	0	400
LONE1-326	104	6	0	0	1	0	231	11	4	0	4	0	0	0	0	0	0	63	2	0	0	0	0	0	0	0	0	0	426
LONE1-577	130	10	1	0	0	0	214	16	3	0	0	0	0	0	0	0	0	45	1	0	0	0	0	0	0	0	0	0	420
LONE1-612	94	19	6	0	0	0	241	26	0	0	1	0	0	0	0	0	0	23	0	0	0	0	0	0	0	0	0	0	410
LONE1-766	78	16	0	0	0	0	214	32	1	0	0	0	0	0	0	0	0	68	0	0	0	0	0	0	0	0	0	0	409
LONE1-892	88	3	1	0	0	0	263	15	0	0	0	0	0	0	0	0	0	35	0	0	0	0	0	0	0	0	0	0	405
LONE1-1071	69	3	4	0	0	0	278	23	2	0	11	0	0	0	0	0	0	41	0	0	0	0	0	0	0	0	0	0	431
LONE1-1197	83	7	7	0	0	0	291	32	0	0	2	0	0	0	0	0	0	14	0	0	2	0	0	0	0	0	0	0	438
LONE1-1225	108	9	0	0	0	0	203	17	6	0	6	0	0	0	0	0	0	53	0	0	0	0	0	0	0	0	0	0	402
LONE1-1570	49	6	10	0	0	0	273	22	1	0	38	0	0	0	0	0	0	12	0	0	1	0	0	0	0	0	0	0	412
LONE1-1572	61	2	5	0	0	0	287	26	1	0	19	0	0	0	0	0	0	9	0	0	1	1	0	0	0	0	0	0	412
LONE1-1575	52	8	7	0	0	0	323	15	0	0	22	0	0	0	0	0	0	12	0	0	2	0	0	0	0	0	0	0	441
LMN (Lava Mountain North) N=19																													
LMN1-24.7	76	25	39	0	0	0	119	91	0	0	0	0	0	0	0	0	0	32	0	0	0	15	1	2	0	0	0	0	400
LMN1-39	72	23	21	0	0	0	170	65	0	0	0	0	0	0	0	0	0	36	0	0	0	6	0	6	0	0	0	0	399
LMN1-71	76	39	12	0	0	0	114	88	0	0	0	0	0	0	2	0	0	51	0	0	0	20	0	0	0	1	0	0	403
LMN1-100.5	94	25	34	0	1	0	138	54	0	1	0	0	0	0	3	0	0	35	0	0	0	14	1	0	0	0	0	0	400
LMN1-180.3	82	26	30	0	0	0	134	85	1	0	0	0	0	0	1	0	0	31	0	0	0	17	0	0	1	0	0	0	408
LMN1-211	44	56	113	0	0	0	86	75	0	1	0	0	0	0	5	0	0	14	0	0	0	0	5	0	1	0	0	0	400
LMN1-257	40	46	44	0	0	0	122	101	2	1	0	0	0	0	0	0	0	44	0	0	0	0	0	0	0	0	0	0	400
LMN1-315	88	14	19	0	0	0	208	42	0	0	0	0	0	0	6	0	0	16	0	0	0	5	0	0	0	2	0	0	400
LMN1-387	56	54	31	0	0	0	107	118	0	0	0	0	0	0	1	0	0	31	0	0	0	0	0	0	0	2	0	0	400
LMN1-406	64	44	20	0	0	0	118	104	0	0	0	0	0	0	4	0	0	35	0	0	0	6	1	0	1	4	0	0	400
LMN1-458	60	44	25	0	0	0	135	100	0	0	0	0	0	0	1	0	0	29	0	0	0	0	0	1	0	5	0	0	400
LMN1-500	27	65	104	0	0	0	62	98	0	0	0	0	0	0	3	0	0	35	0	0	0	0	5	0	1	0	0	0	400
LMN1-553	63	32	24	0	0	0	144	104	0	0	0	0	0	0	0	0	0	30	0	0	0	1	0	0	0	2	0	0	400
LMN1-599	57	32	23	0	0	0	143	77	0	0	0	0	0	0	1	0	0	65	0	0	0	0	1	0	0	1	0	0	400
LMN1-623	79	32	15	0	0	0	156	62	0	0	0	0	0	0	6	0	0	34	0	0	0	3	0	0	0	13	0	0	400
LMN1-682	66	45	51	0	0	0	122	60	0	0	0	0	0	0	1	0	0	51	0	0	0	0	4	0	0	0	0	0	400

Table 7. Raw point-count data for sandstone samples of the Arkose Ridge Formation

Sample	Qm	Qm/Pl	Qpq	Qe	C	Cm	P	P/Pl	K	K/Pl	Lvl	Lvu	Lvf	Lva	Lss	Lsm	Lsa	Lmm	Lmt	Lmc	Cp	Ol	Am	Mu	Bi	M/Pl	Sp	Zr	n
LMN1-740	72	41	27	0	0	0	141	74	0	0	0	0	0	0	0	0	0	40	0	0	0	0	2	0	0	0	3	0	400
LMN1-780	74	30	37	0	0	0	159	52	0	0	0	0	0	0	0	0	0	45	0	0	0	0	0	0	0	0	1	0	400
LMN1-871	41	61	29	0	1	0	109	101	0	0	0	0	0	0	0	1	0	44	0	0	0	0	12	2	0	0	2	0	401

GR (Gray Ridge) N=22

Sample	Qm	Qm/Pl	Qpq	Qe	C	Cm	P	P/Pl	K	K/Pl	Lvl	Lvu	Lvf	Lva	Lss	Lsm	Lsa	Lmm	Lmt	Lmc	Cp	Ol	Am	Mu	Bi	M/Pl	Sp	Zr	n
GR-61.5	62	43	25	0	0	0	74	80	22	33	0	0	0	0	0	0	0	58	0	0	0	0	0	2	1	0	0	0	400
GR-78	83	26	20	1	0	0	128	68	21	21	0	0	0	0	0	0	0	29	0	0	0	1	0	1	0	0	3	0	402
GR-105	13	11	8	0	0	0	71	18	3	0	71	0	110	11	5	3	5	12	0	1	1	8	49	1	0	0	0	0	401
GR-179	57	10	28	0	0	0	68	11	21	10	14	0	77	41	19	5	17	20	0	0	0	0	0	2	0	0	0	1	401
GR-282	38	22	29	0	0	0	57	26	14	11	65	0	97	5	12	1	16	5	1	0	0	0	0	1	0	0	0	0	400
GR-292	40	19	35	0	1	0	67	8	12	24	60	0	99	9	8	2	9	6	1	1	0	0	0	0	0	0	0	0	400
GR-335.1	70	5	10	10	0	0	50	10	36	7	14	0	162	7	4	3	7	3	1	1	0	0	0	0	0	0	0	0	400
GR-404	18	9	15	0	0	1	46	8	4	3	89	0	176	5	6	6	3	11	0	0	0	0	0	0	0	0	0	0	400
GR-406.6	14	9	7	0	1	0	77	12	5	2	113	0	133	3	10	4	6	3	1	0	0	0	0	0	0	0	0	0	400
GR-455.7	29	22	19	0	0	0	78	21	9	15	88	0	105	4	3	3	1	3	1	0	0	0	0	0	1	0	0	1	402
GR-471.2	73	9	9	13	0	0	102	15	43	3	9	0	114	0	4	0	3	3	0	0	0	0	0	0	1	0	0	1	401
GR-500.6	84	7	53	6	0	1	62	11	85	26	10	0	38	3	1	9	4	0	0	0	0	0	0	0	0	0	0	0	400
GR-592.2	29	13	23	2	1	0	69	14	8	1	47	0	154	12	1	18	3	5	0	0	0	0	0	0	0	0	1	0	401
GR-656.8	41	13	38	0	1	3	59	24	10	3	61	0	95	17	14	4	4	10	1	2	0	0	0	0	0	0	0	1	401
GR-678.7	29	16	14	0	1	0	70	31	17	14	52	0	121	5	9	7	7	10	0	0	0	0	0	0	0	0	0	0	400
GR-708.2	40	41	27	1	1	0	82	53	27	16	21	0	61	9	6	5	2	7	0	0	0	0	0	1	0	0	0	0	400
GR-727.2	68	20	14	1	0	0	124	35	63	32	0	0	5	7	2	4	0	23	0	0	0	0	0	2	0	0	0	0	400
GR-752.6	78	19	23	0	4	0	125	29	26	13	4	0	42	1	20	2	4	8	2	0	0	0	0	2	0	0	0	0	402
GR-813.8	26	30	36	0	8	7	40	45	10	19	74	0	78	7	0	2	19	5	0	0	0	0	0	0	0	0	0	0	406
GR-834.6	37	19	27	0	1	0	58	12	13	4	80	0	78	12	25	10	20	4	0	0	0	0	0	0	0	0	0	0	400
GR-861.3	15	23	28	0	8	0	58	52	4	9	68	0	93	5	4	8	18	5	2	0	0	0	0	1	0	0	0	0	400
GR-930.6	42	43	18	0	8	0	44	65	10	12	60	0	50	11	0	2	21	12	1	0	0	0	0	1	0	0	0	0	400

Notes: N= number of samples point counted; n = number of grains counted; Sample codes denote position above base of the measured section.
Example: Sample LONE1-131.5 was collected 131.5 m above the base of section LONE1. See Figure X for sample locations. See Tables 6 and 8 for grain definitions and recalculated data, respectively.

Table 8. Recalculated point-count data for sandstone samples of the Arkose Ridge Formation

Sample	%Q-F-L			%Qm-F-Lt			%Qm-P-K			%Lv-Ls-Lm			%Lv-(Ls+Lm)-Pl		
	Q	F	L	Qm	F	Lt	Qm	P	K	Lv	Ls	Lm	Lv	Ls+Lm	Pl
LONE (Arkose Ridge)															
LONE1-131.5	28.17	62.91	8.92	24.22	64.27	11.51	27.37	70.73	1.90	8.11	0.00	91.89	4.76	55.56	39.68
LONE1-208	22.25	68.50	9.25	19.70	69.19	11.11	22.16	75.57	2.27	5.41	0.00	94.59	3.51	61.40	35.09
LONE1-326	26.06	57.75	16.20	24.76	58.57	16.67	29.71	69.14	1.14	5.80	0.00	94.20	4.65	75.58	19.77
LONE1-577	33.57	55.48	10.95	31.71	56.83	11.46	35.81	63.36	0.83	0.00	0.00	100.00	0.00	63.89	36.11
LONE1-612	29.02	65.12	5.85	24.04	68.29	7.67	26.04	73.96	0.00	4.17	0.00	95.83	1.45	33.33	65.22
LONE1-766	22.98	60.39	16.63	19.85	62.85	17.30	24.00	75.69	0.31	0.00	0.00	100.00	0.00	58.62	41.38
LONE1-892	22.72	68.64	8.64	21.89	69.15	8.96	24.04	75.96	0.00	0.00	0.00	100.00	0.00	66.04	33.96
LONE1-1071	17.63	70.30	12.06	16.12	70.79	13.08	18.55	80.91	0.54	21.15	0.00	78.85	14.10	52.56	33.33
LONE1-1197	22.25	74.08	3.67	19.35	75.29	5.36	20.44	79.56	0.00	12.50	0.00	87.50	3.64	25.45	70.91
LONE1-1225	29.10	56.22	14.68	27.48	57.51	15.01	32.34	65.87	1.80	10.17	0.00	89.83	7.06	62.35	30.59
LONE1-1570	15.85	71.95	12.20	12.13	73.02	14.85	14.24	85.47	0.29	76.00	0.00	24.00	48.72	15.38	35.90
LONE1-1572	16.59	76.59	6.83	14.95	76.96	8.09	16.27	83.47	0.27	67.86	0.00	32.14	33.93	16.07	50.00
LONE1-1575	15.26	76.99	7.74	12.06	78.42	9.51	13.33	86.67	0.00	64.71	0.00	35.29	38.60	21.05	40.35
Mean	**23.19**	**66.53**	**10.28**	**20.64**	**67.78**	**11.58**	**23.41**	**75.87**	**0.72**	**21.22**	**0.00**	**78.78**	**12.34**	**46.72**	**40.95**
LMN (Lava Mountain North)															
LMN1-24.7	36.65	54.97	8.38	26.44	54.97	18.59	32.48	67.52	0.00	0.00	0.00	100.00	0.00	21.62	78.38
LMN1-39	29.97	60.72	9.30	24.55	60.72	14.73	28.79	71.21	0.00	0.00	0.00	100.00	0.00	29.03	70.97
LMN1-71	33.25	52.88	13.87	30.10	52.88	17.02	36.28	63.72	0.00	0.00	3.77	96.23	0.00	29.44	70.56
LMN1-100.5	40.00	50.13	9.87	30.91	50.13	18.96	38.14	61.54	0.32	0.00	7.89	92.11	0.00	32.20	67.80
LMN1-180.3	35.38	56.41	8.21	27.69	56.41	15.90	32.93	66.77	0.30	0.00	3.13	96.88	0.00	22.38	77.62
LMN1-211	54.06	41.12	4.82	25.38	41.12	33.50	38.17	61.45	0.38	0.00	26.32	73.68	0.00	12.58	87.42
LMN1-257	32.50	56.50	11.00	21.50	56.50	22.00	27.56	71.47	0.96	0.00	0.00	100.00	0.00	22.92	77.08
LMN1-315	30.79	63.61	5.60	25.95	63.61	10.43	28.98	71.02	0.00	0.00	27.27	72.73	0.00	28.21	71.79
LMN1-387	35.43	56.53	8.04	27.64	56.53	15.83	32.84	67.16	0.00	0.00	3.13	96.88	0.00	15.69	84.31
LMN1-406	32.90	57.07	10.03	27.76	57.07	15.17	32.73	67.27	0.00	0.00	10.26	89.74	0.00	20.86	79.14
LMN1-458	32.74	59.64	7.61	26.40	59.64	13.96	30.68	69.32	0.00	0.00	3.33	96.67	0.00	17.24	82.76
LMN1-500	49.75	40.61	9.64	23.35	40.61	36.04	36.51	63.49	0.00	0.00	7.89	92.11	0.00	18.91	81.09
LMN1-553	29.97	62.47	7.56	23.93	62.47	13.60	27.70	72.30	0.00	0.00	0.00	100.00	0.00	18.07	81.93
LMN1-599	28.14	55.28	16.58	22.36	55.28	22.36	28.80	71.20	0.00	0.00	1.52	98.48	0.00	37.71	62.29

Table 8. Recalculated point-count data for sandstone samples of the Arkose Ridge Formation

Sample	%Q-F-L			%Qm-F-Lt			%Qm-P-K			%Lv-Ls-Lm			%Lv-(Ls+Lm)-Pl		
	Q	F	L	Qm	F	Lt	Qm	P	K	Lv	Ls	Lm	Lv	Ls+Lm	Pl
LMN1-623	32.81	56.77	10.42	28.91	56.77	14.32	33.74	66.26	0.00	0.00	15.00	85.00	0.00	29.85	70.15
LMN1-682	40.91	45.96	13.13	28.03	45.96	26.01	37.88	62.12	0.00	0.00	1.92	98.08	0.00	33.12	66.88
LMN1-740	35.44	54.43	10.13	28.61	54.43	16.96	34.45	65.55	0.00	0.00	0.00	100.00	0.00	25.81	74.19
LMN1-780	35.34	52.88	11.78	26.07	52.88	21.05	33.02	66.98	0.00	0.00	4.26	95.74	0.00	36.43	63.57
LMN1-871	34.11	54.26	11.63	26.36	54.26	19.38	32.69	67.31	0.00	0.00	2.22	97.78	0.00	21.74	78.26
Mean	35.80	54.33	9.87	26.42	54.33	19.25	32.86	67.04	0.10	0.00	6.21	93.79	0.00	24.94	75.06
GR (Gray Ridge)															
GR-61.5	32.75	52.64	14.61	26.45	52.64	20.91	33.44	49.04	17.52	0.00	0.00	100.00	0.00	27.10	72.90
GR-78	32.75	59.95	7.30	27.71	59.95	12.34	31.61	56.32	12.07	0.00	0.00	100.00	0.00	20.14	79.86
GR-105	9.36	26.90	63.74	7.02	26.90	66.08	20.69	76.72	2.59	88.07	5.96	5.96	77.73	10.53	11.74
GR-179	23.87	27.64	48.49	16.83	27.64	55.53	37.85	44.63	17.51	68.39	21.24	10.36	58.93	27.23	13.84
GR-282	22.31	27.07	50.63	15.04	27.07	57.89	35.71	49.40	14.88	82.67	14.36	2.97	63.98	13.41	22.61
GR-292	23.75	27.75	48.50	14.75	27.75	57.50	34.71	44.12	21.18	86.60	9.79	3.61	68.57	10.61	20.82
GR-335.1	23.75	25.75	50.50	21.25	25.75	53.00	45.21	31.91	22.87	90.59	6.93	2.48	81.70	8.48	9.82
GR-404	10.75	15.25	74.00	6.75	15.25	78.00	30.68	61.36	7.95	85.44	5.07	3.72	85.44	8.23	6.33
GR-406.6	7.75	24.00	68.25	5.75	24.00	70.25	19.33	74.79	5.88	91.21	7.33	1.47	84.12	8.11	7.77
GR-455.7	17.46	30.67	51.87	12.72	30.67	56.61	29.31	56.90	13.79	94.71	3.37	1.92	74.06	4.14	21.80
GR-471.2	26.00	40.75	33.25	23.75	40.75	35.50	36.82	45.35	17.83	92.48	5.26	2.26	76.88	6.25	16.88
GR-500.6	37.75	46.00	16.25	24.25	46.00	29.75	34.52	25.98	39.50	78.46	21.54	0.00	46.79	12.84	40.37
GR-592.2	17.00	23.00	60.00	11.00	23.00	66.00	32.35	61.03	6.62	88.75	9.17	2.08	79.48	10.07	10.45
GR-656.8	24.00	24.00	52.00	13.50	24.00	62.50	36.00	55.33	8.67	83.17	10.58	6.25	69.76	14.11	16.13
GR-678.7	15.00	33.00	52.00	11.25	33.00	55.75	25.42	57.06	17.51	85.58	9.62	4.81	66.17	11.15	22.68
GR-708.2	27.57	44.61	27.82	20.55	44.61	34.84	31.54	51.92	16.54	81.98	11.71	6.31	41.18	9.05	49.77
GR-727.2	25.88	63.82	10.30	22.36	63.82	13.82	25.95	46.36	27.70	29.27	14.63	56.10	9.38	22.66	67.97
GR-752.6	31.00	48.25	20.75	24.25	48.25	27.50	33.45	53.10	13.45	56.63	31.33	12.05	32.64	25.00	42.36
GR-813.8	26.35	28.08	45.57	13.79	28.08	58.13	32.94	50.00	17.06	85.95	11.35	2.70	56.99	9.32	33.69
GR-834.6	21.00	21.75	57.25	14.00	21.75	64.25	39.16	48.95	11.89	74.24	24.02	1.75	64.39	22.35	13.26
GR-861.3	18.50	30.75	50.75	9.50	30.75	59.75	23.60	68.32	8.07	81.77	14.78	3.45	57.84	12.89	29.27
GR-930.6	27.82	32.83	39.35	21.30	32.83	45.86	39.35	50.46	10.19	77.07	14.65	8.28	43.68	13.00	43.32
Mean	22.83	34.29	42.87	16.54	34.29	49.17	32.26	52.69	15.06	73.13	11.49	15.39	56.35	13.94	29.71

See Tables 6 and 7 for grain definitions and sample codes, respectively.

Figure 8. Photomicrographs of representative framework grains from point counted sandstone samples. (A) and (B) Plutonic fragments with quartz and plagioclase feldspar subgrains. (C) Plutonic lithic grain with plagioclase and potassium feldspar subgrains. (D) and (E) Lathwork and microlitic volcanic lithic grains with plagioclase feldspar laths and sparse quartz subgrains; subordinate mudstone lithic grain with quartz subgrains in the upper right of (E). (F) Microlitic volcanic lithic grain. (G) Biotite schist fragment with minor quartz and plagioclase feldspar. (H) Mudstone lithic grain with siliceous microfossils (probable radiolaria). (A), (B), and (G) are from Lava Mountain. (C), (D), (E), (F), and (H) are from Gray Ridge. (A), (B), (C), (D), and (F) are in cross-polarized light. (E), (G), and (H) are in plane light. Thin sections stained for plagioclase (red stain) and potassium feldspar (green stain).
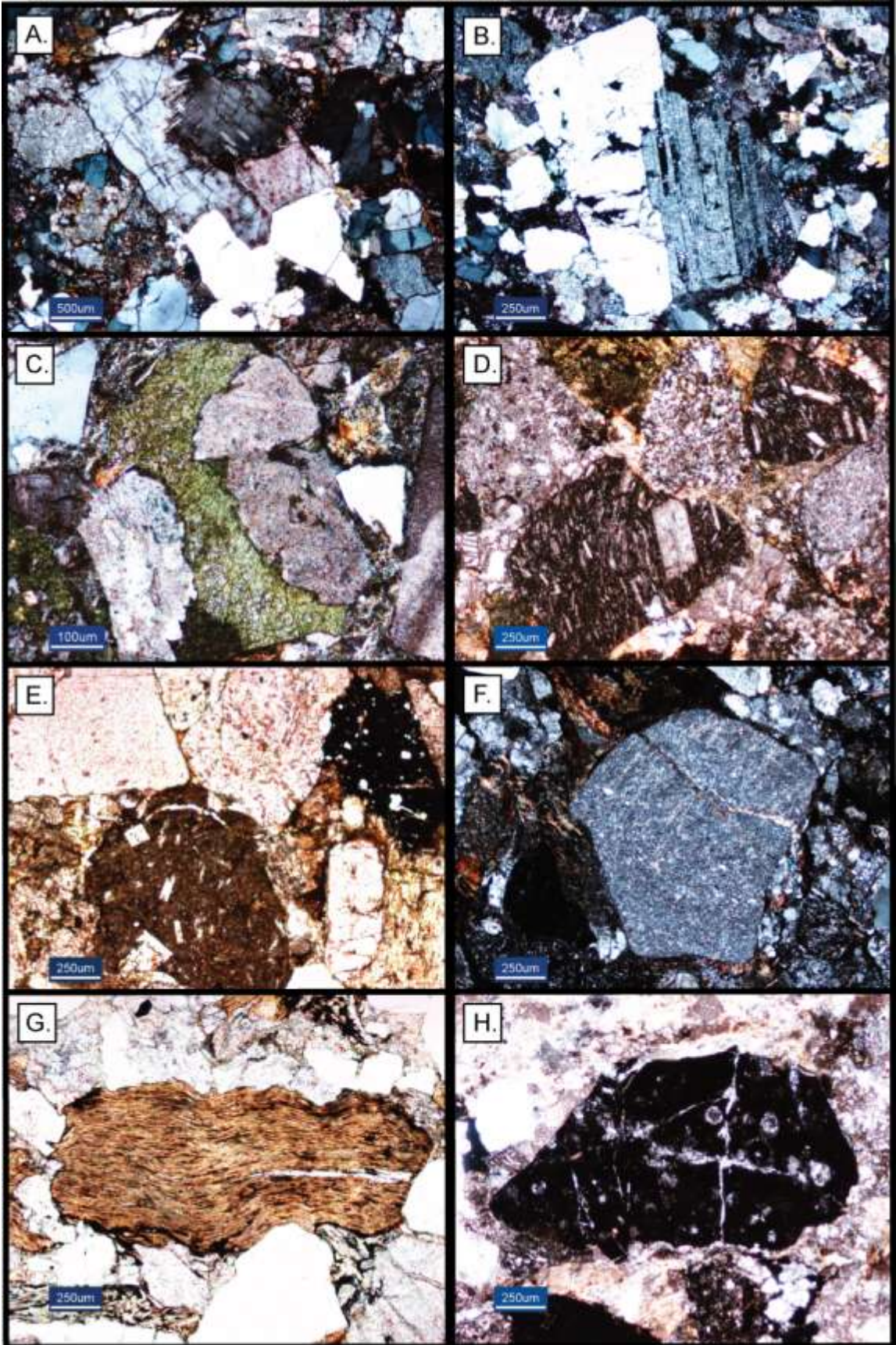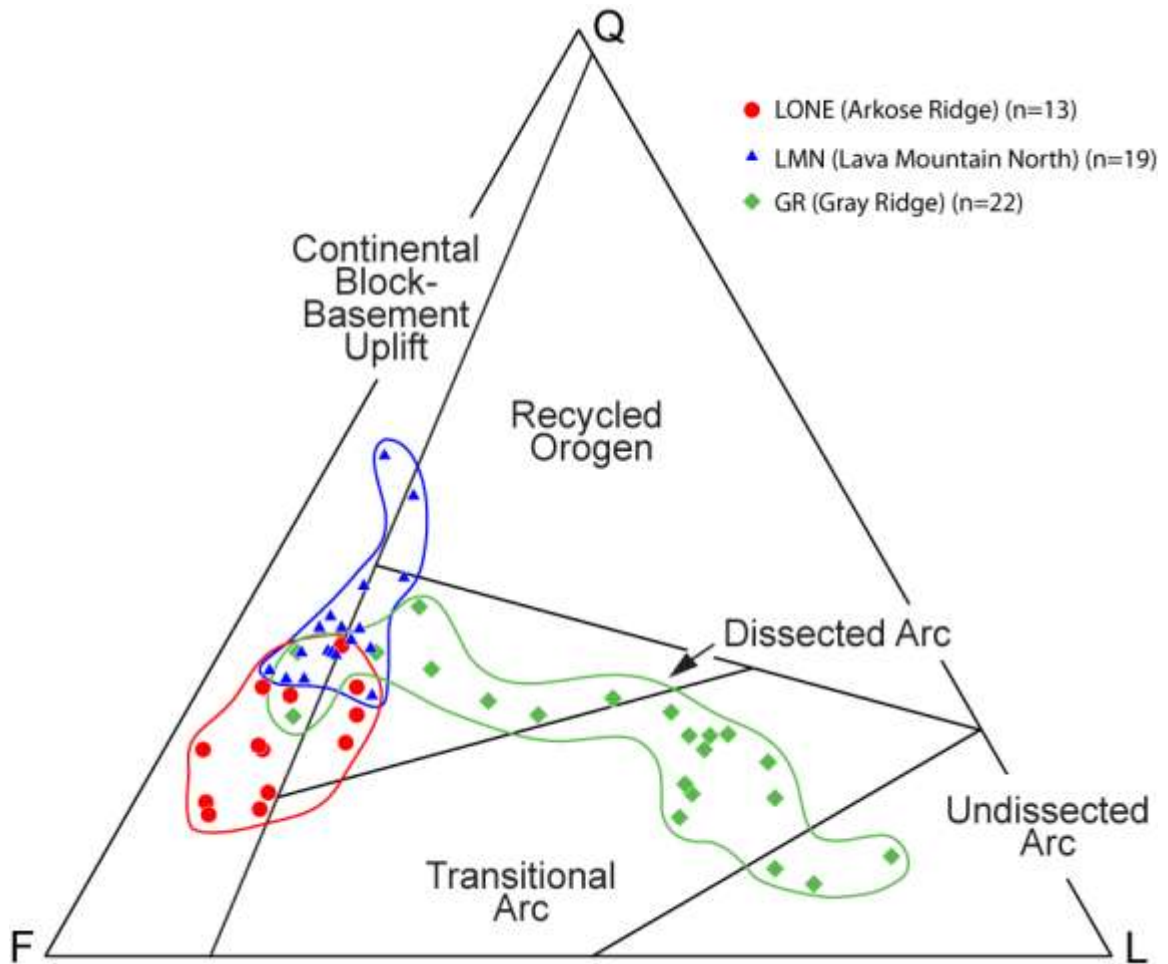
Figure 9. Sandstone point-count data from the Arkose Ridge Formation plotted on a Q-F-L ternary diagram. See Table 6 for grain parameters. Note that western sandstone samples (Arkose Ridge – red circles, and Lava Mountain – blue triangles) largely overlap the continental block-basement uplift provenance fields, whereas eastern sandstone samples (Gray Ridge – green diamonds) mainly overlap the dissected, transitional and undissected volcanic arc provenance fields. Provenance fields are from Dickinson et al. (1983). n = total number of sandstone samples point-counted in each location.
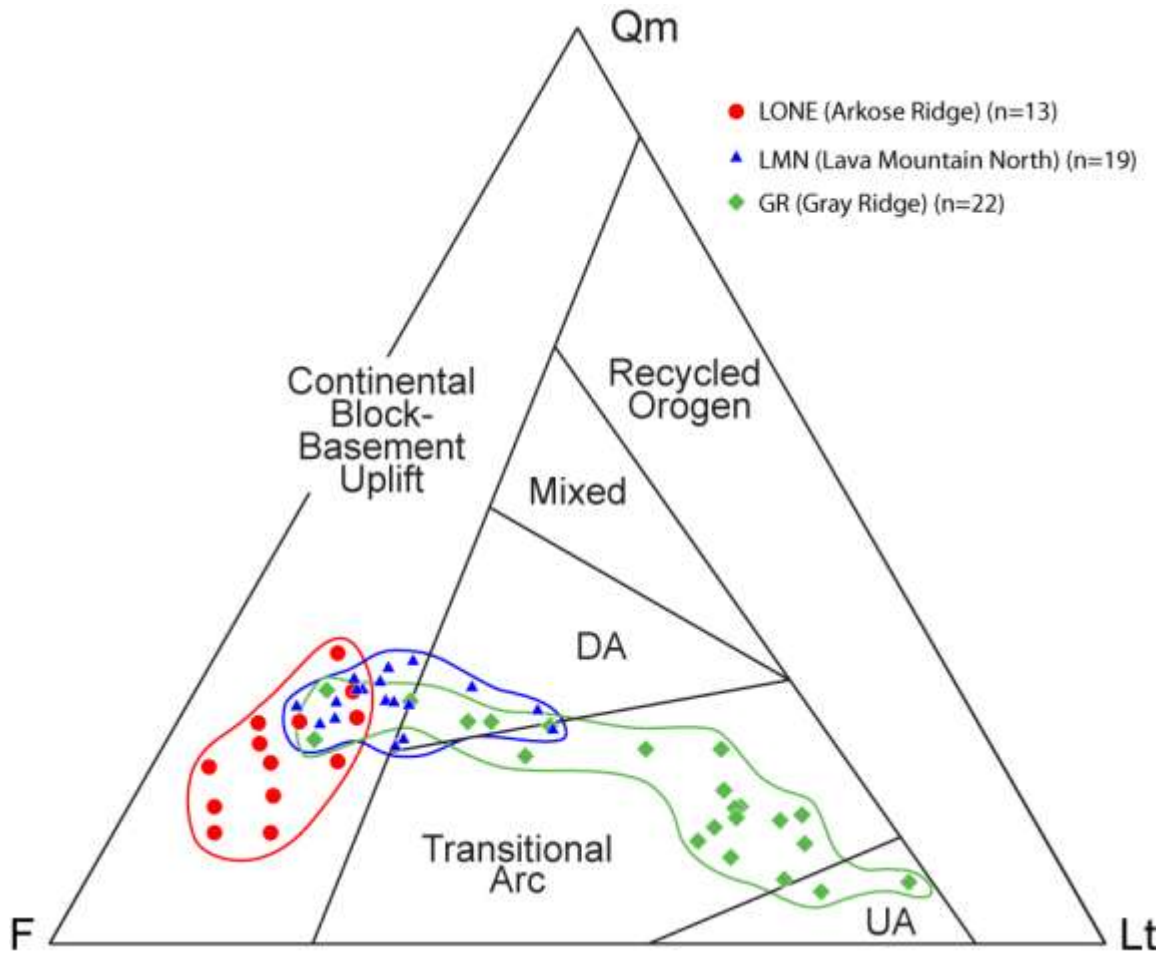
Figure 10. Sandstone point-count data from the Arkose Ridge Formation plotted on a Qm-F-Lt ternary diagram. See Table 6 for grain parameters. Note that western sandstone samples (Arkose Ridge – red circles, and Lava Mountain – blue triangles) largely overlap the continental block-basement uplift provenance fields of Dickinson et al. (1983), whereas eastern sandstone samples (Gray Ridge – green diamonds) mainly overlap the dissected, transitional and undissected volcanic arc provenance fields. n = total number of sandstone samples point-counted in each location.
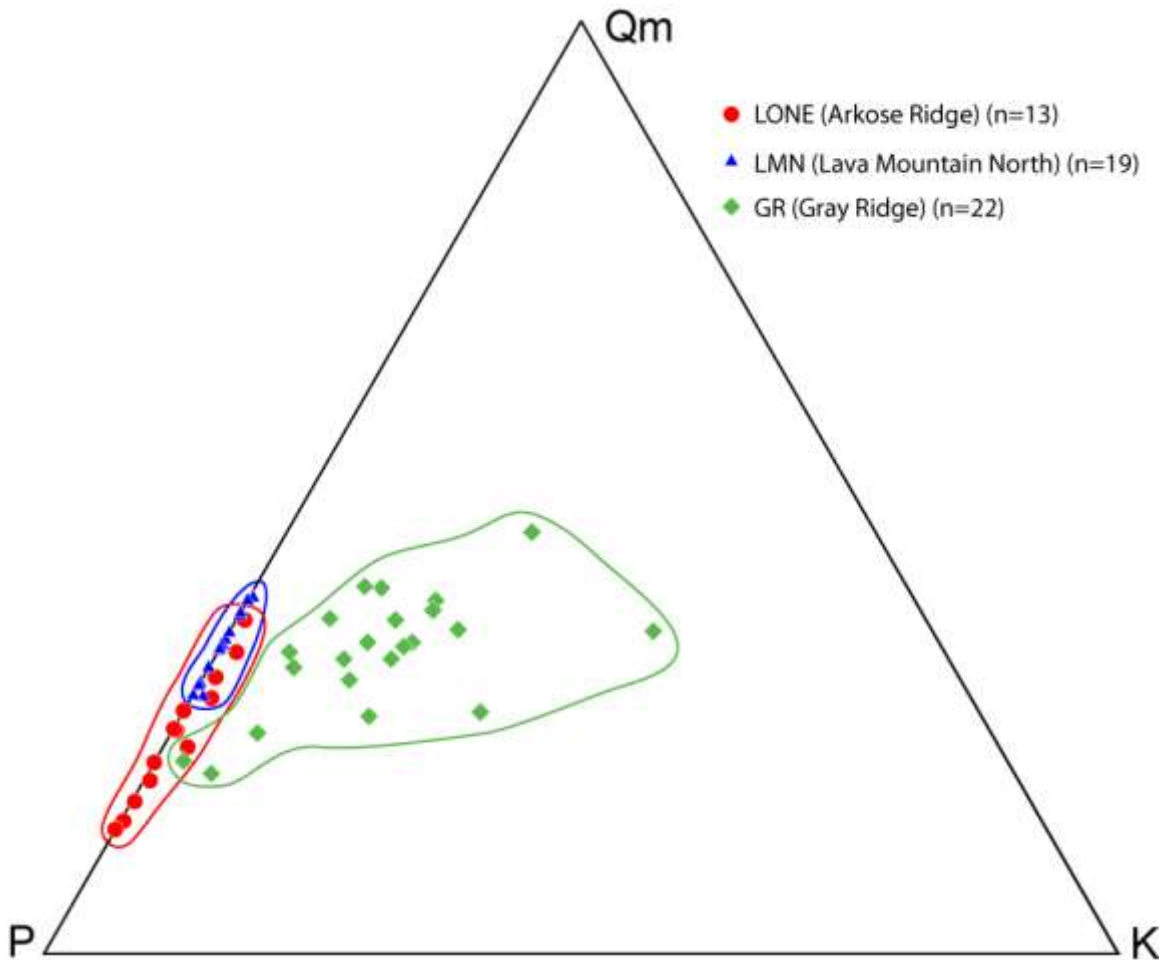
Figure 11. Sandstone point-count data from the Arkose Ridge Formation plotted on a Qm-P-K ternary diagram. See Table 6 for grain parameters. Arkose Ridge sandstone samples are plotted as red circles, Lava Mountain sandstone samples are plotted as blue triangles, and Gray Ridge sandstone samples are plotted as green diamonds. Note overall enrichment of plagioclase feldspar relative to potassium feldspar in Lava Mountain and Arkose Ridge samples, but relative enrichment of potassium feldspar in Gray Ridge samples. n = total number of sandstone samples point-counted at each location.
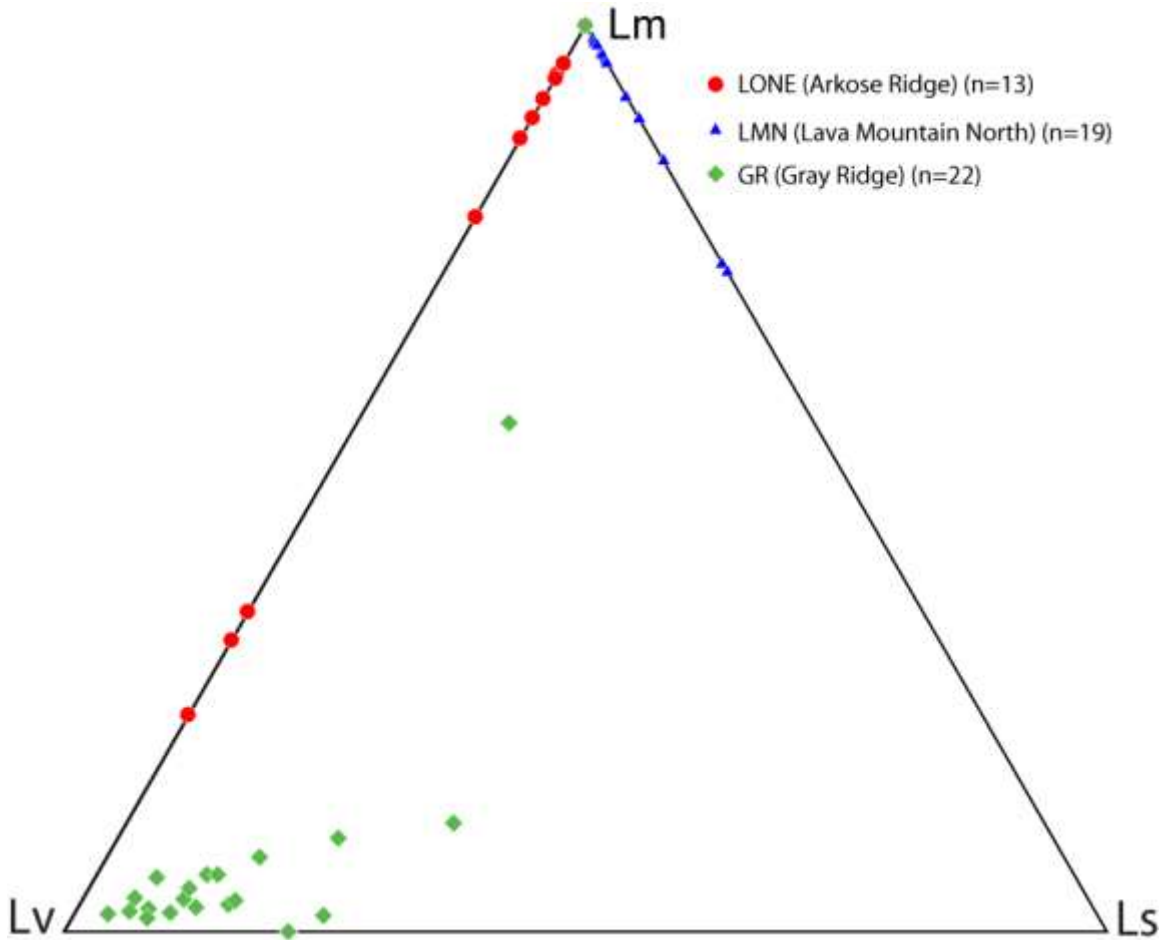
Figure 12. Sandstone point-count data from the Arkose Ridge Formation plotted on a Lm-Ls-Lv ternary diagram. See Table 6 for grain parameters. Note that most western sandstone samples (Arkose Ridge – red circles, and Lava Mountain – blue triangles) are enriched in metamorphic lithic grains, whereas eastern sandstone samples (Gray Ridge – green diamonds) are dominated by volcanic lithics. n = total number of sandstone samples point-counted at each location. Three sandstones from the uppermost Arkose Ridge locality are enriched in volcanic lithics, consistent with reworking of volcanic interbeds in the upper part of the section locally.

49
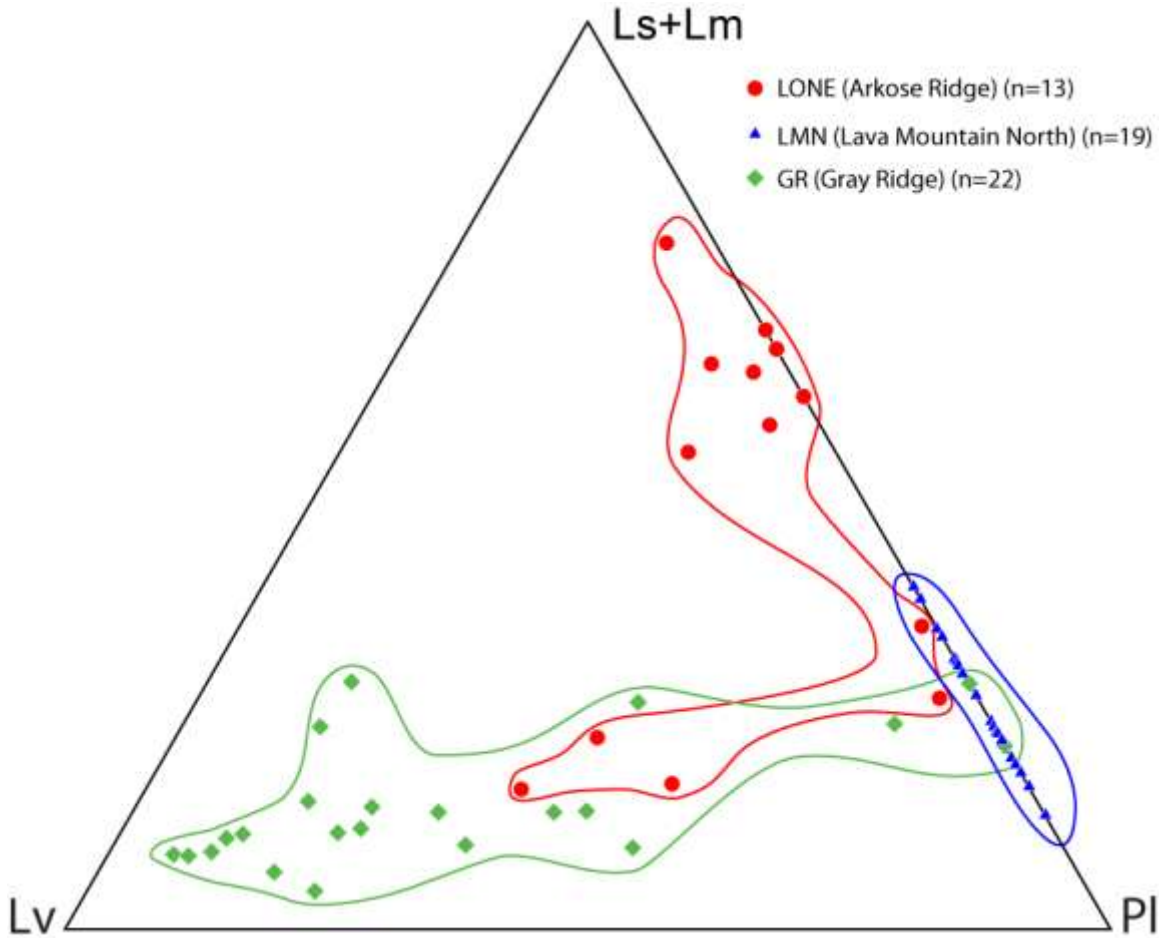
Figure 13. Sandstone point-count data from the Arkose Ridge Formation plotted on a Lv-(Ls+Lm)-Pl ternary diagram. See Table 6 for grain parameters. Note that western sandstone samples (Arkose Ridge – red circles, and Lava Mountain – blue triangles) are dominated by plutonic and metamorphic lithic grains, whereas eastern sandstone samples (Gray Ridge – green diamonds) are dominated by volcanic lithic grains. n = total number of sandstone samples point-counted at each location.

Volcanic Petrofacies

The volcanic petrofacies comprise sandstone modal compositions from the eastern section at Gray Ridge. No sandstone samples for petrography were collected from Box Canyon due to the presence of conglomerate beds throughout the section. Point-counted sandstones are moderately to poorly sorted, with angular to subrounded framework grains. Most samples are closely packed and contain sparse calcite cement and minor volcanic pseudomatrix. Volcanic pseudomatrix was counted as volcanic lithic grains. Overall, modal percentages for the eastern sandstones are dominated by plagioclase feldspar, quartz, and volcanic lithic fragments with subordinate potassium feldspar, plutonic fragments, schist fragments, and sedimentary lithic grains (Fig. 8). Mean modal compositions for the Gray Ridge section are Q:F:L = 23:34:43 and Qm:F:Lt = 17:34:49. On Q:F:L and Qm:F:Lt discrimination diagrams these sandstones classify as feldspathic to lithic arenites and overlap the "continental block-basement uplift", "dissected arc", "transitional arc", and "undissected arc" provenance fields (Fig. 9, 10). Subangular plagioclase feldspars and subordinate potassium feldspars make up the feldspar population (Qm:P:K = 32:53:15) with subordinate feldspars contained within plutonic fragments (Fig. 11). The quartz population consists of monocrystalline quartz, subordinate polycrystalline quartz and quartz within plutonic fragments, and minor embayed quartz, chert, and muddy chert. Lithic fragments include abundant volcanic grains and subordinate metamorphic and sedimentary grains (Lm:Lv:Ls = 15:73:11; Fig. 12). Volcanic grains consist of most felsic and mafic compositions. Mafic volcanic grains contain plagioclase feldspar phenocrysts in a dark glassy matrix, whereas most felsic volcanic grains contain both plagioclase feldspar laths and quartz in a granular,

microlitic texture. Metamorphic grains include mica schist, quartz-mica tectonite, and metachert. Siltstone, shale, and weakly foliated argillite are common sedimentary grains. Plutonic fragments are common and consist mainly of plagioclase feldspar, monocrystalline quartz, potassium feldspar, and muscovite (Fig. 13). Amphiboles, olivine, muscovite, sphene, zircon and clinopyroxene make up the accessory minerals.

Detrital U-Pb Zircon Ages

A total of 15 medium-grained sandstone samples were collected for detrital zircon geochronologic analyses. Detrital zircon analyses were collected from four stratigraphic sections; Arkose Ridge (3 of 15 detrital zircon samples collected) and Lava Mountain (5) in the west, and Gray Ridge (4) and Box Canyon (3) in the east (Fig. 6). U-Pb zircon analyses of 1415 individual grains document mainly Mesozoic to Cenozoic ages (98.2% of analyzed grains) and minor Precambrian to Paleozoic ages (1.8%). Three Mesozoic-Cenozoic age populations dominate the analyzed grains: 60-48 Ma (Late Paleocene to Eocene; 17.2%), 85-60 Ma (Latest Cretaceous to Early Paleocene; 62.5%), and 200-100 Ma (Jurassic to Early Cretaceous; 12.5%). Subordinate Mesozoic populations are 100-85 Ma (Early Late Cretaceous; 5.4%) and 251-200 (Triassic to Early Jurassic; 0.6%). Precambrian-Paleozoic populations include 416-318 Ma (Devonian-Mississippian; 1.3%), Cambrian (0.1%), and Precambrian (0.4%) ages. See Table 9 for summary of detrital zircon geochronologic analyses. Greater than 99% of analyzed zircons yield U/Th values <10, and greater than 97% of analyzed zircons are <200 Ma (Fig. 14).

Akin to the compositional data, the detrital samples may be separated into two distinct chronofacies based on detrital zircon age populations. Overall, the distinction

Table 9. Summary of detrital ages for sandstone samples of the Arkose Ridge Formation

Period	Late Paleocene-Eocene	Latest Cretaceous-Early Paleocene	Early Late Cretaceous	Early Cretaceous-Jurassic	Triassic	Devonian-Mississippian	Cambrian	Precambrian	Total
Age (Ma)	60-48 Ma	85-60	100-85	200-100	251-200	416-318	488-542	>542 Ma	Total
Summary of detrital ages from Arkose Ridge (N=3)									
# grains	0	263	26	7	1	0	0	0	297
%	0.0%	88.6%	8.8%	2.4%	0.3%	0.0%	0.0%	0.0%	100.0%
Summary of detrital ages from Lava Mountain (N=5 including Sheep Valley)									
# grains	6	280	31	87	5	3	0	1	413
%	1.5%	67.8%	7.5%	21.1%	1.2%	0.7%	0.0%	0.2%	100.0%
Summary of detrital ages from Gray Ridge (N=4)									
# grains	128	207	6	36	0	4	0	1	382
%	33.5%	54.2%	1.6%	9.4%	0.0%	1.0%	0.0%	0.3%	100.0%
Summary of detrital ages from Box Canyon (N=3)									
# grains	110	135	13	48	1	11	1	4	323
%	34.1%	41.8%	4.0%	14.9%	0.3%	3.4%	0.3%	1.2%	100.0%
Summary of detrital ages from all Arkose Ridge Formation samples (N=15)									
# grains	244	885	76	177	8	18	1	6	1415
%	17.2%	62.5%	5.4%	12.5%	0.6%	1.3%	0.1%	0.4%	100.0%

Notes: N = number of samples analyzed. See Figure 3 for sample locations.
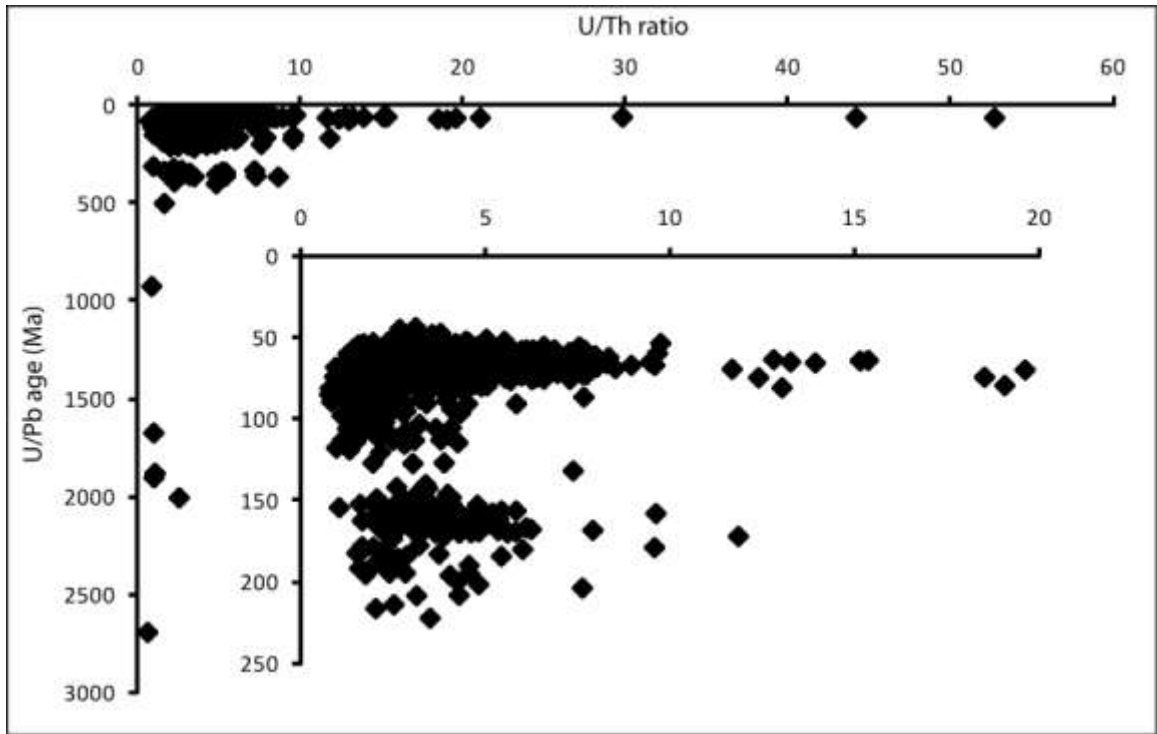
Figure 14. U/Th vs. U/Pb age of spot analyses of 1415 detrital zircons from 15 sandstone samples. Note that >97% of zircons are <200 Ma and >99% of zircons have <10 U/Th ratios. Inset shows details for grains <250 Ma and <20 U/Th.

between the two chronofacies is made by the amount of Late Paleocene-Eocene (60-48 Ma) grains present. The western sections comprise a Jurassic-early Paleocene chronofacies that contains a sparse population of 60-48 Ma grains whereas the eastern sections comprise a Late-Paleocene-Eocene chronofacies that contains a major 60-48 Ma detrital zircon population. Western sections (Arkose Ridge and Lava Mountain) that make up the plutonic petrofacies based on compositional data contain mainly Latest Cretaceous-Early Paleocene (85-60 Ma) and Jurassic-Early Cretaceous (200-100 Ma) detrital age populations consistent with the Jurassic-early Paleocene chronofacies. A total of three detrital geochronologic samples were collected at Arkose Ridge. U-Pb analyses of 297 individual zircon grains document mainly Latest Cretaceous-Early Paleocene (85-60 Ma; 88.6%) ages (Fig. 15). Subordinate Mesozoic populations are 100-85 Ma (Early Late Cretaceous; 8.8%), 200-100 Ma (Jurassic-Early Cretaceous; 2.4%), and 251-200 Ma (Triassic-Early Jurassic; 0.3%). There are no reported Precambrian-Paleozoic ages. It is important to note there are also no reported Late Paleocene-Eocene (60-48 Ma) ages from the westernmost section at Arkose Ridge. A total of five samples were collected at Lava Mountain. Analyses of 413 grains document mainly Mesozoic ages. Two Mesozoic-Cenozoic populations dominate: 85-60 Ma (Latest Cretaceous-Early Paleocene; 67.8%) and 200-100 Ma (Jurassic-Early Cretaceous; 21.1%) (Fig. 16). Subordinate populations are 60-48 Ma (Late Paleocene-Eocene; 1.5%), 100-85 Ma (Early Late Cretaceous; 7.5%), 251-200 Ma (Triassic-Early Jurassic; 1.2%), 416-318 Ma (Devonian-Mississippian; 0.7%), and Precambrian (0.2%). Note that 60-48 Ma (Late Paleocene-Eocene) grains only constitute 1.5% of Lava Mountain detrital zircon samples.
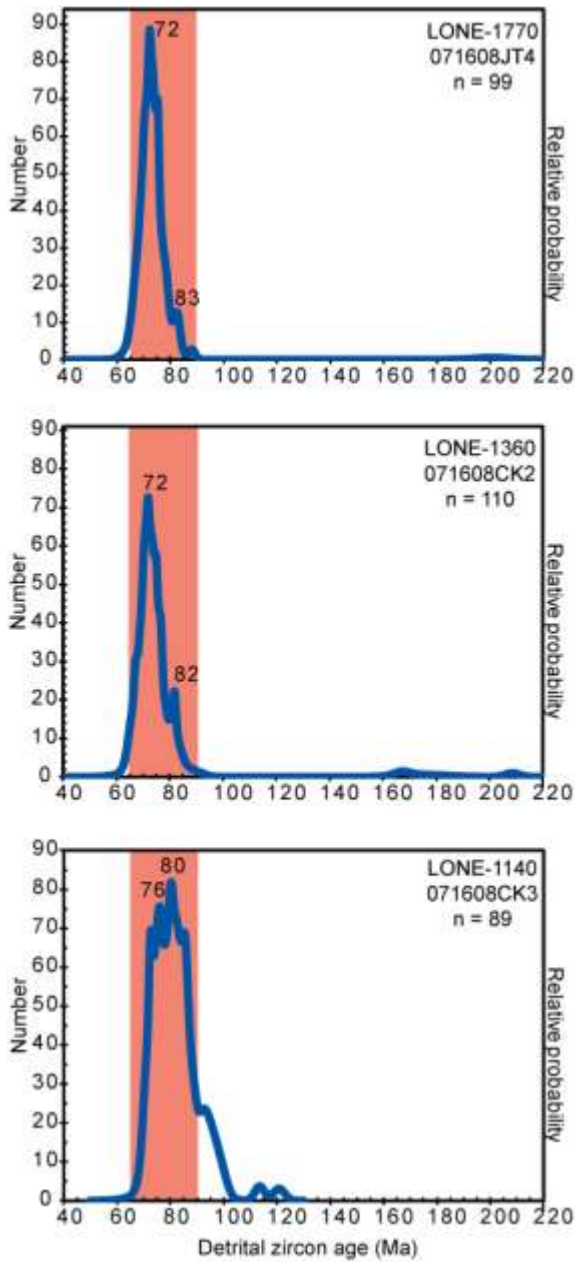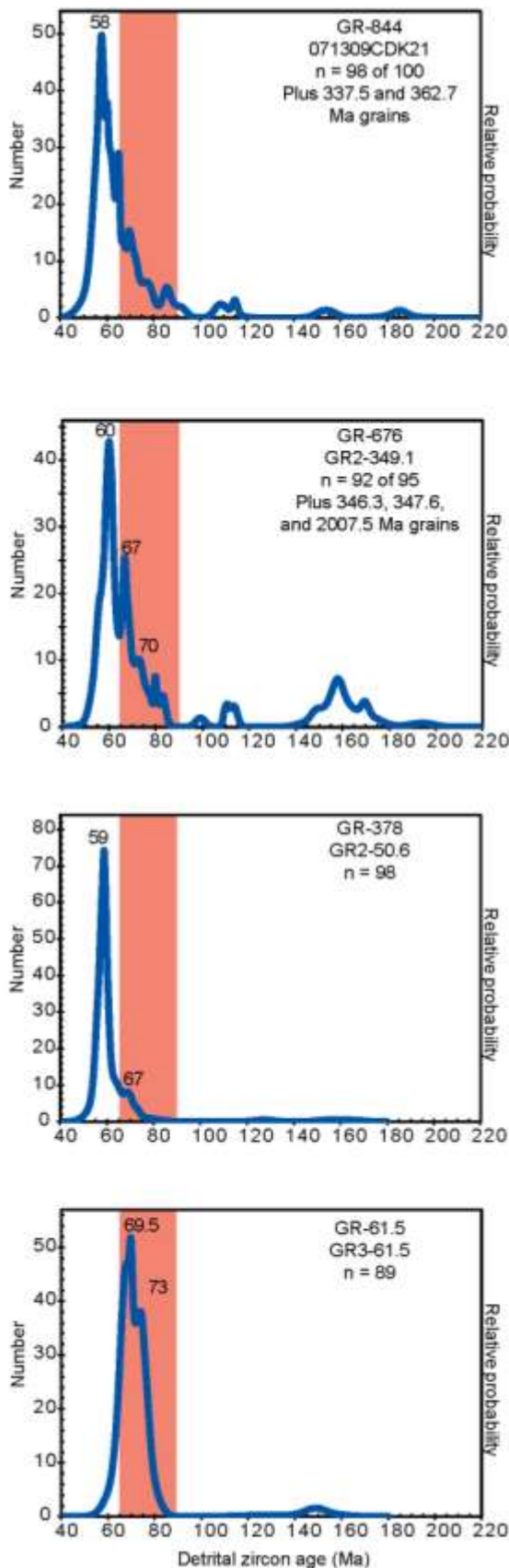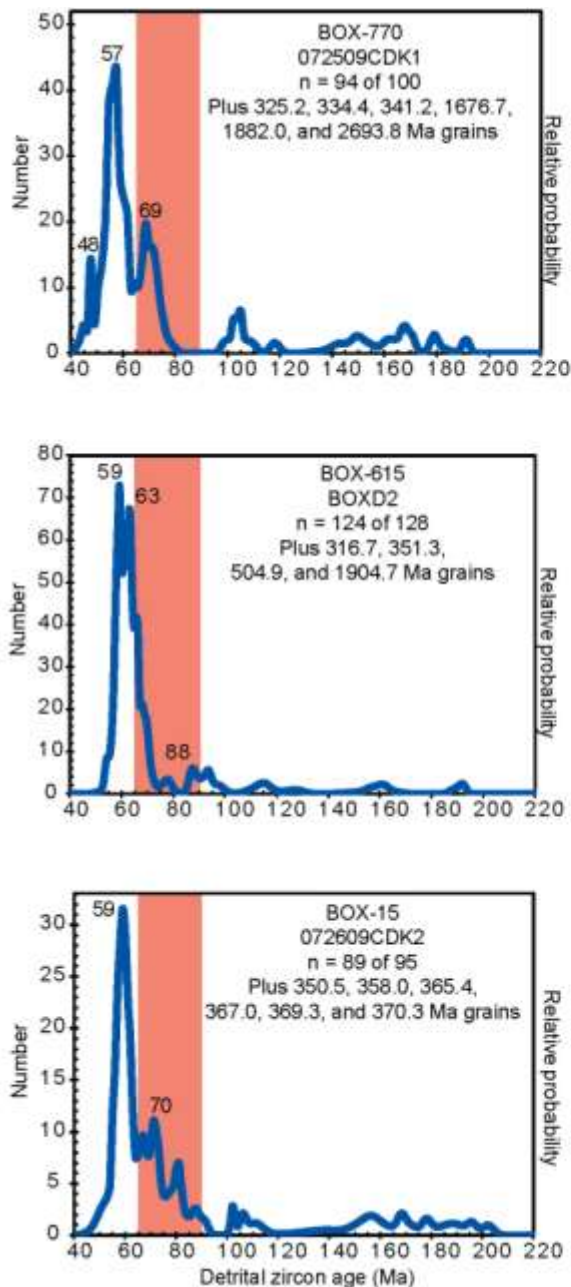
Figure 15. Age probability plots showing distribution of U-Pb age determinations for 298 detrital zircon grains from three sandstone samples collected from the Arkose Ridge section of the Arkose Ridge Formation. Age determinations represent individual spot analyses from separate detrital zircon grains. U-Pb ages are plotted as a normalized relative-probability distribution (Ludwig, 2003). Relative heights of peaks correspond to statistical significance. Orange bar denotes 65-90 Ma age range of adjacent/underlying plutons (TKg on Fig. 3). Note dominance of 70-90 Ma populations consistent with TKg age range.
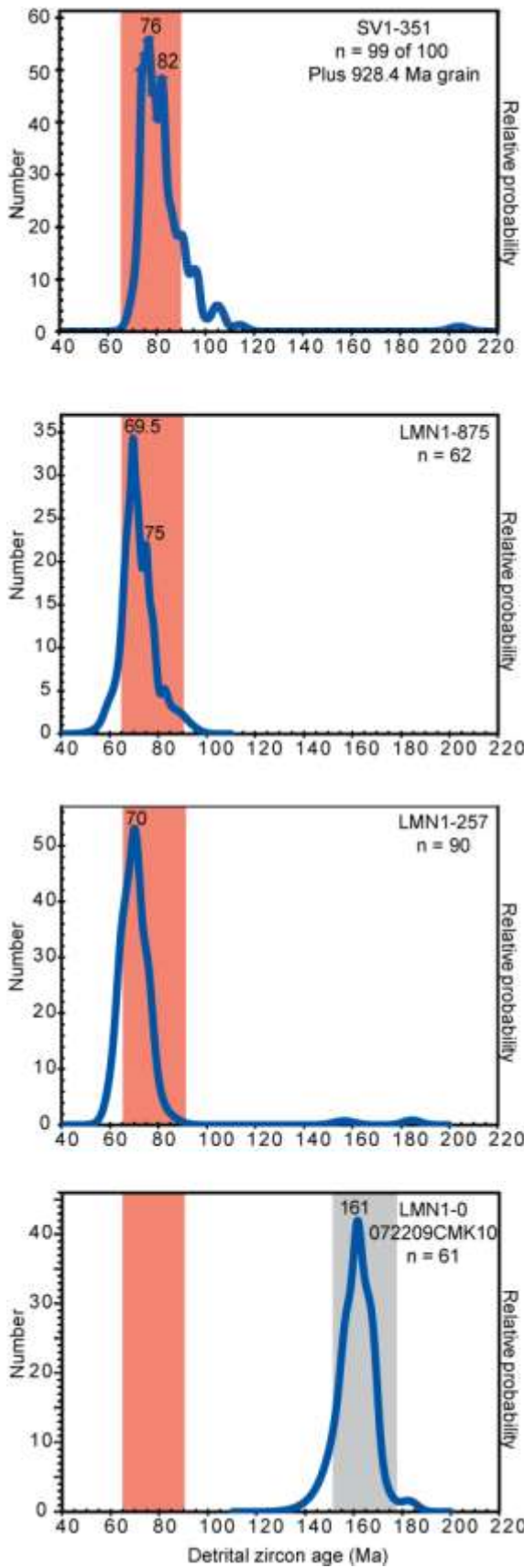
Figure 16. Age probability plots showing distribution of U-Pb age determinations for 413 detrital zircon grains from five sandstone samples collected from the Lava Mountain section of the Arkose Ridge Formation. Age determinations represent individual spot analyses from separate detrital zircon grains. U-Pb ages are plotted as a normalized relative-probability distribution (Ludwig, 2003). Relative heights of peaks correspond to statistical significance. Orange bar denotes 65-90 Ma age range of adjacent Cretaceous plutons (TKg on Fig. 3). Gray bar denotes 152-177 Ma age range of adjacent/underlying Jurassic plutons (Jpu on Fig. 3). Note upsection change from 150-170 Ma age populations consistent with Jpu age range at the base of the section to 65-80 Ma age populations consistent with TKg age range upsection.

Lava Mountain samples also display a distinct upsection change in dominant age population from 200-100 Ma to 85-60 Ma grains (Fig. 16).

Although the eastern sections at Gray Ridge and Box Canyon contain substantial populations of 85-60 Ma and 200-100 Ma detrital grains, they are separated into a separate chronofacies due to the addition of another major age population consisting of Late Paleocene to Eocene (60-48 Ma) grains. A total of four samples and 382 grains were analyzed from Gray Ridge. Three Mesozoic-Cenozoic populations dominate the analyzed grains: 60-48 Ma (Late Paleocene-Eocene; 33.5%), 85-60 Ma (Latest Cretaceous-Early Paleocene; 54.2%), and 200-100 Ma (Jurassic-Early Cretaceous; 9.4%) (Fig. 17). Subordinate populations are 100-85 Ma (Early Late Cretaceous; 1.6%), 416-318 Ma (Devonian-Mississippian; 1.0%), and Precambrian (0.3%). Analyses of 323 grains from three samples collected at Box Canyon document mainly Mesozoic to Cenozoic ages (Fig. 18). Dominant populations are 60-48 Ma (Late Paleocene-Eocene; 34.1%), 85-60 Ma (Late Cretaceous-Early Paleocene; 41.8%), and 200-100 Ma (Jurassic-Early Cretaceous; 14.9%). Subordinate Mesozoic populations include 100-85 Ma (Early Late Cretaceous; 4.0%) and 251-200 Ma (Triassic; 0.3%). Paleozoic and Precambrian age populations are 416-418 Ma (Devonian-Mississippian; 3.4%), 488-542 Ma (Cambrian; 0.3%), and Precambrian (1.2%). There is an upsection increase in 60-48 Ma grains as well as an upsection younging of the 60-48 Ma age population peak in both Gray Ridge and Box Canyon samples (Fig. 17, 18). For example, at Gray Ridge the youngest major age peak evolves upsection from 69.5 to 60-59 to 58 Ma over a stratigraphic thickness of 844 meters (Fig. 17).

Figure 17. Age probability plots showing distribution of U-Pb age determinations for 382 detrital zircon grains from four sandstone samples collected from the Gray Ridge section of the Arkose Ridge Formation. Age determinations represent individual spot analyses from separate detrital zircon grains. U-Pb ages are plotted as a normalized relative-probability distribution (Ludwig, 2003). Relative heights of peaks correspond to statistical significance. Orange bar denotes 65-90 Ma age range of adjacent Cretaceous plutons (TKg on Fig. 3). Note upsection change from 60-75 Ma age populations consistent with TKg age range to <60 Ma age populations consistent with ages of the slab window volcanic center (Tv on Fig. 3).

59

Figure 18. Age probability plots showing distribution of U-Pb age determinations for 323 detrital zircon grains from three sandstone samples collected from the Box Canyon section of the Arkose Ridge Formation. Age determinations represent individual spot analyses from separate detrital zircon grains. U-Pb ages are plotted as a normalized relative-probability distribution (Ludwig, 2003). Relative heights of peaks correspond to statistical significance. Orange bar denotes 65-90 Ma age range of adjacent Cretaceous plutons (TKg on Fig. 3). Note dominance of <60 Ma age populations consistent with ages of the slab window volcanic center (Tv on Fig. 3).

DISCUSSION

Provenance Interpretation

Compositional and detrital zircon data from the Arkose Ridge Formation indicate sediment derived mainly from Jurassic-Eocene igneous source terranes exposed north of the sampled forearc strata. This interpretation is consistent with the lithofacies trend that shows a southward decrease in grain size, from boulder conglomerate and cross-stratified sandstones of the Arkose Ridge Formation to thick packages of mudstones and coals of the Chickaloon Formation (Winkler, 1992; Trop et al., 2003). This southward lithofacies trend is further supported by paleocurrent data that show a general south- to southwestward-directed paleoflow (Fig. 5). Modal data from sandstone and conglomerate display two distinct petrofacies and chronofacies, respectively. Together, these provenance data support deposition of the Arkose Ridge systems in at least two separate drainage networks that may have been separated by a significant drainage divide.

Separation of the Arkose Ridge Formation spatially into at least two distinct and separate coeval river systems is based on five major lines of evidence. First and foremost, the eastern sections contain abundant volcanic lithic grains and <60 Ma detrital zircons (34% of zircons), whereas the western sections contain sparse volcanic lithic grains and <60 Ma detrital zircons (0.8% of zircons are <60 Ma) (Fig. 9, 10, 19, and 20). Second, the western sections have the highest abundance of mica schist lithic grains, but sparse sedimentary lithic grains, whereas the eastern sections a have much lower amount of metamorphic grains together with a substantially higher abundance of sedimentary lithic grains (Fig. 12). Third, western sections have very minor amounts of potassium
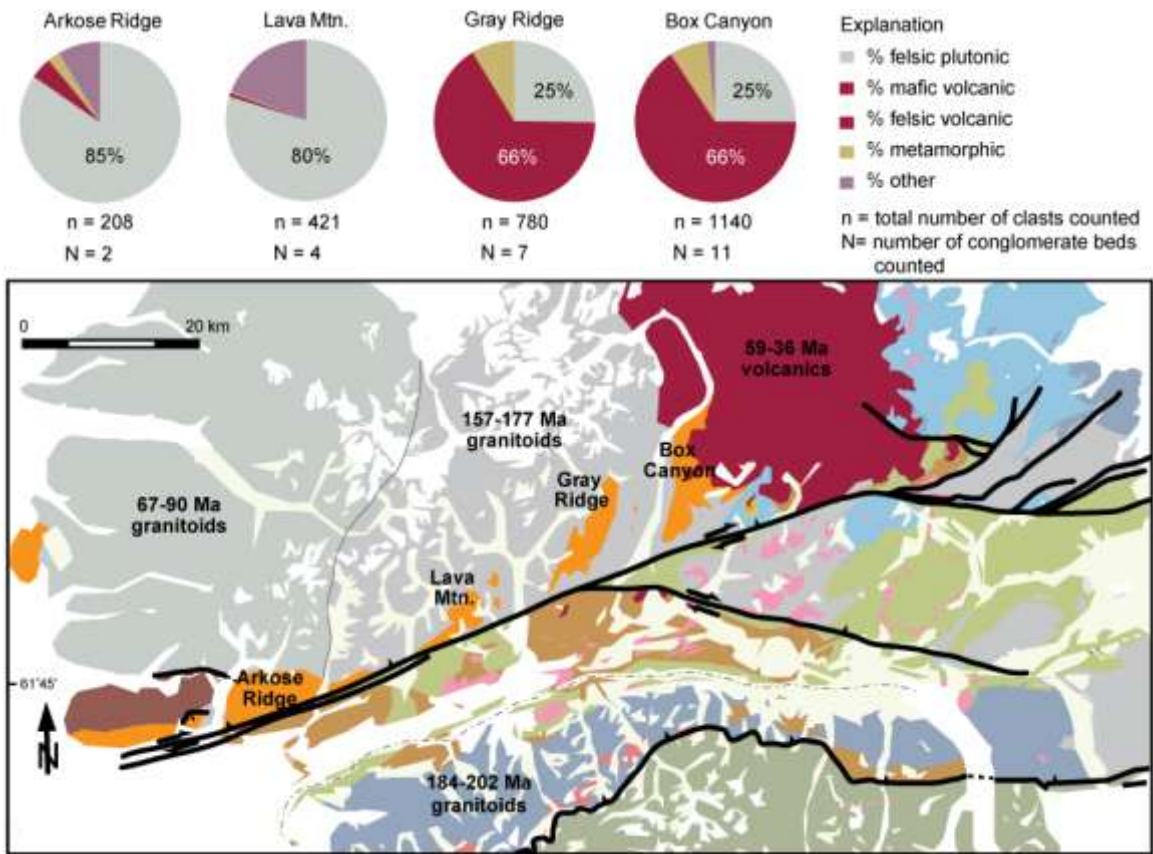
Figure 19. Pie diagrams summarizing conglomerate clast counts for each stratigraphic section (Arkose Ridge, Lava Mountain, Gray Ridge, and Box Canyon). See Fig. 3 for explanation of geologic map units. See Tables 2, 3, 4, and 5 for raw and summary clast count data. Note that western strata (Arkose Ridge and Lava Mountain) are dominated by felsic plutonic clasts, consistent with derivation from Mesozoic arc plutons exposed directly north of the sampled strata, whereas eastern strata (Gray Ridge and Box Canyon) are dominated by volcanic clasts, consistent with derivation from the Paleocene-Eocene volcanic field exposed east of the ARF outcrop belt. Detrital geochronologic ages support this interpretation (Fig. 20).
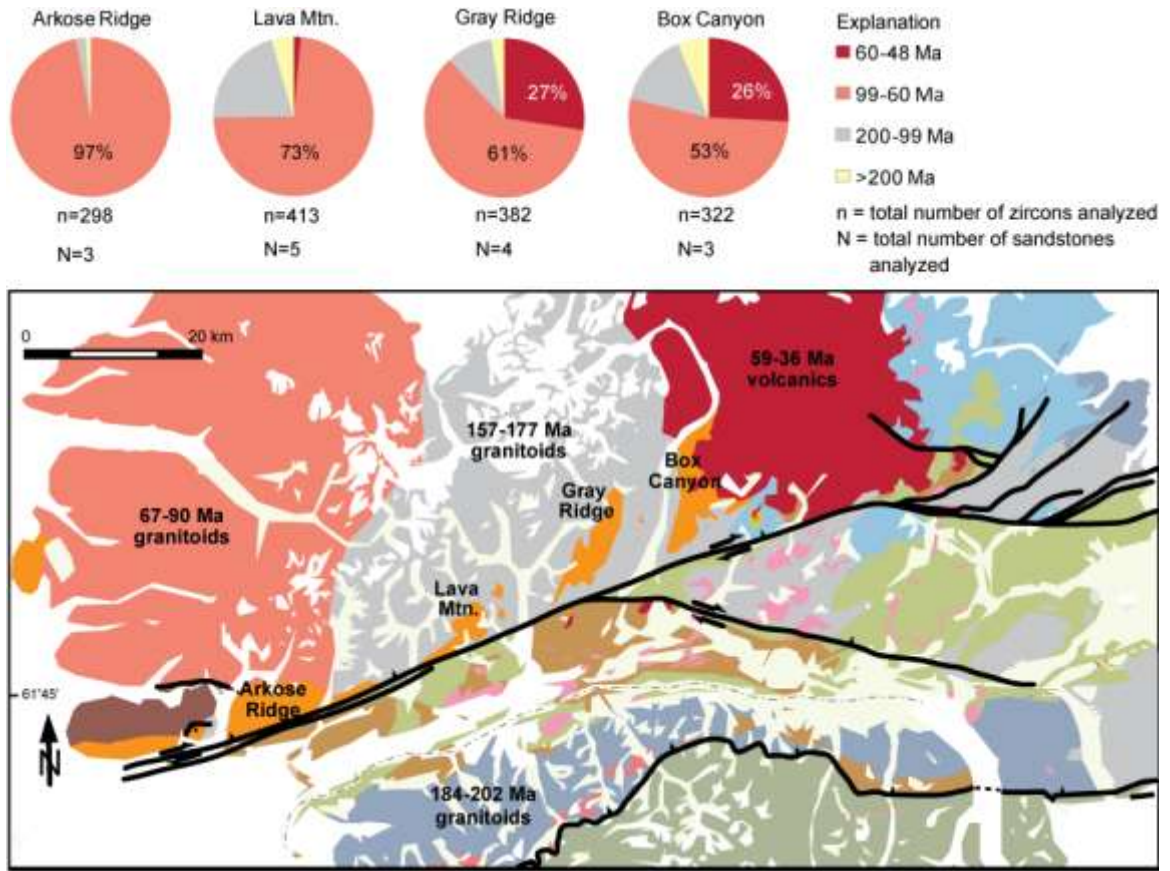
Figure 20. Pie diagrams summarizing detrital zircon analyses for each stratigraphic section (Arkose Ridge, Lava Mountain, Gray Ridge, and Box Canyon). See Fig. 3 for explanation of geologic map units. See Figs. 15, 16, 17, and 18 for relative probability plots. Note that western detrital zircon samples (Arkose Ridge and Lava Mountain) are dominated by 200-60 Ma grains, consistent with derivation from 177-67 Ma arc plutons exposed directly north of the sampled strata, whereas eastern detrital zircons samples (Gray Ridge and Box Canyon) are enriched in <60 Ma grains, consistent with derivation from the 59-35 Ma volcanic field exposed east of the sampled strata. Compositional data support this interpretation (Fig. 19).

feldspar compared to the eastern sections (Fig. 11). Fourth, western sections contain rare grains of Paleozoic to Precambrian detrital zircons (0.6%), whereas eastern sections contain much more (3.0%). Fifth, Triassic aged zircons are in higher relative abundance in the western sections (6 grains total) than in the eastern sections (1 grain total).

The combination of provenance data from the Arkose Ridge Formation allows for a detailed discussion of source terranes and the geometry of the drainage basin. The following sections will provide a detailed interpretation of these data. The plutonic petrofacies contained in the western half of the outcrop belt at Arkose Ridge and Lava Mountain is most similar to detritus derived from continental block-basement uplift belts (Fig. 9, 10). The abundance of plutonic clasts in conglomerate, in combination with sandstone enriched in quartz, feldspar, and plutonic rock fragments indicates derivation from mainly plutonic source terranes. This petrofacies is consistent with sediment derived from underlying Jurassic-Paleocene arc plutons exposed directly north of the Arkose Ridge and Lava Mountain sections; specifically, plutons from the late Cretaceous-Paleocene Alaska Range-Talkeetna Mountains belt (90-67 Ma; Bleick et al., 2009) and the Jurassic Talkeetna magmatic arc (177-153 Ma; Rioux et al., 2007) (Fig. 19). The dominant detrital zircon age populations (85-60 Ma and 200-100 Ma) from Arkose Ridge and Lava Mountain directly overlap with the ages of these two local source terranes. Moreover, the clast types identified in the conglomerate and sandstone from the western sections are closely similar to lithologies exposed in these igneous source terranes. A slight decrease in peak age of the detrital age populations upsection from 80 to 72 Ma supports unroofing of different Alaska Range-Talkeetna Mountains arc plutons through time (Fig. 15, 16). Alternatively, migration of drainage networks through time

produced the observed changes in detrital peaks, such as northward erosion as drainages expanded or stream capture.

The volcanic petrofacies contained in the eastern half of the outcrop belt at Gray Ridge and Box Canyon is most similar to detritus derived from dissected, transitional and undissected volcanic arcs (Fig. 9, 10). The abundance of volcanic clasts in conglomerate, and volcanic lithic grains and plagioclase feldspar in sandstone coupled with subordinate plutonic clasts in conglomerate and plutonic fragments in sandstone indicate derivation from mainly volcanic and plutonic source terranes. The abundance of volcanic detritus in this petrofacies is consistent with sediment derived from the Paleocene-Eocene Caribou Creek volcanic center that crops out to the east of the Arkose Ridge Formation (59-36 Ma; Cole et al., 2006) (Fig. 19). A major 60-48 Ma detrital zircon age population from Gray Ridge and Box Canyon is consistent with derivation from the volcanic center (Fig. 20). Moreover, the observed upsection increase in volcanic lithic grains and <60 Ma detrital zircons in eastern deposystems reflects the incorporation of higher proportions of juvenile volcanic detritus through time, consistent with adjacent construction of the slab-window volcanic center during deposition (Fig. 7). Subordinate plutonic detritus and substantial 85-60 Ma and 200-100 Ma zircon age populations are consistent with derivation of subordinate detritus from the Alaska Range-Talkeetna Mountains and Jurassic Talkeetna arc plutons (Fig. 19, 20). Given the prevalence of plutonic grains and Jurassic-Cretaceous detrital zircon ages in the Gray Ridge and Box Canyon sections, the proposed eastern fluvial network must have received detritus from arc plutons that cropped out along the drainage divide or further north.

Subordinate metamorphic and sedimentary fragments in both the gravel and sand indicate minor non-igneous source terranes provided sediment to the Arkose Ridge Formation (Fig. 12). The change in abundance of mica schist fragments from the plutonic petrofacies (~9% of the sands) to the volcanic petrofacies (~2% of sands) is consistent with the higher concentration of potential metamorphic sources exposed to the west. The low-grade metamorphic clasts common in western samples are lithologically comparable with bedrock exposed directly north and west of the sampled strata. At Hatcher Pass (Fig. 3), biotite schist with 75 Ma and older detrital zircons crops out <10 km west of Arkose Ridge strata at Arkose Ridge (Bradley et al., 2009). Largely unexplored metamorphic rocks reportedly also crop out among the Mesozoic plutons exposed between Arkose Ridge and Lava Mountain (Winkler, 1992). Metamorphic lithologies are also presented in more distant sources in the northern Talkeetna Mountains (Wilson et al., 1998), but unstable, fine-grained lithic grains would likely break down into monocrystalline grains during long distance (>100 km) transport.

The Late Cretaceous-Paleocene schist of Hatcher Pass is greenschist-facies schist with a bracketed depositional age between 61 Ma (age of peak metamorphism) and 77-75 Ma (maximum depositional age, Bradley et al., 2009). Harlan and others (2003) reported Paleogene metamorphic ages using the $^{40}Ar/^{39}Ar$ method (61 to 57 Ma). Detrital zircon ages yielded probability density curves with four Cretaceous peaks from 76 to 102 Ma (the youngest four zircons determine a maximum depositional age of 77-75 Ma), two Late Jurassic peaks at 155 and 166 Ma, three early Jurassic to Late Triassic peaks at 186, 197, and 213 Ma, minor Carboniferous peaks at 303 and 346 Ma, and a minor Paleoproterozoic peak at 1828 Ma (Bradley et al., 2009). Recycling of the Hatcher Pass

schist detrital zircons into the Arkose Ridge Formation is consistent with the observed detrital ages from Arkose Ridge and Lava Mountain. The largely unexplored metamorphic rocks that reportedly crop out among the Mesozoic plutons between Arkose Ridge and Lava Mountain reportedly comprise intermixed amphibolites, foliated quartz diorite and lesser trondhjemite. Although the metamorphic rocks are principally amphibolites, they include minor biotite-quartz-feldspar gneiss present locally. The amphibolites and associated metamorphic rocks are correlated to rocks exposed further north that have a K-Ar age of 176 Ma (Cjestey and others, 1978). The foliated quartz diorite probably represents a broad contact zone with Jurassic arc plutons (Winkler, 1992). Given its proximity to the western sections, the Hatcher Pass schist is most likely the primary source of metamorphic grains seen in thin section in western samples. Unfortunately, it is not possible to support this conclusion using detrital zircon ages due to the overlap of detrital zircon ages in the schist with the crystallization ages of zircons in the surrounding plutons. Therefore, through the ages alone we were unable to resolve individual detrital zircons in the Arkose Ridge strata of metamorphic origin from those of igneous origin. However, >99% of analyzed zircons yielded <10 U/Th values which is consistent with nearly all detrital zircons being of igneous origin. This suggests that the surrounding igneous rocks (plutons and volcanic centers) mainly supplied detrital zircons to the Arkose Ridge Formation and not local metamorphic rocks.

Siltstone, shale, and argillite fragments in Arkose Ridge Formation sandstones suggest erosion and recycling of Jurassic-Cretaceous sedimentary strata such as the Jurassic Tuxedni, Chinitna, and Naknek Formations (Winkler, 1992) and Cretaceous Matanuska Formation (Trop, 2003), as well as more distant strata, including the late

Jurassic-Cretaceous Kahiltna Assemblage and Caribou Pass Formation, exposed >50 km north of the basin. Sediment recycling is consistent with the presence of an angular unconformity between the Arkose Ridge Formation and underlying Jurassic-Cretaceous sedimentary strata in the Matanuska Valley/Talkeetna Mountains (Winkler, 1992). The sedimentary fragments are most common in the volcanic petrofacies (~6% of the sands) and less common in the plutonic petrofacies (~0% of the sands). This increase in abundance from west to east is notably opposite of the east to west increase in abundance of mica schist fragments. Rare chert and metachert grains likely indicate minor sediment derivation from the Proterozoic-Paleozoic Yukon-Tanana Terrane. Similarly, detrital age populations show that Paleozoic to Precambrian grains are more prevalent in the eastern petrofacies (~3.0%) than in the western facies (~0.6%). Paleozoic-Precambrian ages are interpreted to be recycled from the Kahiltna and Caribou Pass Formations and/or sourced directly from the Yukon-Tanana Terrane, exposed >100 km north of the sampled strata (Hampton et al., 2007).

The general paucity of lithologies commonly contained in the Chugach accretionary prism such as metachert, metabasalt, metasandstone, and argillite in the compositional data indicates that the medisedimentary and metavolcanic strata of the Chugach accretionary prism did not contribute abundant detritus to the Arkose Ridge Formation. Additionally, the Castle Mountain Fault that bounds the Arkose Ridge Formation to the south is an active dextral strike-slip fault that is thought to have been active since Mesozoic time. However, the displacement history of this fault is poorly constrained. Late Cretaceous-Tertiary piercing points record 20-40 km of offset, but do not constrain timing of displacement (Grantz, 1966; Clardy, 1974; Detterman et al., 1976;

Fuchs, 1980; Trop et al., 2003). Trop et al. (2005) infers ~130 km of dextral offset through correlation of the Bruin Bay and Little Oshetna fault systems that Pavlis and Roeske (2007) hypothesize to be strike slip displacement transferred over from the Border Ranges fault system. To help constrain the displacement history of the Castle Mountain fault, provenance data may be used to link any source terranes across the fault to the Arkose Ridge Formation. Any well-defined source terranes across the fault may then be able to provide a rough piercing point across the fault. However, the general compositional and detrital zircon data are unable to resolve any strike-slip motion on the Castle Mountain Fault post-deposition of the Arkose Ridge Formation. Since the fault bounds the formation to the south and all sediment is interpreted to be sourced from the hanging wall, no piercing points are available to estimate the amount of strike separation.

Depositional Model

In Late Cretaceous (Campanian-Maastrichtian) time, sedimentary strata were deposited in a forearc position between a coeval continental-margin arc to the north and a trench-accretionary prism to the south (Trop, 2008). In the southern Talkeetna Mountains and Matanuska Valley, submarine slope and ramp strata of the Matanuska Formation were deposited on a trenchward (southward) dipping basin floor (Trop, 2008). Sedimentation into the forearc basin was interrupted during Paleocene time when a mid-ocean spreading ridge subducted underneath southern Alaska (Bradley et al., 2003; Cole et al., 2006; Trop and Ridgway, 2007). Progressively thicker, more buoyant oceanic crust in front of the spreading ridge subducted shallowly causing subaerial uplift of the forearc and cessation of marine deposition in the basin. Additionally, the shallow

subduction angle caused the cessation of continental arc magmatism, prompted the erosion of the volcanic edifice, and exhumation of subvolcanic plutons (TKg on Fig. 3). Subsequent erosion and unconformity development occurred in the forearc basin, apparently until the slab-window passed underneath the forearc region. Slab-window magmatism associated with ridge subduction led to the construction of the Caribou Creek slab-window volcanic center from Paleocene to Eocene time (59-36 Ma) (Cole et al., 2006). Coeval to the formation of the volcanic center, the absence of subducting crust in the slab-window prompted rapid subsidence and resumption of sedimentation in the now subaerially exposed Matanuska forearc basin as fluvial-lacustrine systems of the Arkose Ridge and Chickaloon Formations (Trop et al., 2003; Kortyna et al., 2009; Kassab et al., 2009; Ridgway et al., in press). River systems flowed from the north and northeast regions of the Matanuska Basin based on paleocurrent data and lithofacies trends (Trop et al., 2003). Provenance data from this study supports deposition of the Arkose Ridge systems in at least two separate drainage networks that may have been separated by a significant drainage divide where the western river network primarily fed plutonic detritus from Mesozoic remnant arc plutons that cropped out to the northwest of the Matanuska basin and the eastern river network primarily fed volcanic detritus from the nascent Caribou Creek volcanic center that was being constructed northeast of the basin coeval with deposition (Fig. 21). Furthermore, the western river system transported minor schist fragments from local metamorphic sources exposed northwest of the sampled strata whereas the eastern river system transported recycled sedimentary fragments from Mesozoic sedimentary rocks exposed to the northeast. Additionally, the amount of volcanic detritus supplied to the eastern river systems increased through time

Figure 21. Paleogeographic reconstruction of the Matanuska basin during late Paleocene-Eocene time, based on integration of lithofacies, paleocurrent, compositional, and detrital geochronologic data. Black circles represent detrital geochronologic samples analyzed from the Arkose Ridge Formation. Note that the black circles are grouped into discrete localities, from left to right, Arkose Ridge, Lava Mountain, Gray Ridge, and Box Canyon. Note that western fluvial-lacustrine deposystems (Arkose Ridge and Lava Mountain) deposited plutonic and metamorphic detritus derived (eroded) from Mesozoic arc plutons and metamorphic rocks that cropped out to the northwest of the basin. Eastern fluvial-lacustrine deposystems (Gray Ridge and Box Canyon) primarily deposited juvenile volcanic detritus from a coeval slab window volcanic center located northeast of the basin (Caribou Creek volcanic field, CV). Abbreviations are as follows: Paleogene sedimentary basins: MB-Matanuska basin; CIB-Cook Inlet basin. Major Paleogene volcanic belts: CTV-Central Talkeetna Mountains volcanics; JV-Jack River volcanics; CB-Cantwell basin volcanics. Major faults: DF-Denali fault; CMF-Castle Mountain fault; BRF-Border Ranges fault. Intrusive igneous rocks: MI-Matanuska intrusives; PI-Prince William sound intrusives. #A-City of Anchorage. Adapted from Trop and Ridgway (2007).

Late Paleocene-Eocene

Orocline Hinge Area

Yukon Tanana terrane plutons with 110-85, 215-175 Ma and 380-330 Ma U-Pb zircon ages (Foster et al., 1994; Dusel-Bacon et al., 2004)

CB

Chisana arc plutons and volcanic rocks with 140-113 Ma K-Ar and Ar-Ar ages (Snyder and Hart, 2007)

DF

60-55 Ma (CB) and 63-50 Ma (JV) plutons and volcanics from remnant arc mantle wedge (Cole et al., 2007)

?

Caribou Pass Fm.? (Hampton et al., 2007)

JV

Wrangellia with 285-320 Ma arc plutons

Granitoids with 63-55 Ma Ar-Ar ages, volcanic rocks with 56-60 Ma Ar-Ar ages (Cole et al., 2007)

PzTr

Arc plutons with 178-152 Ma U-Pb zircon ages (Rioux et al., 2007)

CTV   Jpu

Arc plutons with 68-63 Ma U-Pb zircon ages (David and McPhillips, 2007)

PzTr

CV

59-35 Ma slab-window volcanic and intrusive rocks (CTV, CV, MI; Cole et al., 2006)

Jpu

Arc plutons with 90-67 Ma U-Pb zircon ages (Bleick et al., 2009)

Kg

MI

?

Detachment fault and schist with 75+ detrital zircon, 61 Ma peak metamorphism (Bradley et al., 2009; Harlan et al., 2003)

MB

CMF

Axial fluvial strata with Mesozoic-Cenozoic detrital zircons derived from north and south (Trop et al, 2009)

BRF

A

Arc magmatism until ca. 56 Ma.

57 Ma

CIB

Diachronous near-trench plutonism during northeastward oblique subduction of spreading ridge

58 Ma

Alluvial-fluvial-estuarine deposition in southwestward-tilted remnant forearc basin (CIB, MB)

PI

52 Ma

60 Ma

62 Ma

Resurrection Plate

Kula Plate

Ridge migration

as the slab-window volcanic center was constructed. The following sections will outline the depositional history for each stratigraphic section.

Arkose Ridge

The section at Arkose Ridge was deposited as part of the western drainage network (Fig. 21). This section of the river was adjacent to and infilled paleovalleys incised into the Latest Cretaceous-Early Paleocene plutonic belt from which it received the majority of its sediment based on high concentrations of plutonic clasts in conglomerate (85% of clasts), quartz, plagioclase feldspar, and plutonic fragments (Q:F:L = 23:67:10; Lv:(Ls+Lm):Pl = 12:47:41), and a main detrital age population (85-60 Ma; 88.6%) that matches the age of the Late Cretaceous-Early Paleocene arc plutons. Additionally, subordinate plutonic sediment that couldn't be compositionally resolved from the main Late-Cretaceous-Early Paleocene belt carried by tributary streams that drained from nearby Jurassic and Early Late Cretaceous plutons based on detrital ages (200-100 Ma; 2.4%; 100-85 Ma; 8.8%). Alternatively, these ages could reflect recycling of zircons from local metamorphic rocks (e.g. Hatcher Pass schist), but the U/Th-U/PB age data indicate that the detrital zircons are mainly of igneous origin (Fig. 14). The relative abundance of mica schist (Lm:Lv:Ls = 79:21:0; ~9% of total grains) is probably derived primarily from the local Hatcher Pass schist northwest of the basin, although the source terrane could also potentially be the poorly constrained Jurassic amphibolite unit to the north or no longer exposed at the surface. Upsection decreases in the age peaks of the detrital zircon age populations could represent the unroofing of the Late Cretaceous plutons or the migration of drainage networks through time such as northward erosion as the drainages expanded or stream capture.

Lava Mountain

The Lava Mountain section was deposited within the western river system near the middle of the basin (Fig. 21). It received a majority of its sediment from the Late Cretaceous-Early Paleocene Alaska Range-Talkeetna Mountains and Jurassic Talkeetna magmatic arcs based on high concentrations of plutonic clasts in conglomerate (85% of clasts), quartz, plagioclase feldspar, and plutonic fragments (Q:F:L = 23:67:10; Lv:(Ls+Lm):Pl = 12:47:41), and a main detrital age population (85-60 Ma; 88.6%) that matches the age of the Late Cretaceous-Early Paleocene arc. Relatively abundant mica schist grains (Lm:Lv:Ls = 94:0:6) were most likely derived from the Hatcher Pass schist that cropped out along the northwest margin of the basin. At the base of the section, the dominant age population is 200-100 Ma grains that match the Jurassic Talkeetna magmatic arc plutons. Additionally, plutonic clasts in the basal boulder conglomerate are the same lithology as the Jurassic arc plutons. This signature is completely overridden by a Late Cretaceous-Early Paleocene detrital age signature upsection. This relationship is consistent with the base of the section being deposited in paleovalleys incised into the underlying bedrock (in this case, Jurassic granitoids with which the Lava Mountain section shares a high-relief, unconformable contact) from which the main signature is the underlying bedrock.   As the basin matures, this local Jurassic bedrock source was overridden by sediment from nearby Cretaceous granitoids of the Alaska Range-Talkeetna Mountains arc.

Gray Ridge

The Gray Ridge section was deposited within the eastern river network near the middle of the basin (Fig. 21). It received sediment from the Eocene volcanic center that

was constructed by slab-window magmatism northeast of the basin based on abundant volcanic detritus and <60 Ma (33.5%) detrital grains that match the compositional and age signature of the volcanic field. Gray Ridge also continued to receive sediment eroded from granitoids related to the Late Cretaceous-Early Paleocene Alaska Range-Talkeetna Mountains arc and the Jurassic Talkeetna arc based on the presence of plutonic detritus in conglomerate and sandstone and detrital age populations (85-60 Ma and 200-100 Ma; 54.2% and 14.9%, respectively). The distinct change in petrofacies and chronofacies between Gray Ridge and Lava Mountain underlies the need for a drainage divide between the eastern and western river networks. Near the base of the Gray Ridge section, the dominant detrital signature is plutonic based on a high abundance of plutonic detritus and 85-60 Ma zircons, before quickly grading to volcanic detritus and <60 Ma age peaks upsection. This upsection increase in volcanic detritus and <60 Ma zircons is consistent with the construction and growth of the adjacent volcanic field during deposition of the Arkose Ridge Formation.

Box Canyon

The Box Canyon section was deposited within the eastern river network on the east side of the basin (Fig. 21). It received sediment from the Eocene volcanic center that was constructed by slab-window magmatism northeast of the basin based on abundant volcanic detritus and <60 Ma (34.1%) detrital grains that match the compositional and age signature of the volcanic field. Box Canyon continued to receive sediment eroded from granitoids related to the Late Cretaceous-Early Paleocene Alaska Range-Talkeetna Mountains arc and the Jurassic Talkeetna arc as well, based on the presence of plutonic detritus in conglomerate and sandstone and detrital age populations (85-60 Ma and 200-

100 Ma; 41.8% and 9.4%, respectively). Box Canyon, however, has a high abundance of volcanic detritus and <60 Ma grains throughout the section unlike Gray Ridge which had plutonic detritus and >60 Ma grains at the base, although the zircon age peaks do young upsection. This slight difference between the eastern sections is due to the proximity of Box Canyon to the nascent volcanic center.

Both Gray Ridge and Box Canyon were apparently isolated from metamorphic sources exposed north of the basin (e.g. Hatcher Pass schist), evidenced by the relatively minor metamorphic detritus whereas a relative abundance of sedimentary fragments and >245 Ma zircons show it received recycled material from Mesozoic sedimentary strata such as the local Tuxedni, Chititna, Naknek, and Matanuska Formations (Trop, 2008; Winkler, 1992), as well as the more distant Caribou Pass Formation, Kahiltna Assemblage, and Yukon-Tanana Terrane that the western sections did not.

General Implications for Forearc Basin Development

Previous forearc basin studies, such as studies from the Great Valley forearc basin, show that as a volcanic arc denudes, sandstone modal analyses record an increase in quartz and feldspar and a decrease in lithic grains (DeGraaff-Surpless et al., 2002; Dickinson, 1982; Dickinson, 1995; Ingersoll and Eastmond, 2007; Fig. 22A). This change occurs throughout the forearc as the volcanic edifice erodes and an increasingly larger amount of the underlying arc plutons are exposed. In Alaska, Upper Cretaceous marine forearc strata (uppermost Matanuska Formation) and the western strata of the Arkose Ridge Formation are consistent with this progression (Fig. 22B). The composition of the Upper Cretaceous Matanuska Formation is most similar to sandstone derived from dissected volcanic arcs (Trop, 2008). The abundance of volcanic lithic

Figure 22. (A) Mesozoic sandstone (purple circles) and modern fluvial sand (U-undissected volcanic arc setting, T-transitional volcanic arc setting, D-dissected volcanic arc setting, B- continental block-basement uplift setting) point-count data from studies in the ancient and modern Great Valley forearc basin plotted on a Q-F-L ternary diagram (Dickinson and Gehrels, 2000; Ingersoll and Eastmond, 2007). See Table 6 for grain parameters. Note that as a volcanic arc denudes, modal analyses in both modern sands and ancient sandstones record an increase in quartz and feldspar grains and a decrease in lithic grains (indicated by arrow). (B) Cretaceous marine sandstone (green squares; Trop, 2008) and Paleogene fluvial sandstone (blue circles and triangles and red diamonds; this study) detrital modes from the Matanuska-Talkeetna Mountains forearc basin plotted on a Q-F-L ternary diagram. Blue circles and triangles are point-count data from the western sandstones (Arkose Ridge and Lava Mountain). Red diamonds are point-count data from the eastern sandstones (Gray Ridge). Note that the progression from the Upper Cretaceous marine strata to the western sandstones of the Paleogene fluvial strata matches the general progression towards enrichment of quartz and feldspar at the expense lithic grains, similar to the Great Valley forearc basin (Fig. 22A), consistent with progressive denudation of the volcanic arc edifice and increased sediment sourcing from dissected subvolcanic arc plutons. Eastern sandstones record an opposite progression, due to proximity to a newly constructed volcanic center linked to slab window magmatism associated with ridge subduction. (C) Relative probability plots of detrital ages from representative western and eastern sandstone samples. Yellow bar denotes depositional age of the Arkose Ridge Formation. Note in the western sandstone, detrital age populations reflect erosion from remnant arc plutons and are older than the age of

deposition (yellow bar). In the eastern sandstone, however, juvenile volcanics from the constructing slab window volcanic center results in erosion of syndepositional volcanic, providing a detrital zircon peak that matches the depositional age (yellow bar).
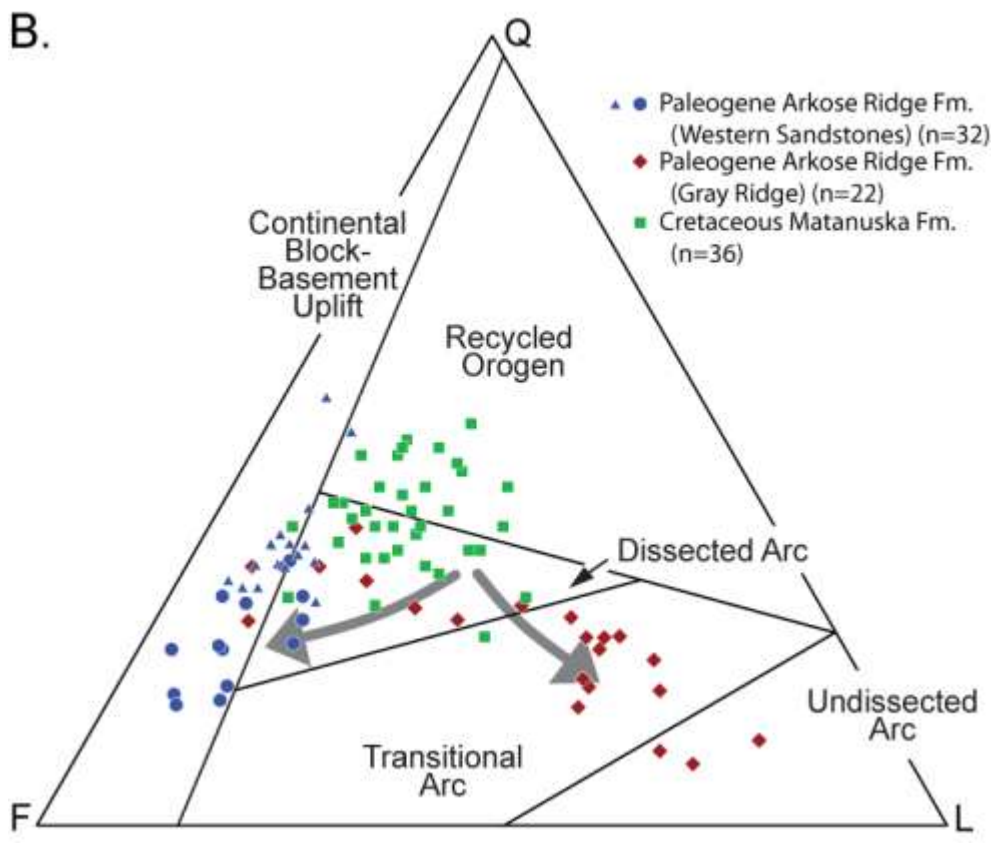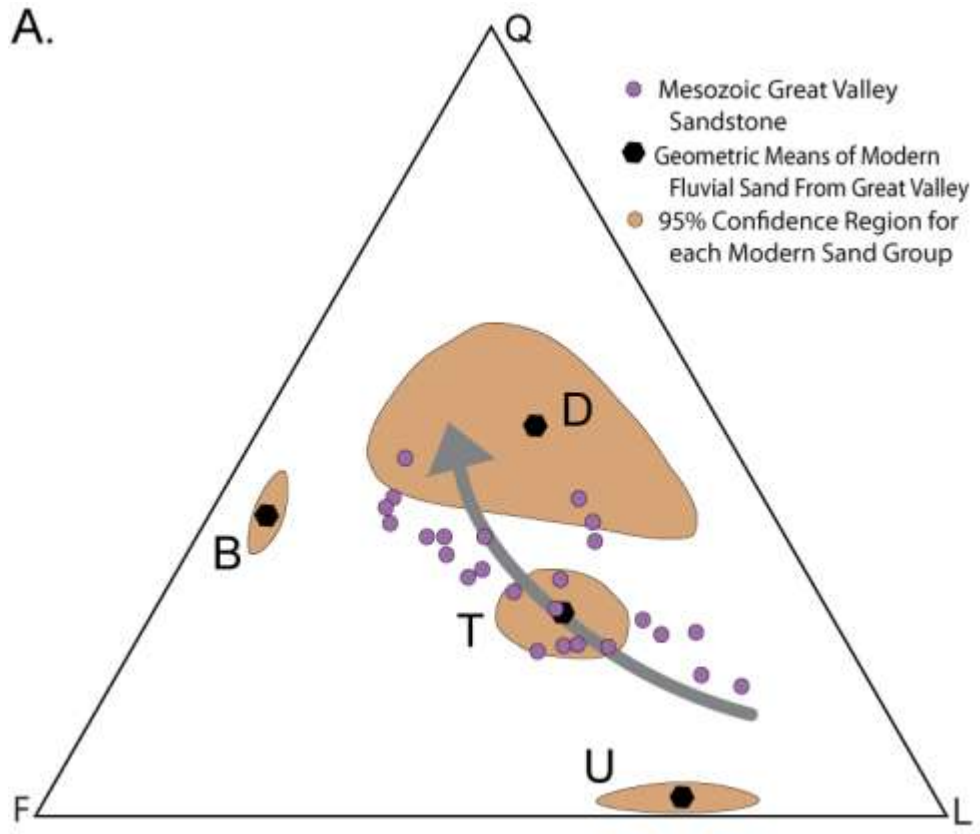
C.

Western samples draining dissected arc
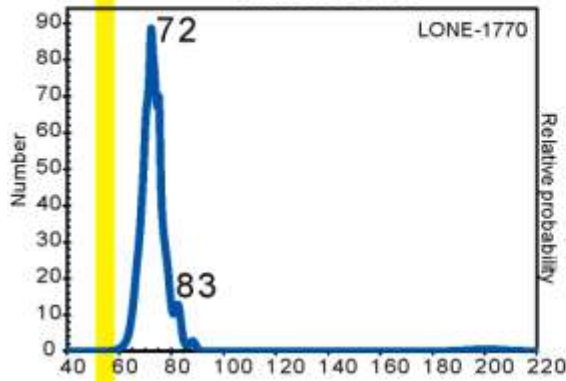
Eastern samples draining slab-window volcanic center

LONE-1770 — 72, 83

BOX-770 — 57

LONE-1360 — 72

BOX-615 — 59

LONE-1140 — 80

BOX-15 — 59

Detrital zircon age (Ma)

80
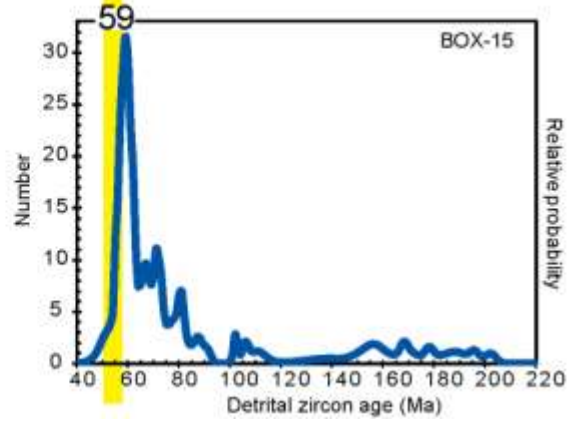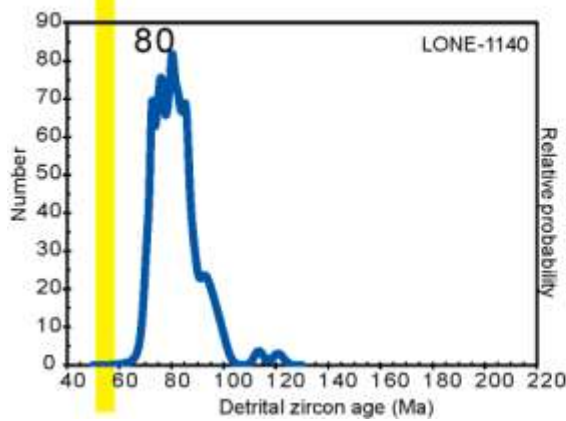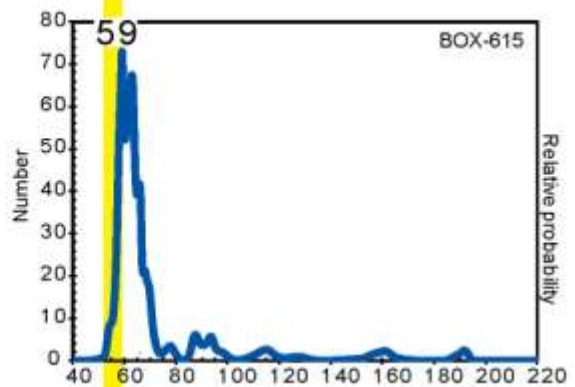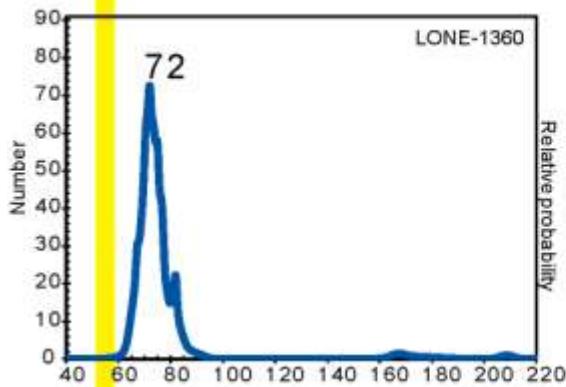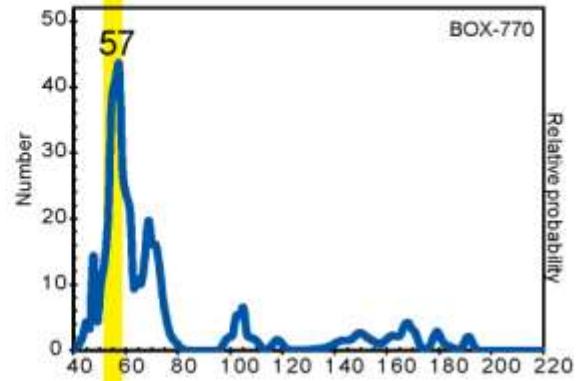
grains, plutonic rock fragments, and plagioclase feldspar indicate derivation from both volcanic and plutonic source terranes that is concordant with denuding the late Cretaceous Alaska Range-Talkeetna Mountains magmatic belt (Trop, 2008). The composition of the western strata of the Paleocene-Eocene Arkose Ridge Formation is most similar to sandstone derived from continental block-basement uplift setting (this study). The abundance of plutonic rock fragments and plagioclase feldspar indicate derivation from plutonic source terranes, and is compatible with the further denudation of the late Cretaceous Alaska Range-Talkeetna Mountains magmatic belt. Additionally, the paucity of volcanic lithic grains is consistent with the complete erosion of the volcanic edifice. This relationship is consistent with the progression towards quartz and feldspar traditionally seen in forearc basins as the volcanic arc denudes. The eastern strata of the Arkose Ridge Formation, however, record an opposite progression, with increasing volcanic lithic grains through time at the expense of quartz and feldspar (Fig. 22B). This is due to its depositional proximity to a slab-window volcanic center.

Furthermore, as the volcanic arc denudes through time, the detrital U-Pb zircon age populations of a sedimentary formation in a typical forearc setting become significantly older than the age of deposition (Fig. 22C). The western strata of the Arkose Ridge Formation are consistent with this progression with major age populations of Latest Cretaceous-Early Paleocene (85-60 Ma) and Jurassic-Early Cretaceous (200-100 Ma), but a depositional age of Early Paleocene-Eocene. The eastern strata of the Arkose Ridge Formation, however, contain a third major age population (Late Paleocene-Eocene; 60-48 Ma) that significantly overlaps with the depositional age of the Arkose Ridge Formation due to local juvenile volcanics supplied by a slab-window volcanic

center. Conventional provenance models predict reduced input of volcanic detritus to forearc basins during exhumation of the volcanic edifice and exposure of subvolcanic plutons (Dickinson, 1995). However, Arkose Ridge Formation data show that forearc basins modified by ridge subduction may record upsection localized increases in non-arc, syndepositional volcanic detritus due to contemporaneous construction of slab-window volcanic centers (Kortyna et al., 2010).

CONCLUSIONS

New compositional and detrital geochronologic data from the Arkose Ridge Formation documents the Paleocene-Eocene erosional history of bedrock source terranes, and depositional and tectonic framework of the Matanuska Valley-Talkeetna Mountains forearc basin. Conglomerate and sandstone compositional data document detritus dominated by plutonic clasts, plagioclase feldspar, and monocrystalline quartz in western sections, and volcanic clasts, plagioclase feldspar and subordinate plutonic clasts in the eastern sections. Detrital zircon geochronologic data show three main age populations of 200-100 Ma, 85-60 Ma, and 60-48 Ma, and may be split into two chronofacies. Western sections are dominated by a Jurassic-early Paleocene chronofacies and sparse 60-48 Ma grains, whereas eastern sections are dominated by a Late Paleocene-Eocene chronofacies that has a major 60-48 Ma population. Overall, the detrital zircon and compositional data are consistent with the paleocurrent data and lithofacies trends that show a southward decrease in grain size in the Arkose Ridge Formation and Chickaloon Formations. This is concordant with sediment derivation from northern source terranes. A western, plutonic petrofacies is most similar to a continental block-basement uplift setting that,

along with the Jurassic-early Paleocene chronofacies, is consistent with the erosion of Mesozoic arc plutons that presently crop out to the northwest of the Matanuska basin and directly underlie the sampled sections. An eastern, volcanic petrofacies is most similar to a dissected-undissected volcanic arc setting that, along with a Late Paleocene-Eocene chronofacies, is concordant with the erosion of the Paleocene-Eocene Caribou Creek volcanic center that presently crops out along the eastern margin of the basin. The paucity of metasedimentary detritus suggests the Chugach accretionary prism did not supply significant sediment to the Arkose Ridge Formation. The eastern strata received higher proportions of juvenile volcanic detritus through time despite not being in an active arc setting, consistent with construction of the adjacent slab-window volcanic center, likely due to subduction of an oceanic spreading ridge and associated slab-window magmatism. Conventional provenance models predict a decrease in volcanic detritus to forearc basins due to the denudation of the volcanic edifice. These data show that in a forearc basin modified by spreading ridge subduction, non-arc volcanic detritus related to slab-window magmatism provides an important component of forearc basin fills.

REFERENCES

Adams, D.D., Burns, L.E., Pessel, G.H., Little, T.A., Newberry, R.J., and Flynn, L.R.,
1985, Preliminary geologic map of the central Talkeetna Mountains, Alaska:
Alaska Division of Geological and Geophysical Surveys, Public Data File 85-20,
scale 1:25,000, 2 sheets.

Amato, J.M., and Pavlis, T.L., 2010, Detrital zircon ages from the Chugach terrane,
southern Alaska, reveal multiple episodes of accretion and erosion in a subduction
complex: *Geology* v. 38, p. 459-462, doi: 10.1130/G30719.1.

Bleick, H.A., Till, A.B., Bradley, D.C., O'Sullivan, P.B., Trop, J.M., Wooden, J.L.,
Bradley, D.B., Taylor, T.A., Friedman, S.B., and Hults, C.P., 2009, Early Tertiary
exhumation of the flank of a forearc basin, southwest Talkeetna Mountains,
Alaska: *Geological Society of America, Abstracts with Programs*, v. 41, no. 7, p.
303.

Bradley, D., Haeussler, P., O'Sullivan, P., Friedman, R., Till, A., Bradley, D., and Trop,
J., 2009, Detrital zircon geochronology of Cretaceous and Paleogene strata across
the south-central Alaskan convergent margin, *in* Haeussler, P.J., and Galloway,
J.P., eds., Studies by the U.S. Geological Survey in Alaska, 2007: *U.S. Geological
Survey Professional Paper* 1760-F, 36 p.

Bradley, D.C., Kusky, T.M., Haeussler, P.J., Goldfarb, R.J., Miller, M.L., Dumoulin,
J.A., Nelson, S.W., and Karl, S.M., 2003, Geologic signature of early Tertiary
ridge subduction in Alaska, *in* Sisson, V.B., Roeske, S.M., and Pavlis, T.L., eds.,
Geology of a transpressional orogen developed during ridge-trench interaction

along the north Pacific margin: *Geological Society of America Special Paper* 371, pp. 19-49.

Clardy, B.I., 1974, Origin of the Lower and Middle Tertiary Wishbone and Tsadaka formations, Matanuska Valley, Alaska [M.S. thesis]: Fairbanks, Alaska, University of Alaska, 50 p.

Cole, R.B., and Layer, P.W., 2002, Stratigraphy, age, and geochemistry of Tertiary volcanic rocks and associated synorogenic deposits, Mount McKinley quadrangle, Alaska, *in* Wilson, F.H., and Galloway, J.P., eds., Studies by the U.S. Geological Survey in Alaska, 2000: *U.S. Geological Survey Professional Paper* 1662, p. 19-43.

Cole, R.B., Layer, P.W., Hooks, B., Cyr, A.J. and Turner, J., 2007, Magmatism and deformation in a terrane suture zone south of the Denali Fault, northern Talkeetna Mountains, Alaska, *in* Ridgway, K.D., Trop, J.M., Glen, J.M.G., O'Neill, J.M., eds., Tectonic Growth of a Collisional Continental Margin: Crustal Evolution of Southern Alaska: *Geological Society of America Special Paper* 431, pp. 477-506.

Cole, R.B., Nelson, S.W., Layer, P.W., and Oswald, P.J., 2006, Eocene volcanism above a depleted mantle slab window in southern Alaska: *Geologic Society of America Bulletin,* v. 118, p. 140-158.

Coney, P.J., Jones, D.L., and Monger, J.W.H., 1980, Cordilleran suspect terranes: *Nature*, v. 288, p. 329–333, doi: 10.1038/288329a0.

Csejtey, Bela, Jr., Nelson, W.H., Jones, D.L., Silberling, N.J., Dean, R.M., Morris, M.S., Lanphere, M.A., Smith, J.G., and Silberman, M.L., 1978, Reconnaissance geologic map and geochronology, Talkeetna Mountains Quadrangle, northern part

of Anchorage Quadrangle, and southwest corner of Healy Quadrangle, Alaska: *U.S. Geological Survey* Open- File Report 78-558-A, 60 p., 1 sheet, scale 1:250,000.

Davidson, C., and McPhillips, D., 2007, Along Strike variations in metamorphism and deformation of the strata of the Kahiltna basin, south central Alaska, *in* Ridgway, K.D., Trop, J.M., Glen, J.M.G., O'Neill, J.M., eds., Tectonic Growth of a Collisional Continental Margin: Crustal Evolution of Southern Alaska: *Geological Society of America Special Paper* 431, pp. 437-465.

DeGraaff-Surpless, K., Graham, S.A., Wooden, J.L., and McWilliams, M.O., 2002, Detrital zircon provenance analysis of the Great Valley Group, California: Evolution of an arc-forearc system: *Geological Society of America Bulletin*, v. 114, p. 1564–1580.

Detterman, R.L., Plafker, G., Russell, G.T., and Hudson, T., 1976, Features along part of the Talkeetna segment of the Castle Mountain–Caribou fault system, Alaska: *U.S. Geological Survey Miscellaneous Field Studies Map MF-738*, scale 1:63,360.

Dickinson, W.R., 1970, Interpreting detrital modes of greywacke and arkose: *Journal of Sedimentary Petrology*, v. 40, p. 695-707.

Dickinson, W.R., 1982, Compositions of sandstones in circum-Pacific subduction complexes and forearc basins: *American Association of Petroleum Geologists Bulletin*, v. 66, p. 121-137.

Dickinson, W.R., 1985, Interpreting provenance relations from detrital modes of sandstones: *in* Zuffa, G.G., eds., Provenance of Arenites: *North Atlantic Treaty*

Organization, Advanced Study Institute Series 148, Dordrecht, The Netherlands, D. Reidel, pp. 333-361.

Dickinson, W.R., 1995, Forearc basins: *in* Busby, C.J. and Ingersoll, R.V., eds., *Tectonics of sedimentary basins,* Blackwell Science, Cambridge, pp. 221-261.

Dickinson, W.R., Bear, L.S., Brakenridge, G.R., Erjavec, J.L., Ferguson, R.C., Inman, K.F., Knepp, R.A, Lindberg, F.A., and Ryberg, P.T., 1983, Provenance of North American Phanerozoic sandstones in relation to tectonic setting: *Geological Society of America Bulletin*, v. 94. p. 222-235.

Dusel-Bacon, C., Wooden, J.L., and Hopkins, M.J., 2004, U-Pb zircon and geochemical evidence for bimodal mid-Paleozoic magmatism and syngenetic base-metal mineralization in the Yukon-Tanana terrane, Alaska: *Geological Society of America Bulletin*, v. 116, p. 989-1015.

Eberhart-Phillips, D., Christensen, D., Brocher, T.M., Hansen, R., Ruppert, N.A., Haeussler, P.J., and Abers, G.A., 2006, Imaging the transition from Aleutian subduction to Yakutat collision in central Alaska, with local earthquakes and active source data: *Journal of Geophysical Research*, v. 111, B11303, doi: 10.1029/2005JB004240.

Flores, R.M., and Stricker, G.D., 1993, Early Cenozoic depositional systems, Wishbone Hill District, Matanuska coal field, Alaska: *U.S. Geological Survey Bulletin*, v. 1992, p. 101-117.

Foster, H.L., Keith, T.E.C., and Menzie, W.D., 1994, Geology of the Yukon-Tanana area of east central Alaska, *in* Plafker, G.H., and Berg, H.C., eds., The geology of

Alaska: *Boulder, Colorado, Geological Society of America, Geology of North America,* v. G-1, pp. 205-240.

Fuchs, W.A., 1980, Tertiary tectonic history of the Castle Mountain Fault System in the Talkeetna Mountains [Ph.D. dissertation]: Salt Lake City, Utah, University of Utah, 152 p.

Fuis, G.S., Moore, T.E., Plafker, G., Brocher, T.M., Fisher, M.A., Mooney, W.D., Nokleberg, W.J., Page, R.A., Beaudoin, B.C., Christensen, N.I., Levander, A.R., Lutter, W.J., Saltus, R.W., and Ruppert, N.A., 2008, Trans-Alaska Crustal Transect and continental evolution involving subduction underplating and synchronous foreland thrusting: *Geology*, v. 36, p. 267–270, doi: 10.1130/G24257A.1.

Gehrels, G.E., and Saleeby, J.B., 1987, Geologic framework, tectonic evolution, and displacement history of the Alexander terrane: *Tectonics*, v. 6, p. 151-171, doi: 10.1029/TC006i002p00151.

Gehrels, G., Valencia, V., and Pullen, A., 2006, Detrital zircon geochronology by Laser-Ablation Multicollector ICPMS at the Arizona LaserChron Center, *in* T. Loszewski and W. Huff, eds., *Geochronology: Emerging Opportunities Paper 12*, Paleontological Society, Washington, D.C., pp. 67–76.

Gehrels, G.E., Valencia, V.A., and Ruiz, J., 2008, Enhanced precision, accuracy, efficiency, and spatial resolution of U-Pb ages by laser ablation–multicollector–inductively coupled plasma–mass spectrometry: *Geochemistry, Geophysics, Geosystems*, 9, Q03017, doi:10.1029/2007GC001805.

Grantz, A., 1966, Strike-slip faults in Alaska, *U.S. Geological Survey Open-File Report* 267, 82 p.

Hampton, B.A., Ridgway, K.D., O'Neill, J.M., Gehrels, G.E., Schmidt, J., and Blodgett, R.B., 2007, Pre-, syn-, and postcollisional stratigraphic framework and provenance of Upper Triassic-Upper Cretaceous strata in the northwestern Talketna Mountains, Alaska, *in* Ridgway, K.D., Trop, J.M., Glen, J.M.G., and O'Neill, J.M., eds., Tectonic growth of a collisional continental margin, crustal evolution of southern Alaska: *Geological Society of America Special Paper* 431, pp. 401-438.

Hansen, V.L., and Dusel-Bacon, C., 1998, Structural and kinematic evolution of the Yukon-Tanana upland tectonites, east-central Alaska: A record of Late Paleozoic to Mesozoic crustal assembly: *Geological Society of America Bulletin*, v. 110, p. 211-230, doi: 10.1130/0016-7606(1998)110<0211: SAKEOT>2.3.CO;2.

Haq, B.U., Hardenbol, J., and Vail, P.R., 1988, Mesozoic and Cenozoic chronostratigraphy and cycles of sea-level change, *in* Wilgus, C.K., Hastings, B.S., Kendall, C.G.S.C., Posamentier, H.W., Ross, C.A., and Van Wagoner, J.C., eds., Sea-level changes: An integrated approach: *Society of Economic Paleontologists and Mineralogists Special Publication* 42, p. 78-108.

Harlan, S.S., Snee, L.W., Vielreicher, R.M., Goldfarb, R.G., Mortensen, J.K., and Bradley, D.C., 2003, Age and cooling history of gold deposits and host rocks in the Willow Creek mining district, Talkeetna Mountains, south-central Alaska: *Geological Society of America Abstracts with Programs*, v. 35, no. 6, p. 235.

Ingersoll, R.V., Bullard, T.F., Ford, R.L., Grimm, J.P., Pickle J.D., and Sares, S.W., 1984, The effect of grain size on detrital modes: A test of the Gazzi-Dickinson point-counting method: *Journal of Sedimentary Petrology*, v. 54, p. 103-116.

Ingersoll, R.V., and Eastmond, D.J., 2007, Composition of modern sand from the Sierra Nevada, California, U.S.A.: Implications for actualistic petrofacies of continental-margin magmatic arcs: *Journal of Sedimentary Research*, v. 77, p. 784–796, doi: 10.2110/jsr.2007.071.

Johnston, S., Gehrels, G., Valencia, V., and Ruiz, J., 2009, Small-volume U-Pb zircon geochronology by laser ablation-multicollector-ICP-MS: *Chemical Geology*, v. 259, p. 218-229.

Jones, D.L., Silberling, N.J., and Hillhouse, J., 1977, Wrangellia: A displaced terrane in northwestern North America: *Canadian Journal of Earth Sciences* v. 14, p. 1565-2577, doi: 10.1139/e77222.

Kassab, C.M., Kortyna, C.D., Ridgway, K.D., and Trop, J.M., 2009, Sedimentology, structural framework, and basin analysis of the eastern Arkose Ridge Formation, Talkeetna Mountains, Alaska: *Geological Society of America, Abstracts with Programs*, v. 41, no. 7, p. 304.

Kortyna, C.D., Trop, J.M., Idleman, B., Kassab, C.M., Ridgway, K.D., and Gehrels, G., 2010, Provenance signature of a forearc basin modified by spreading ridge subduction: detrital zircon geochronology and detrital modes from the Paleogene Arkose Ridge Formation, southern Alaska: *Geological Society of America, Abstracts with Programs*, v. 42, no. 5, p. 54.

Kortyna, C.D., Trop, J.M., Lecomte, A.A., Bauer, E., Kassab, C.M., Sunderlin, D., and Ridgway, K.D., 2009, Sedimentology, paleontology, and structural framework of the central Arkose Ridge Formation, Talkeetna Mountains, Alaska: *Geological Society of America, Abstracts with Programs*, v. 41, no. 7, p. 304.

Lecomte, A.A., Sunderlin, D., Kassab, C.M., Kortyna, C.D., Trop, J.M., 2010, Floral Remains in the Paleogene Arkose Ridge Formation, South-Central Alaska: Climatic and Paleoenvironmental Implications: *Geological Society of America Abstracts with Programs,* v. 42, No. 1, p. 162.

Leonard, L.J., Hyndman, R.D., Mazzotti, S., Nykolaishen, L., Schmidt, M., and Hippchen, S., 2007, Current deformation in the northern Canadian Cordillera inferred from GPS measurements: *Journal of Geophysical Research*, v. 112, B11401, doi: 10.1029/2007JB005061.

Little, T.A., 1988, Tertiary tectonics of the Border Ranges fault system, north-central Chugach Mountains, Alaska: Sedimentation, deformation, and uplift along the inboard edge of a subduction complex [Ph.D. thesis]: Stanford, California, Stanford University, 343 p.

Little, T.A., 1990, Kinematics of wrench and divergent-wrench deformation along central part of the Border Ranges fault system, northern Chugach Mountains, Alaska: *Tectonics*, v. 9, p. 585–611.

Little, T.A., and Naeser, C.W., 1989, Tertiary tectonics of the Border Ranges fault system, southern Alaska, USA: *Journal of Geophysical Research*, v. 94, no. B4, p. 4333-4359.

Ludwig, K.R., 2003, Isoplot 3.00, a geochronological toolkit for Microsoft Excel: Berkeley Geochronology Center, *Special Publication* No. 4a, Berkeley, California.

Madsen, J.K., Thorkelson, D.J., Friedman, R.M., and Marshall, D.D., 2006, Cenozoic to Recent plate configurations in the Pacific Basin: ridge subduction and slab window magmatism in western North America: *Geosphere*, v. 1, p. 11-34.

Mortel, C., Pichavant, M., Bourdier, J.L., Traineau, H., Holtz, F., and Scaillet, B., 1998, Magma storage conditions and control of eruption regime in silicic volcanoes: Experimental evidence from Mount Pelee: *Earth and Planetary Science Letters*, v. 156, p. 89-99, doi: 10.1016/S0012-821X(98)00003-X.

Mortensen, J.K., 1992, Pre-mid-Mesozoic tectonic evolution of the Yukon-Tanana terrane: *Tectonics*, v. 11, p. 836-853.

Panuska, B.C., Stone, D.B., and Turner, D.L., 1990, Paleomagnetism of Eocene volcanic rocks, Talkeetna Mountains, Alaska: *Journal of Geophysical Research*, v. 95, p. 6737-6750.

Pavlis, T.L., Monteverde, D.H., Bowman, J.R., Rubenstone, J.L., and Reason, M.D., 1988, Early Cretaceous near-trench plutonism in southern Alaska: A tonalite-trodhjemite intrusive complex injected during ductile thrusting along the Border Ranges fault system: *Tectonics*, v. 7, p. 1179–1199.

Pavlis, T.L., and Roeske, S.M., 2007, The Border Ranges fault system, southern Alaska, *in* Ridgway, K.D., Trop, J.M., Glen, J.M.G., and O'Neill, J.M., eds., Tectonic Growth of a Collisional Continental Margin: Crustal Evolution of Southern Alaska: *Geological Society of America Special Paper* 431, pp. 55-94.

Plafker, G., and Berg, H.C., 1994, Overview of the geology and tectonic evolution of Alaska, *in* Plafker, G., and Berg, H.G., eds., The Geology of Alaska: Boulder, Colorado, *Geological Society of America*, Geology of North America, v. G-1, pp. 989–1021.

Plafker, G., Hudson, T., and Richter, D.H., 1977, Preliminary observations of late Cenozoic displacements along the Totschunda and Denali fault systems: *U.S. Geological Survey Circular* 733, p. 67-69.

Plafker, G., Moore, J.C., and Winkler, G.R., 1994, Geology of the southern Alaska margin, *in* Plafker, G., and Berg, H.G., eds., The Geology of Alaska: Boulder, Colorado, Geological Society of America, Geology of North America, v. G-1, p. 389-450.

Ridgway, K.D., Trop, J.M., and Finzel, E.S., Modification of continental forearc basins by spreading ridge subduction and flat-slab subduction processes: a case study from southern Alaska: submitted to *Recent Advances in Tectonics of Sedimentary Basins*, book volume edited by C. Busby and A. Azor, in press.

Rioux, M., Hacker, B., Mattinson, J., Kelemen, P., Blusztajn, J., and Gehrels, G., 2007, Magmatic development of an intra-oceanic arc; high-precision U-Pb zircon and whole-rock isotopic analyses from the accreted Talkeetna arc, south-central Alaska: *Geological Society of America Bulletin,* v. 119, p. 1168–1184. doi: 10.1130/B25964.1.

Rubatto, D., 2002, Zircon trace element geochemistry: partitioning with garnet and the link between U-Pb ages and metamorphism: *Chemical Geology*, v. 184, p. 123-138.

Scaillet, B., and Evans, B.W., 1999, The 15 June 1991 eruption of Mount Pinatubo: I. Phase equilibria and pre-eruption P-T-fO$_2$-fH$_2$O conditions of the dacite magmas: *Journal of Petrology*, v. 40, p. 381-411, doi: 10/1093/petrology/40.3.381.

Scaillet, B., Whittington, A., Martel, C., Pichavant, M., and Holtz, F., 2001, Phase equilibrium constraints on the viscosity of silicic magmas: II. Implications for mafic-silicic mixing processes, *in* Barbarian, B., Stephens, W.E., Bonin, B., Bouchez, J., Clarke, D.B., Cuney, M., and Martin, H., eds., The origin of granites and related rocks: *Geological Society of America Special Paper* 350, p. 61-72, doi: 10.1130/0-8137-2350-7.61.

Silberman, M.L., and Grantz, A., 1984, Paleogene volcanic rocks of the Matanuska Valley area and the displacement history of the Castle Mountain fault, *in* Coonrad, W.L., and Elliot, R.L., eds., The U.S. Geological Survey in Alaska: Accomplishments during 1981: *U.S. Geological Survey Circular* 868, p. 82–86.

Snyder, D., and Hart, W., 2007, The White Mountains Granitoid Suite: Isotopic constraints on source reservoirs for Cretaceous magmatism within the Wrangellia terrane, *in* Ridgway, K.D., Trop, J.M., Glen, J.M.G., and O'Neill, J.M., eds., Tectonic Growth of a Collisional Continental Margin: Crustal Evolution of Southern Alaska: *Geological Society of America Special Paper* 431, pp. 379−399, doi:10.1130/2007.243(15).

Sunderlin, D., White, J.G., Lecomte, A.A., and Trop, J.M., 2011, Paleobotany and paleoecology of the Early Paleogene Arkose Ridge Formation, Talkeetna Mountains, Alaska: *Geological Society of America, Abstracts with Programs,* v. 43, p. 164.

Triplehorn, D.M., Turner, D.L., and Naeser, C.W., 1984, Radiometric age of the Chickaloon Formation of south-central Alaska: Location of the Paleocene-Eocene boundary: *Geological Society of America Bulletin*, v. 95, p. 740–742.

Trop, J. M., 2008, Latest Cretaceous forearc basin development along an accretionary convergent margin: south-central Alaska: *Geologic Society of America Bulletin*, v. 120, p. 207-224.

Trop, J.M., and Plawman, T., 2006, Bedrock geology of the Glenn Highway from Anchorage to Sheep Mountain, Alaska – Mesozoic-Cenozoic forearc basin development along an accretionary convergent margin: *Geological Society of America Field Trip Guidebook* – Cordillera Section, 45 p.

Trop, J.M., and Ridgway, K.D., 2000, Sedimentology, stratigraphy, and tectonic importance of the Paleocene-Eocene Arkose Ridge Formation, Cook Inlet-Matanuska Valley forearc basin, Alaska, *in* Pinney, D.S. and Davis, P.K., eds., Short notes on Alaskan Geology 1999, *Fairbanks, Alaska, Division of Geological and Geophysical Surveys Professional Report* 119, p. 129-144.

Trop, J.M., and Ridgway, K.D., 2007, Mesozoic and Cenozoic tectonic growth of southern Alaska: a sedimentary basin perspective, *in* Ridgway, K.D., Trop, J.M., Glen, J.M.G., and O'Neill, J.M., eds., Tectonic Growth of a Collisional Continental Margin: Crustal Evolution of Southern Alaska: *Geological Society of America Special Paper* 431, pp. 55-94.

Trop, J.M., Ridgway, K.D., and Spell, T.L., 2003, Sedimentary record of transpressional tectonics and ridge subduction in the Tertiary Matanuska Valley-Talkeetna Mountains forearc basin, southern Alaska, *in* Sisson, V.B., Roeske, S.M., and

Pavlis, T.L., eds., Geology of a transpressional orogen developed during ridge-trench interaction along the North Pacific margin: *Geological Society of America Special Paper* 371, pp. 89-118.

Trop, J.M., Szuch, D.A., Rioux, M., and Blodgett, R.B., 2005, Sedimentology and provenance of the Upper Jurassic Naknek Formation, Talkeetna Mountains, Alaska: Bearings on the accretionary tectonic history of the Wrangellia composite terrane: *Geological Society of America Bulletin*, v. 117, no. 5/6, p. 570-588, doi: 10.1130/B25575.1.

Van Der Plas, L. and Tobi, A.C., 1965, A chart for judging the reliability of point counting results: *American Journal of Science*, v. 263, p. 87-90.

Wilson, F.H., Dover, J.H., Bradley, D.C., Weber, F.R., Bundtzen, T.K., and Haeussler, P.J., 1998, Geologic map of central (interior) Alaska: *U.S. Geological Survey Open-File Report 98-133-A*, 63 p.

Winkler, G.R., 1978, Framework grain mineralogy and provenance of sandstones from the Arkose Ridge and Chickaloon Formations, Matanuska Valley, The United States Geological Survey in Alaksa − Accomplishments during 1977: *U.S. Geological Survey Circular* 772-B, p. B70-B73

Winkler, G. R., 1992, Geologic map and summary geochronology of the Anchorage 1° × 3° quadrangle, southern Alaska: *U.S. Geological Survey Miscellaneous Investigations Series Map I-2283*, scale 1:250,000.

APPENDICES

APPENDIX A:
PHOTOMICROGRAPHS OF POINT-COUNTED SANDSTONES

Appendix A. Labels for photomicrographs of point counted sandstones

Raw	
Am	Amphibole
K	Potassium feldspar (single crystals)
K/Pl	Potassium feldspar, plagioclase feldspar, and quartz in plutonic fragments
Lmm	Mica schist and subordinate chlorite schist lithic fragments, foliated
Lmt	Quartz-mica tectonite and subordinate quartz-mica-feldspar tectonite, foliated
Lsa	Argillaceous metasedimentary lithic fragments, weakly foliated
Lsm	Sedimentary lithic fragments (shale)
Lss	Sedimentary lithic fragments (quartzose to quartzofeldspathic siltstone)
Lvf	Volcanic lithic fragments (felsitic to microlitic textures)
Lvl	Volcanic lithic fragments (lathwork textures)
P	Plagioclase feldspar (single crystals)
Pl	Plagioclase feldspar and quartz in plutonic fragments
Qe	Embayed monocrystalline quartz
Qm	Monocrystalline quartz (single crystals)
Qpq	Polycrystalline quartz

LMN1-24.7
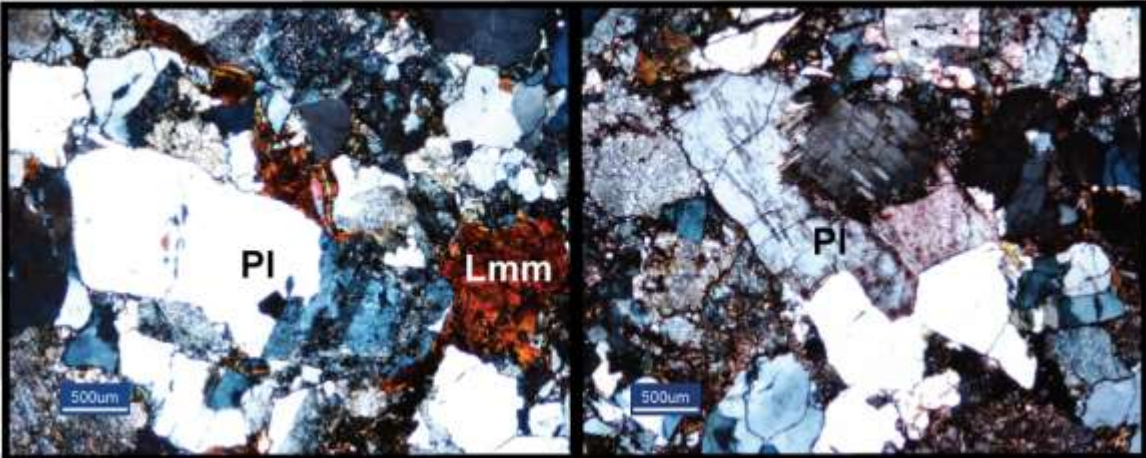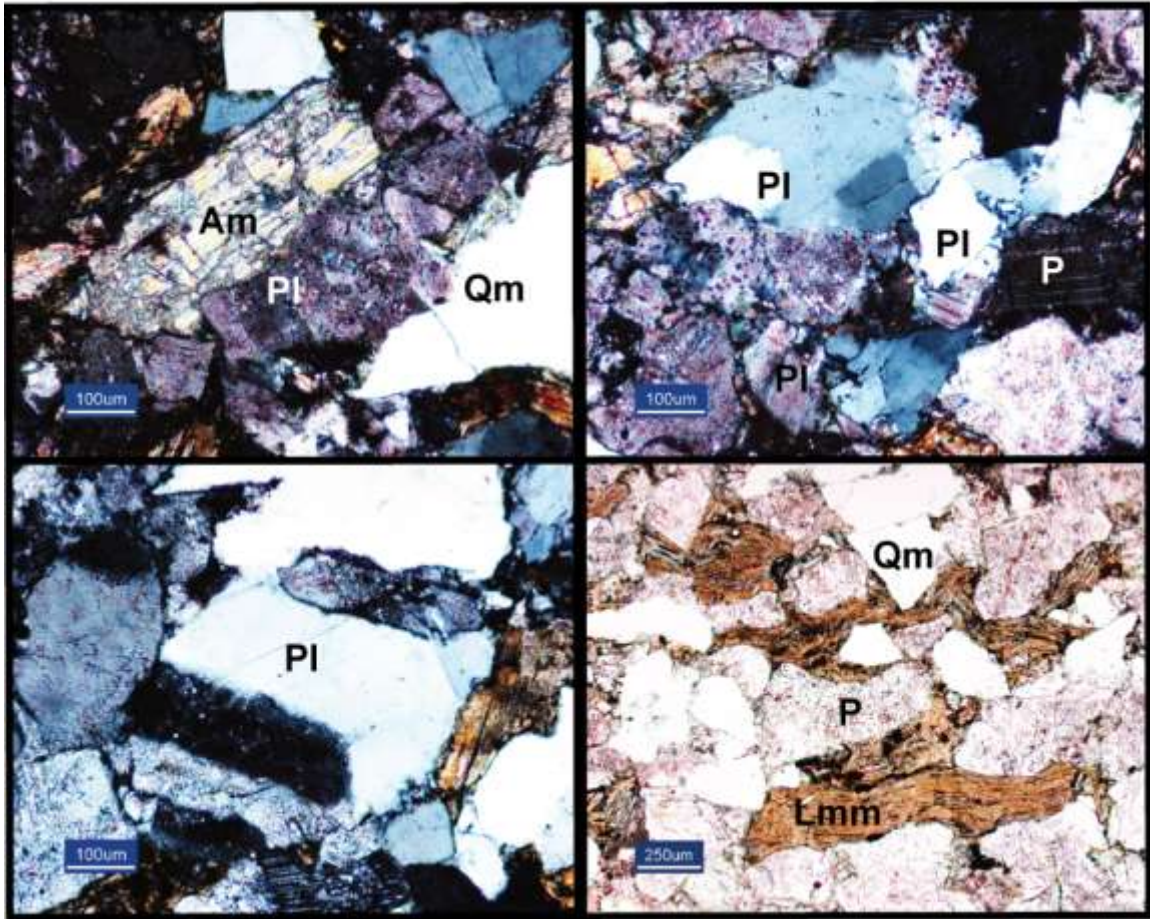
LMN1-71
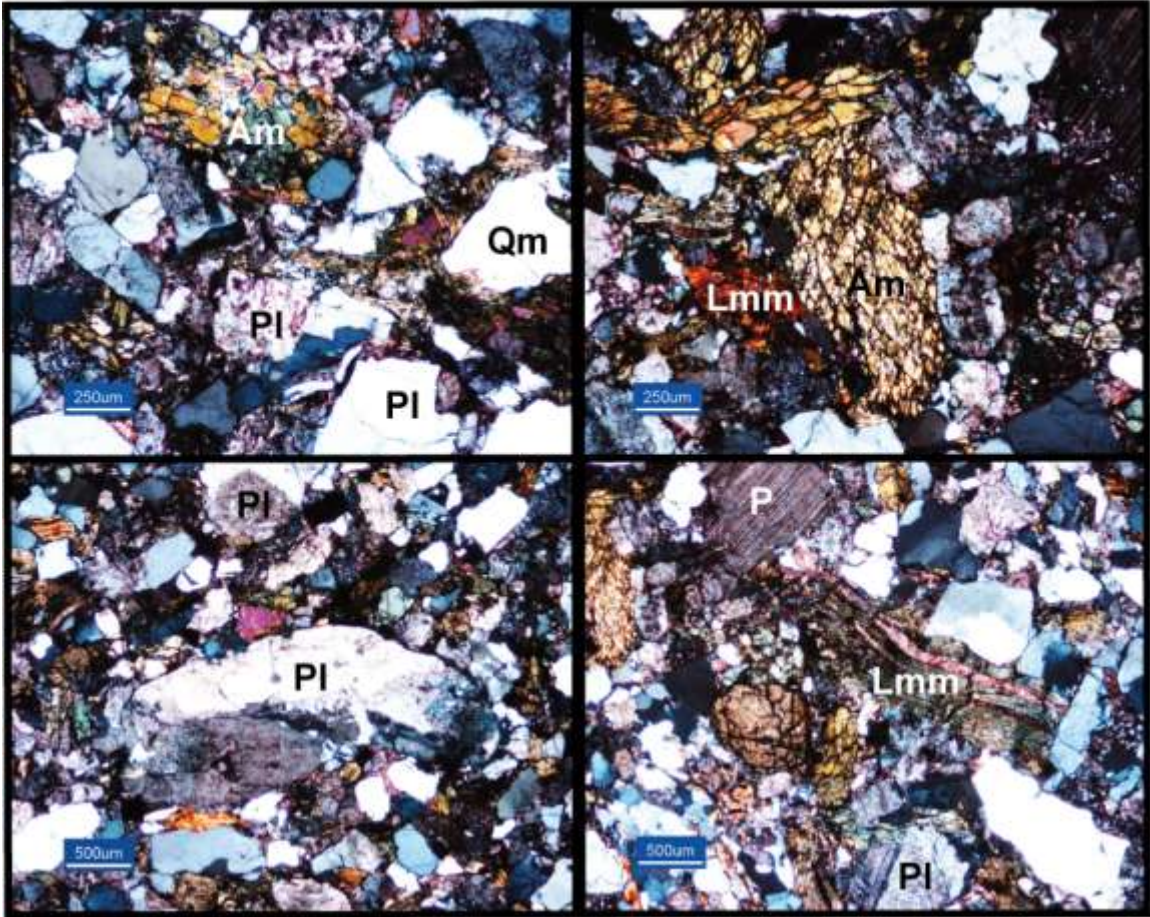
LMN1-100.5
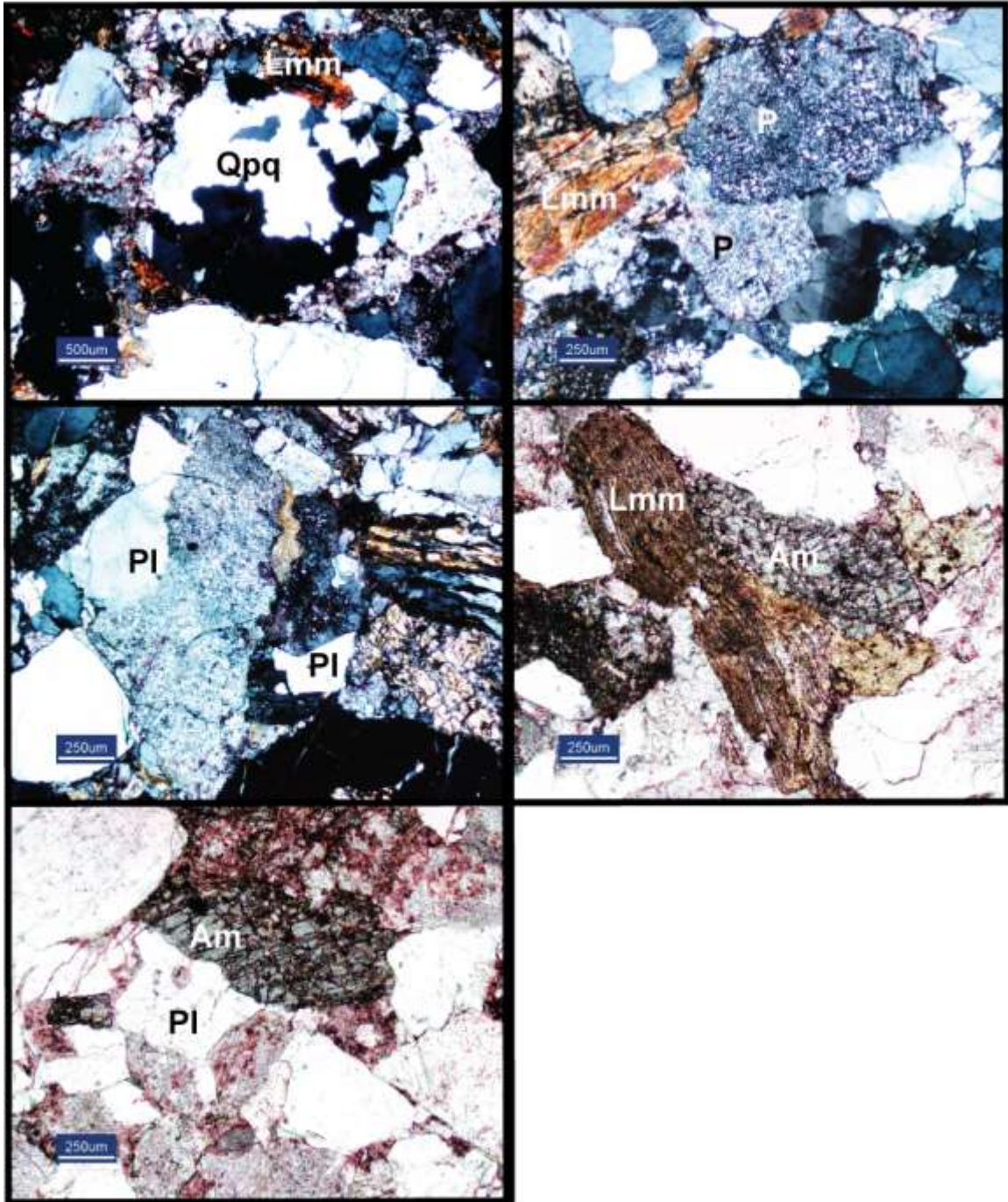
LMN1-180.3
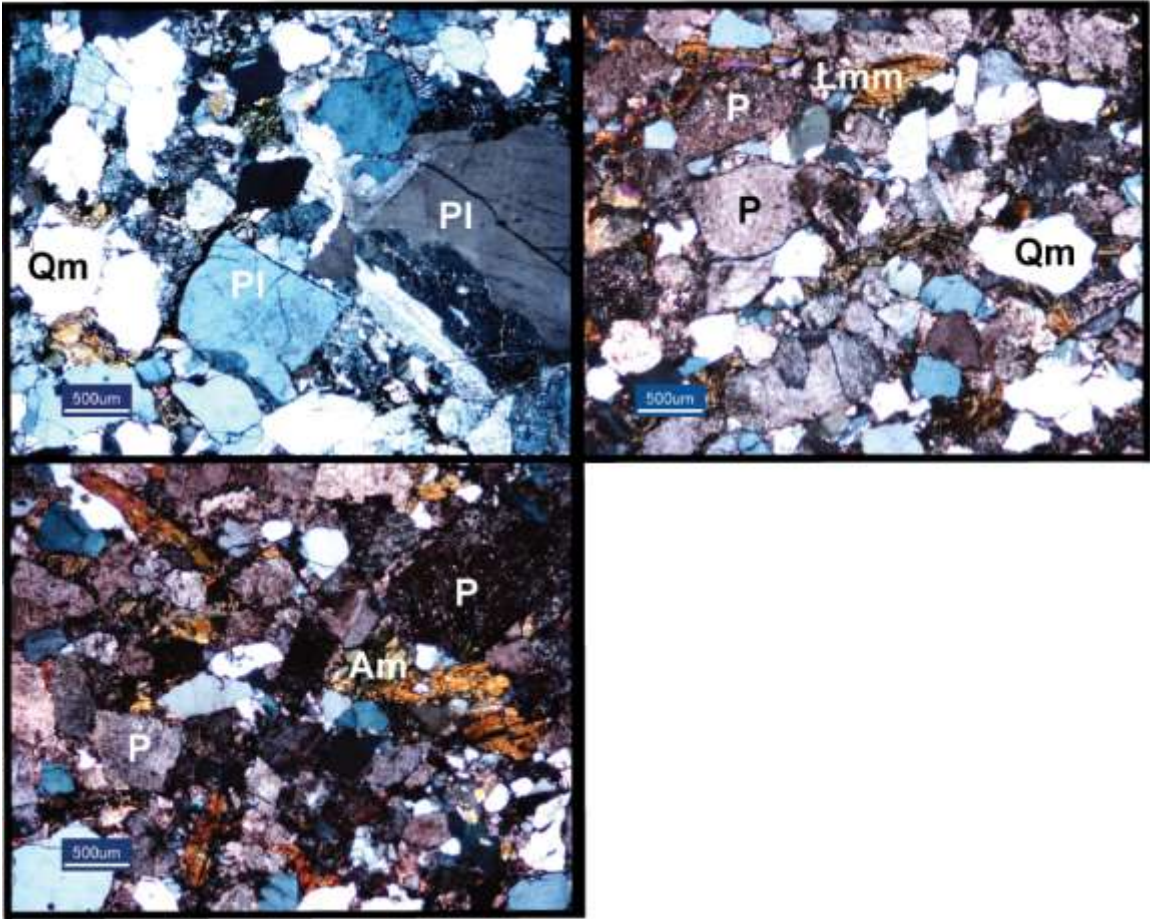
LMN1-211
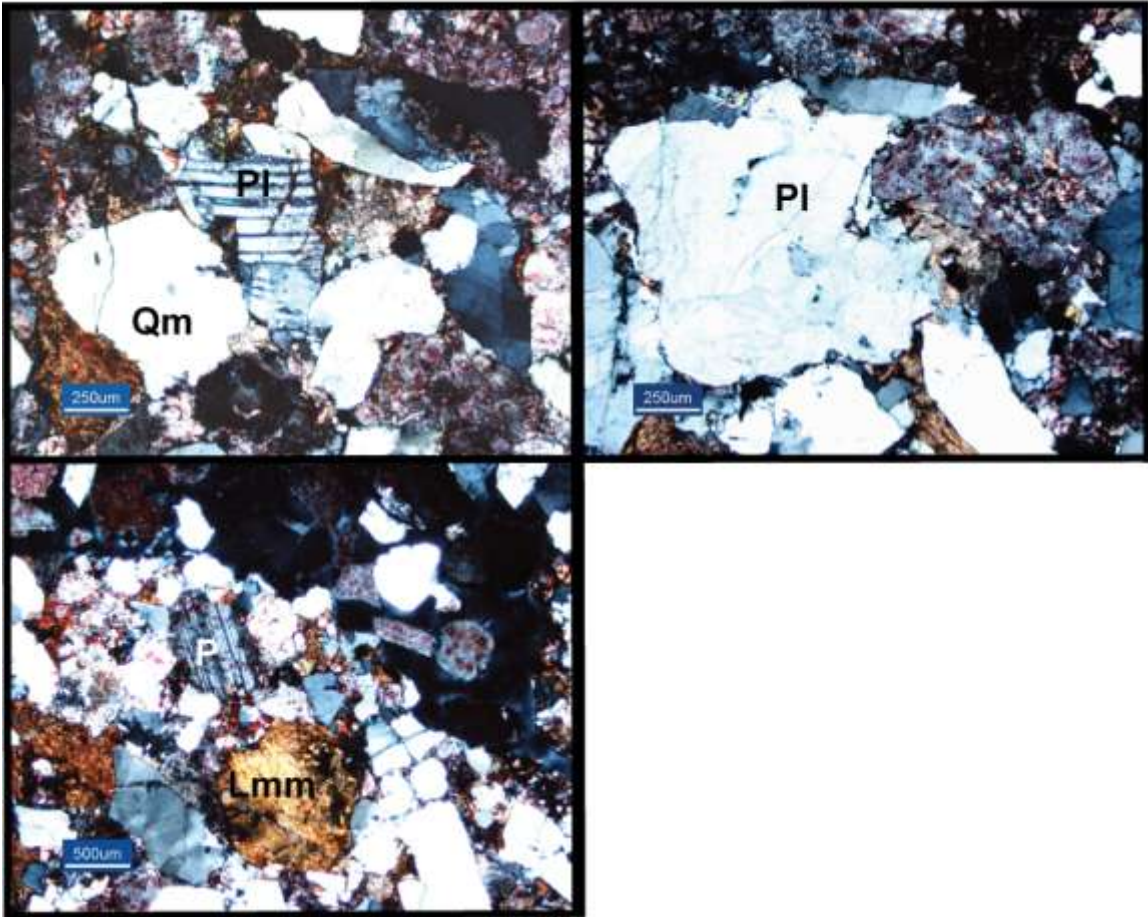
LMN1-257
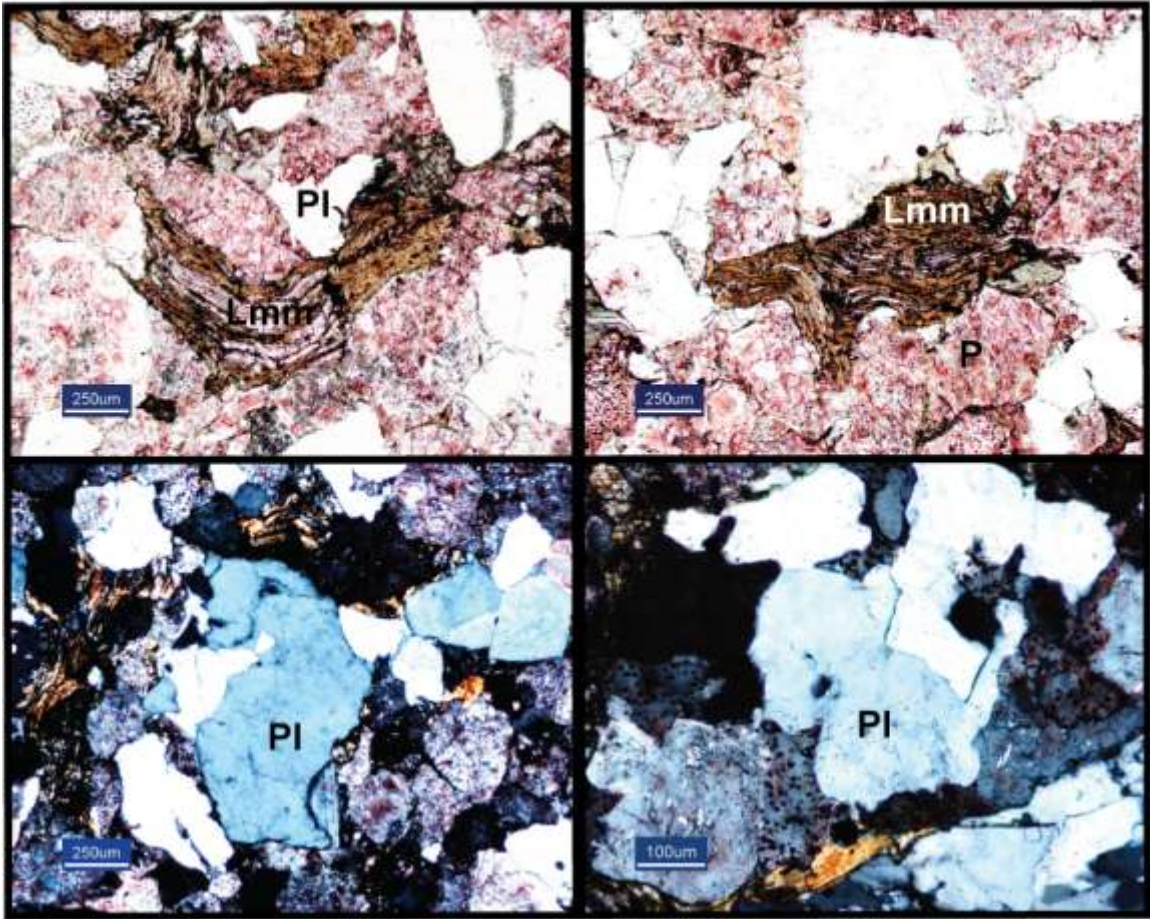
LMN1-315
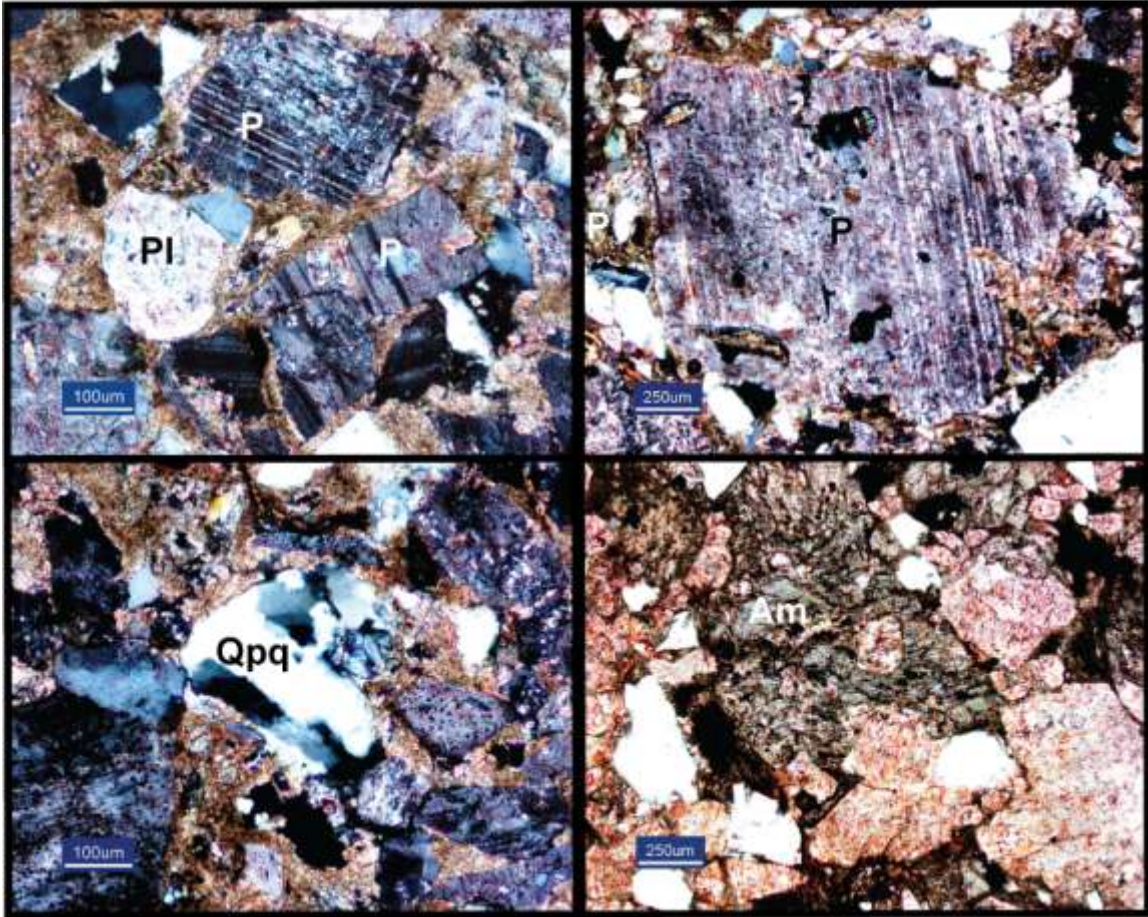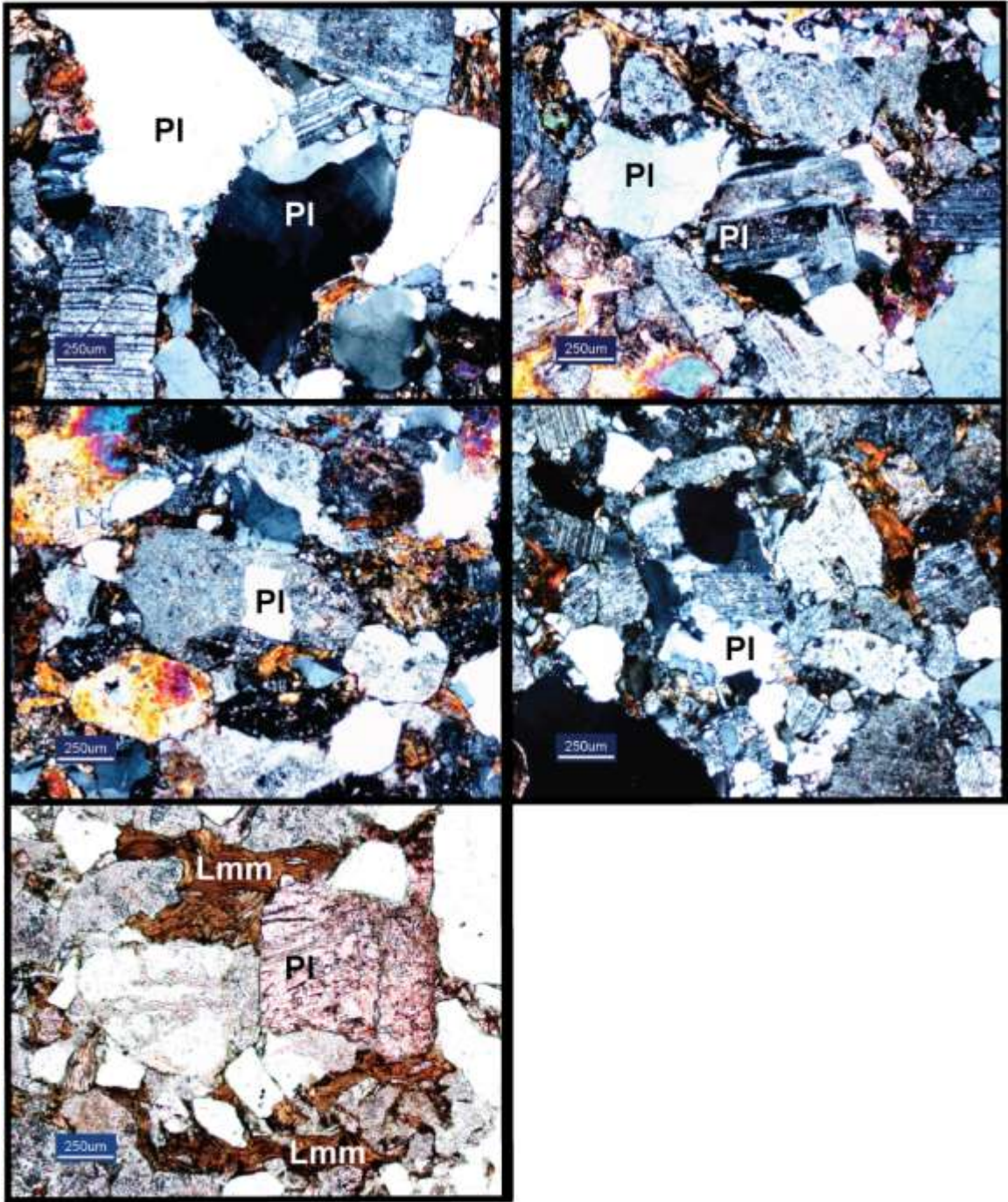
LMN1-406
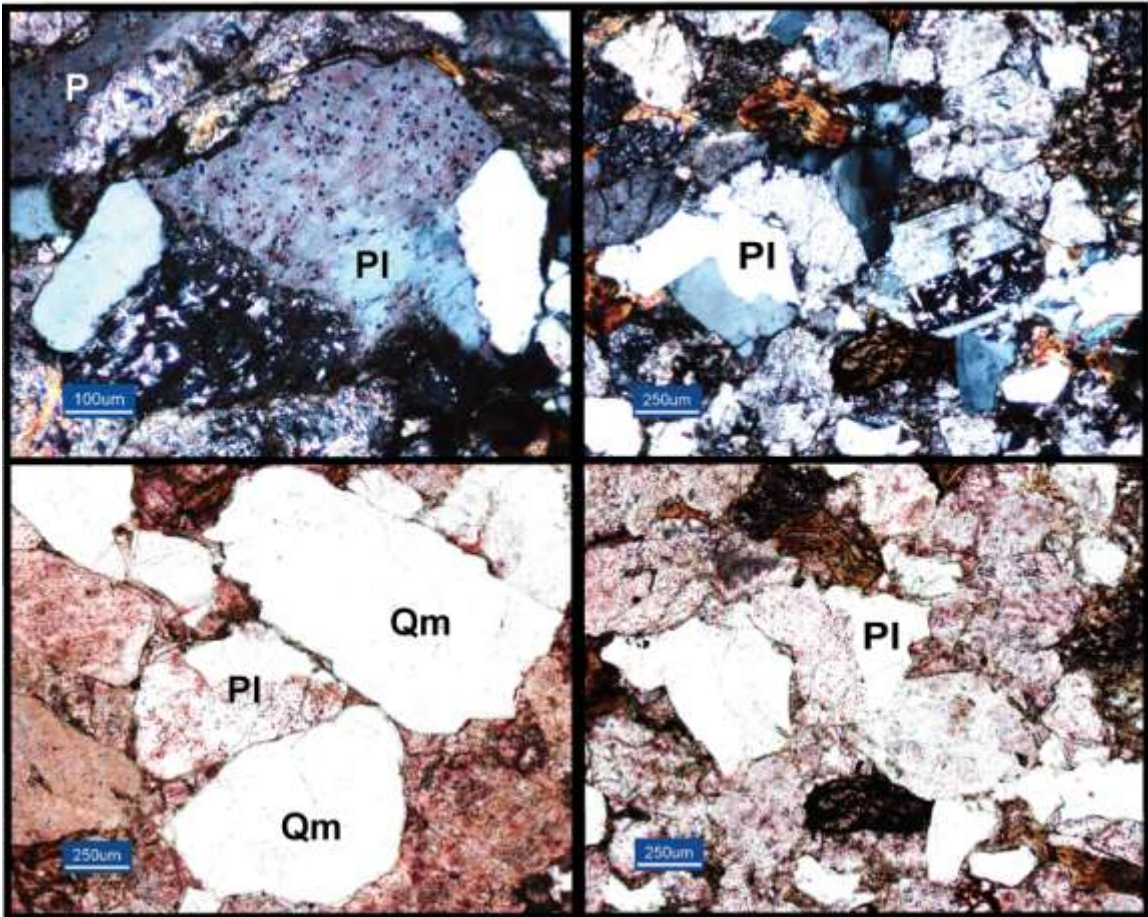
LMN1-458
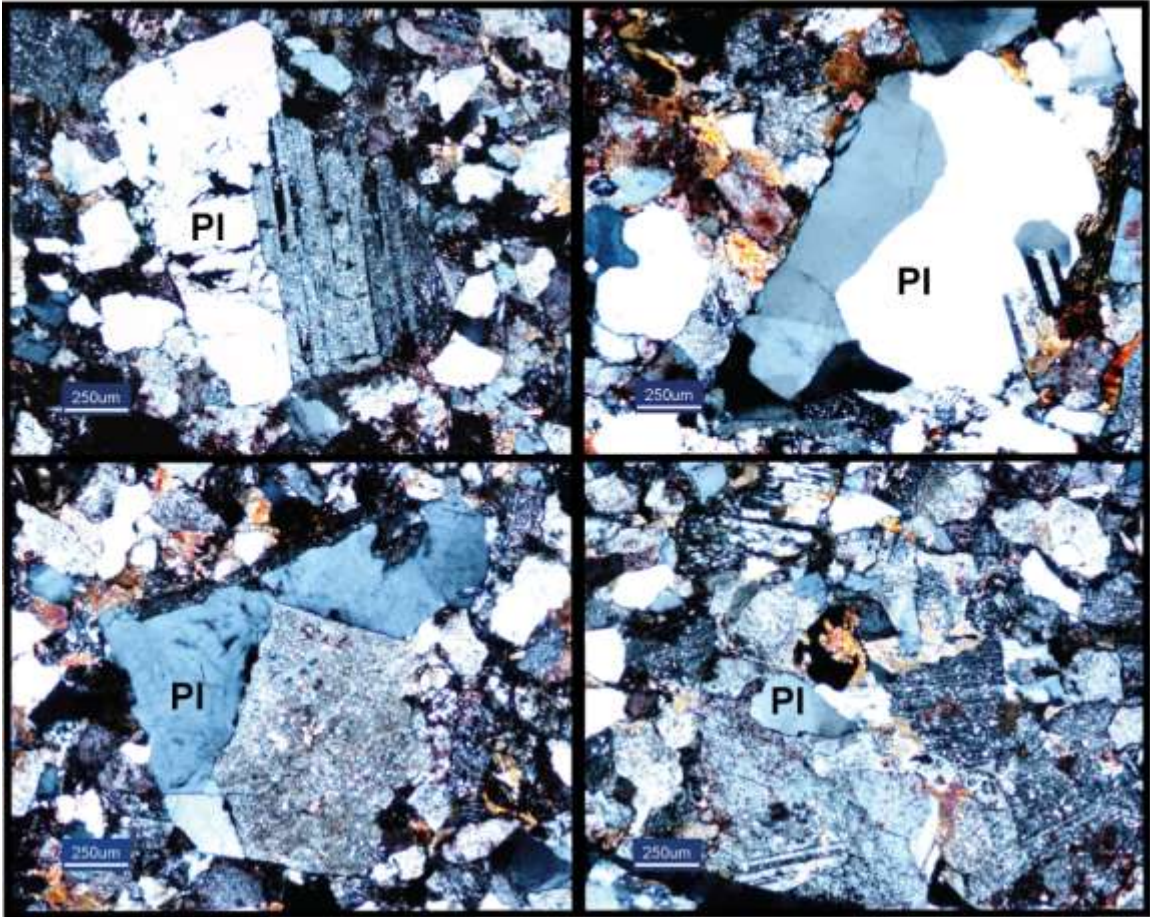
LMN1-500
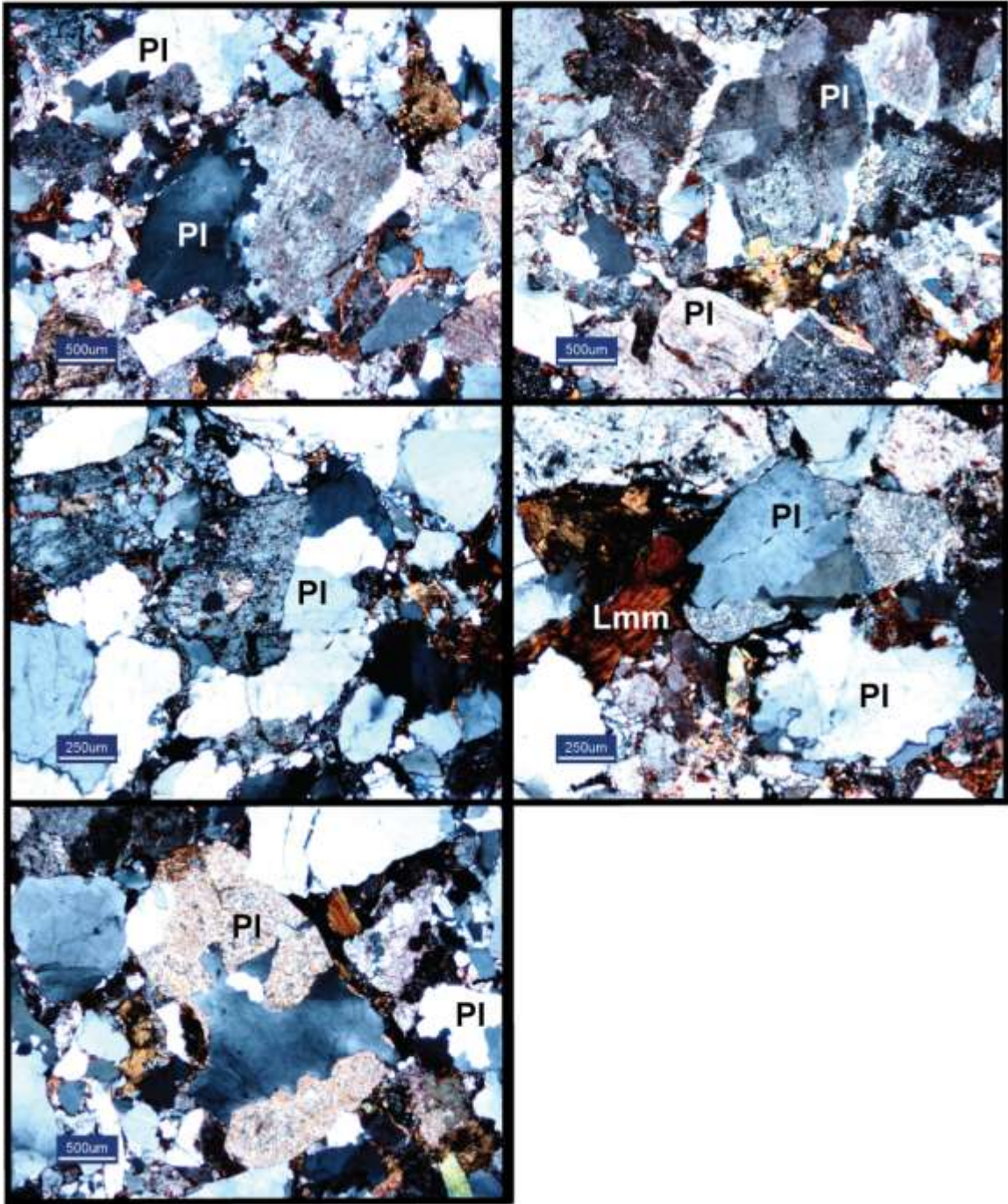
LMN1-553
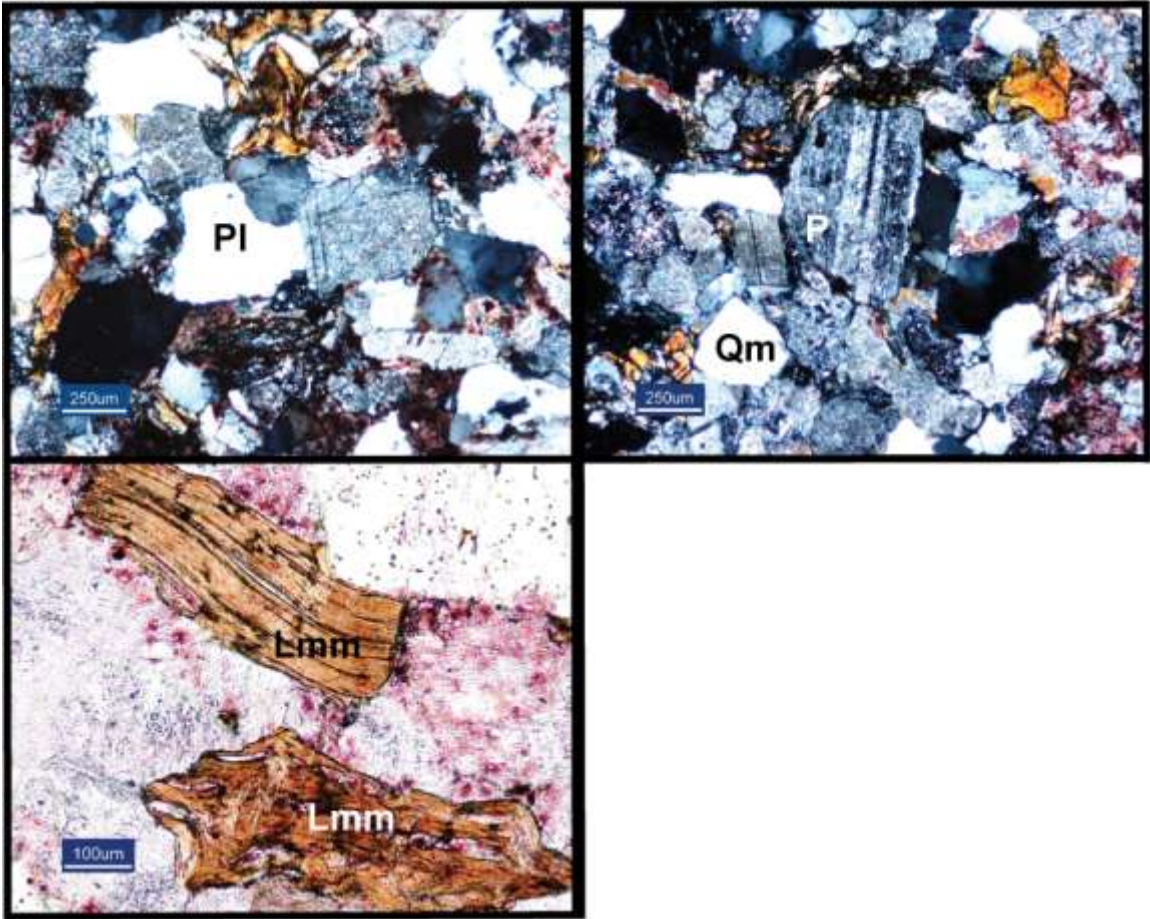
LMN1-599
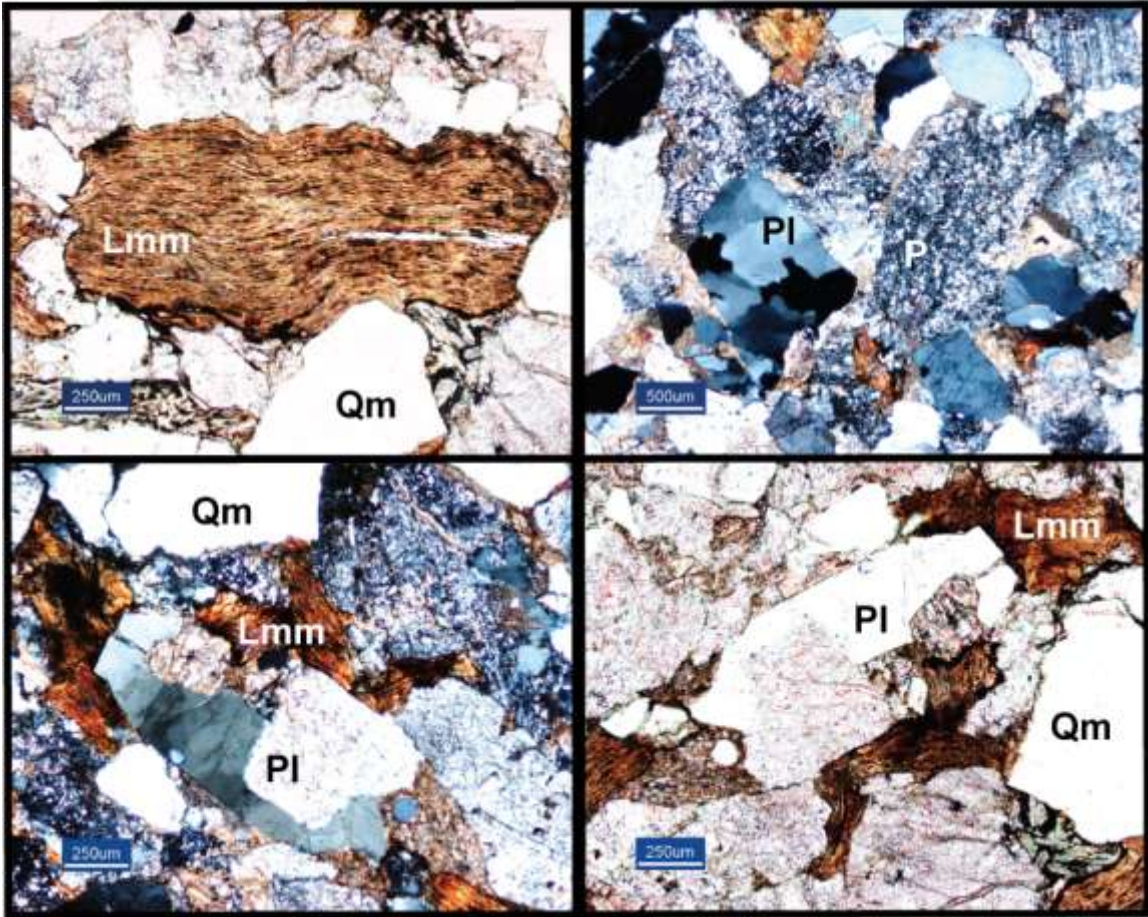
LMN1-623
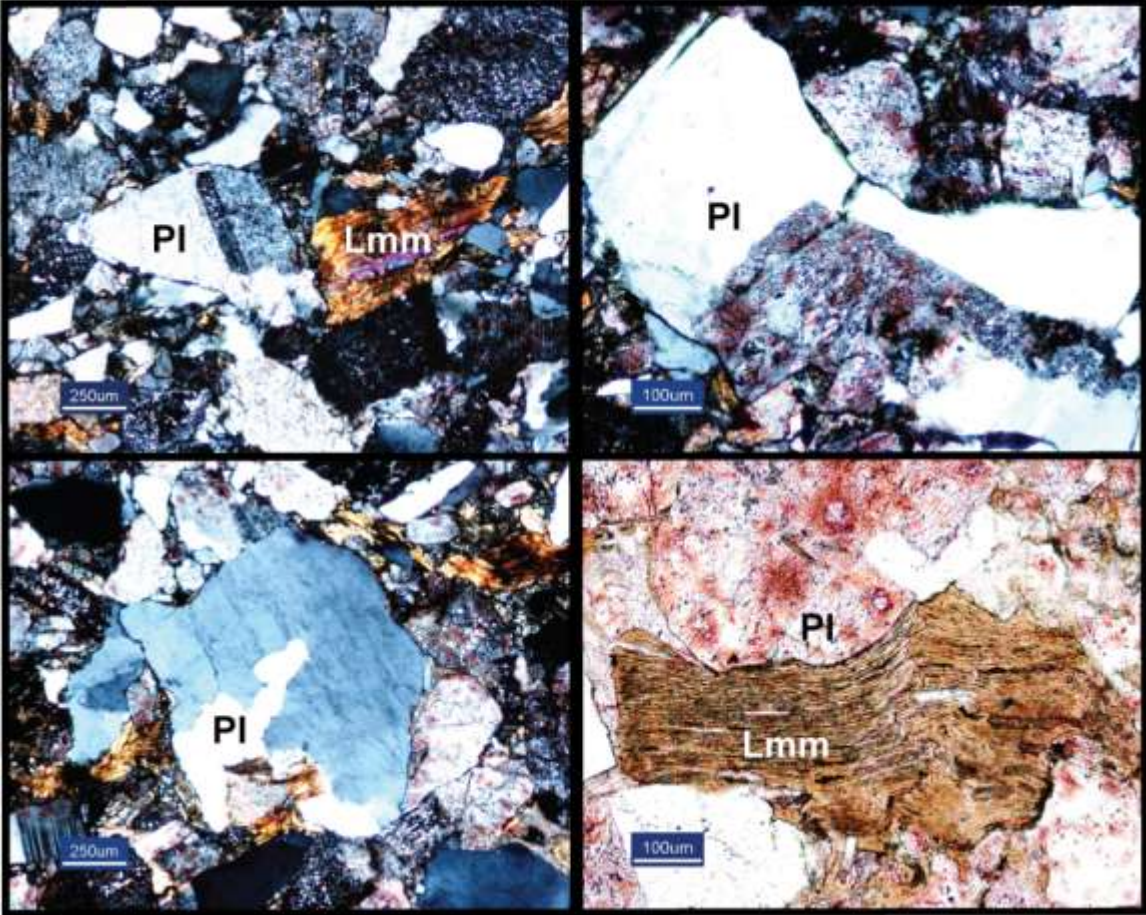
LMN1-780

GR-61.5

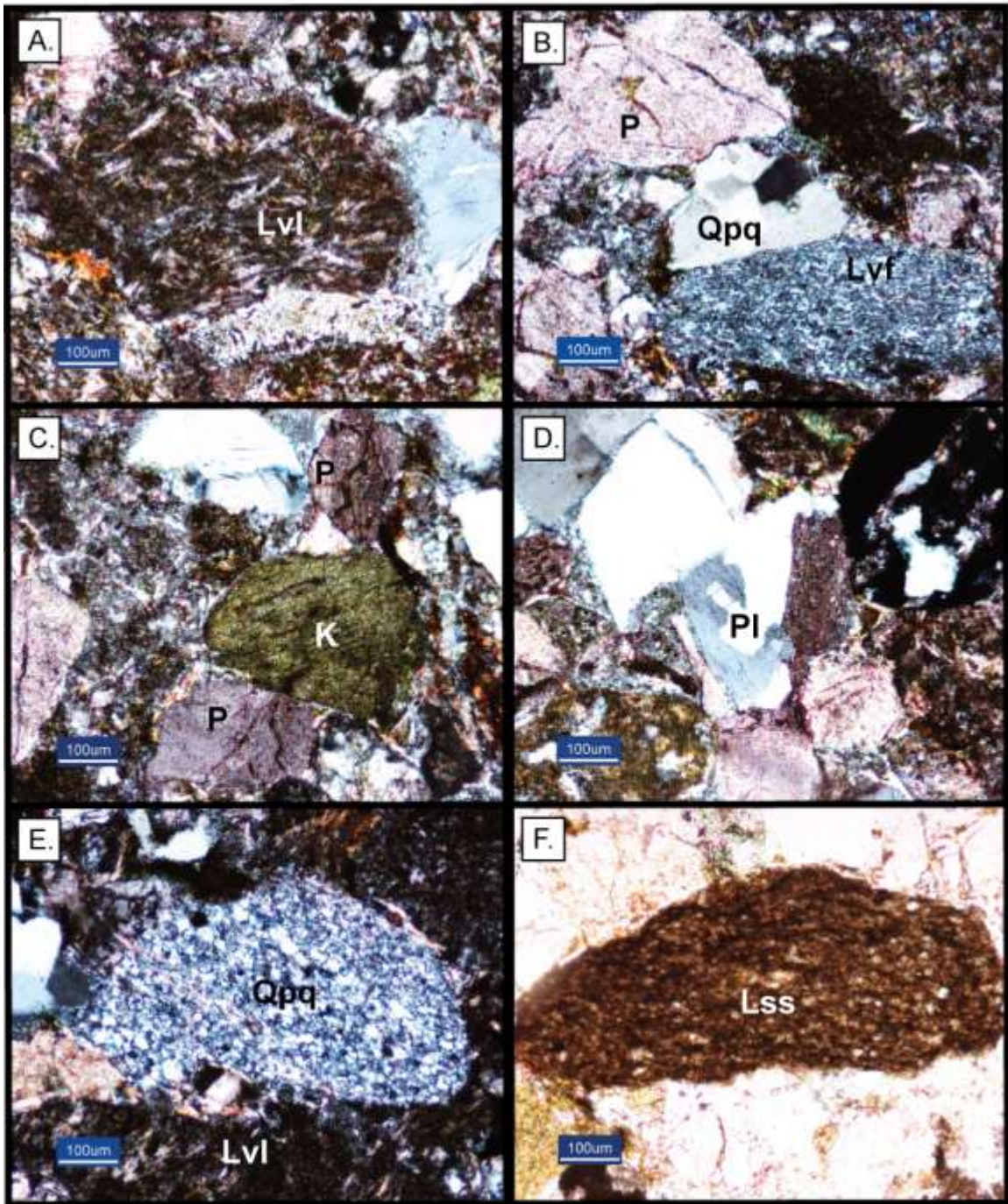

119
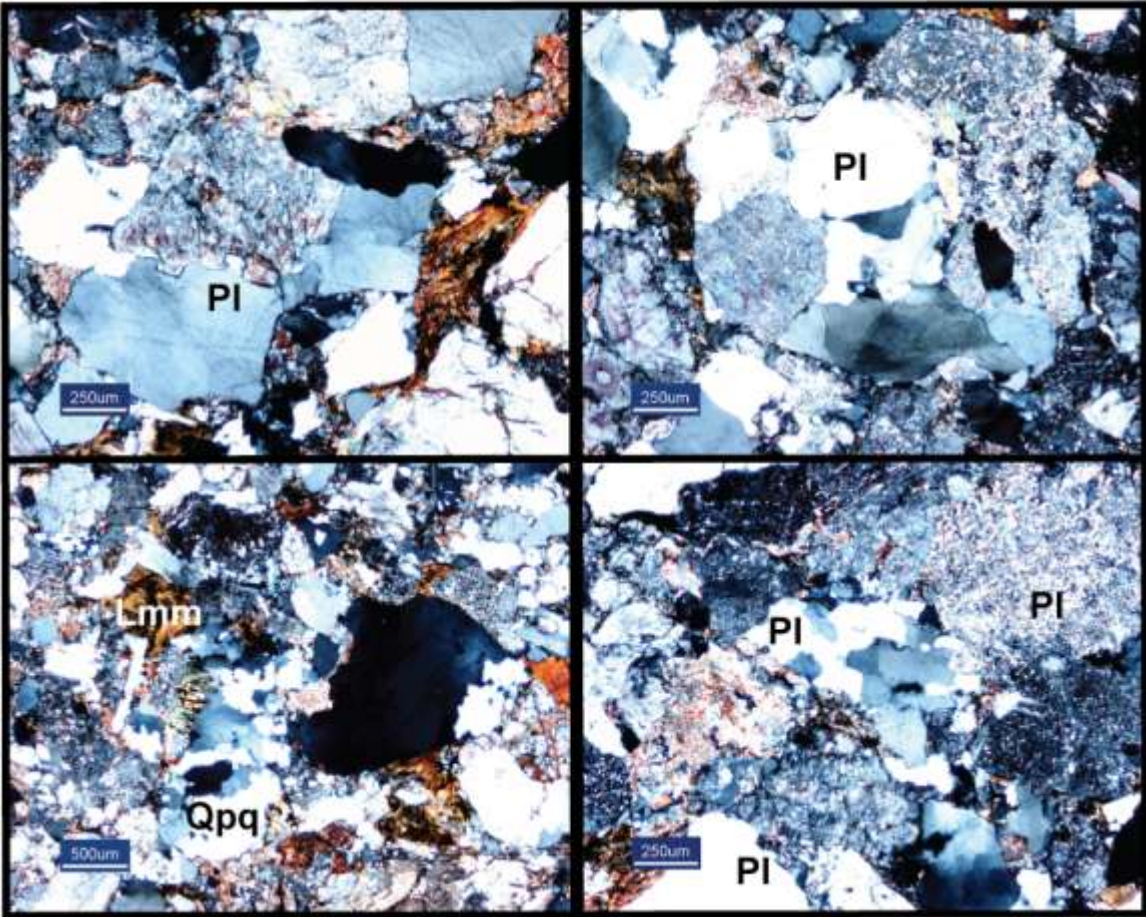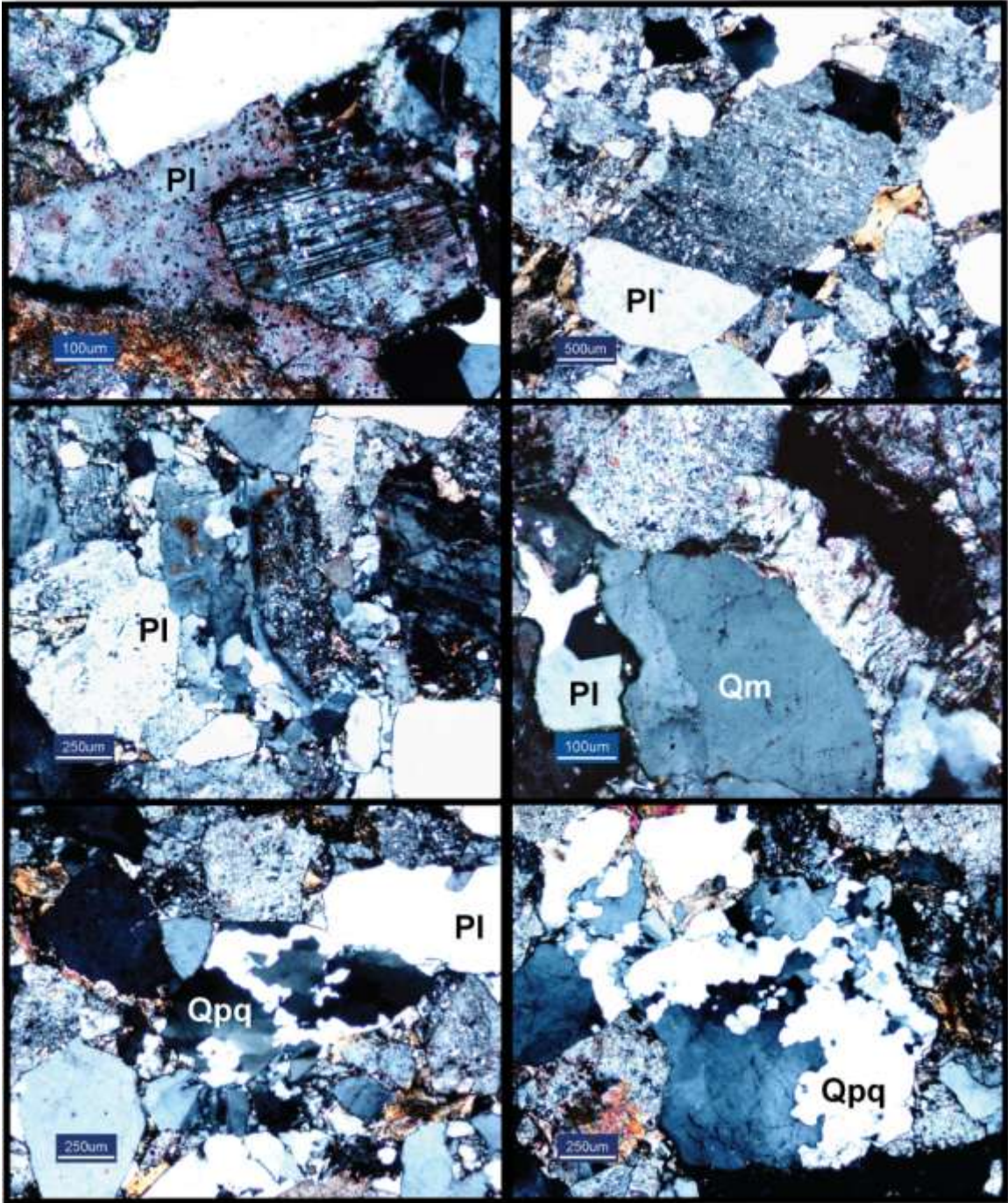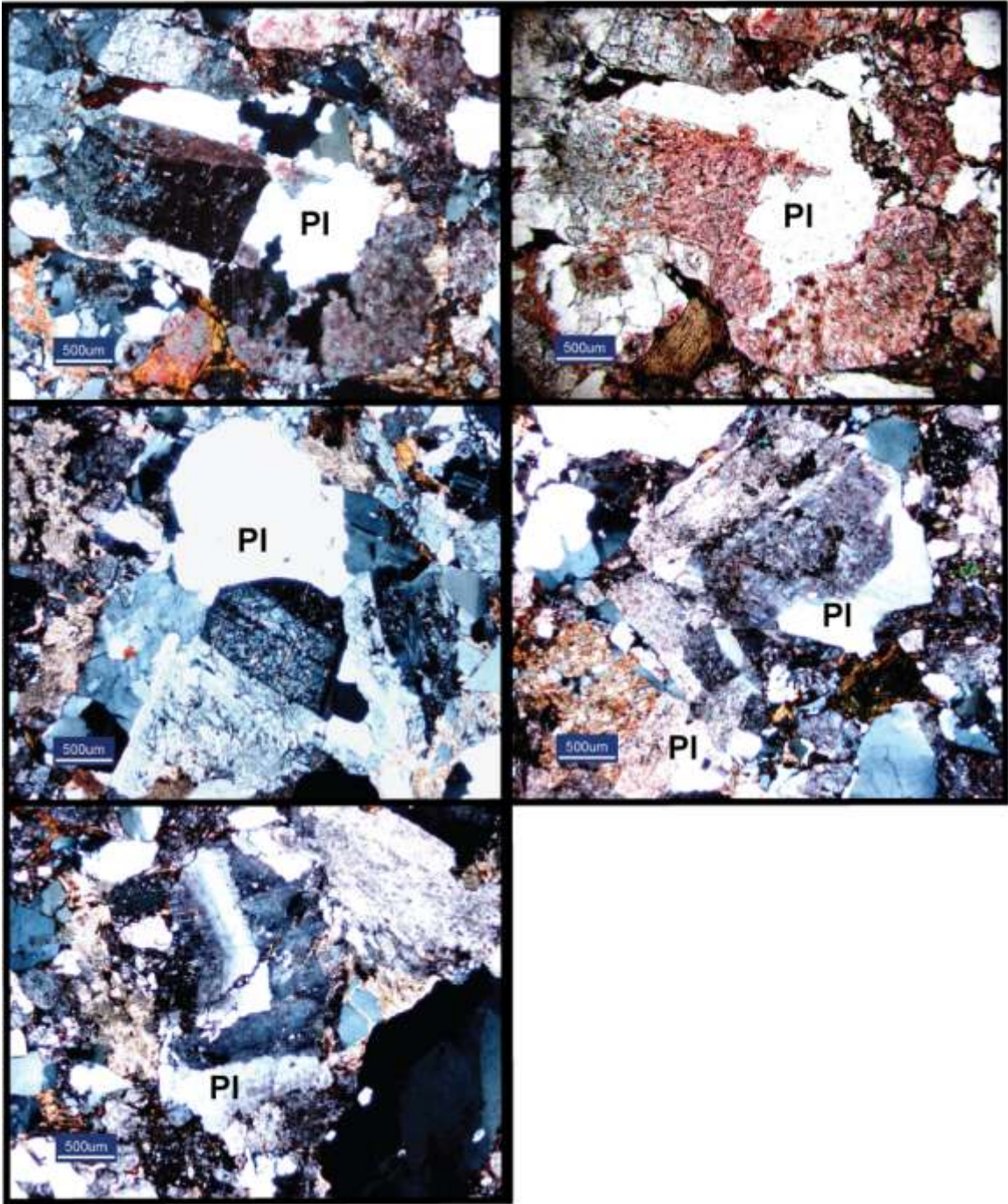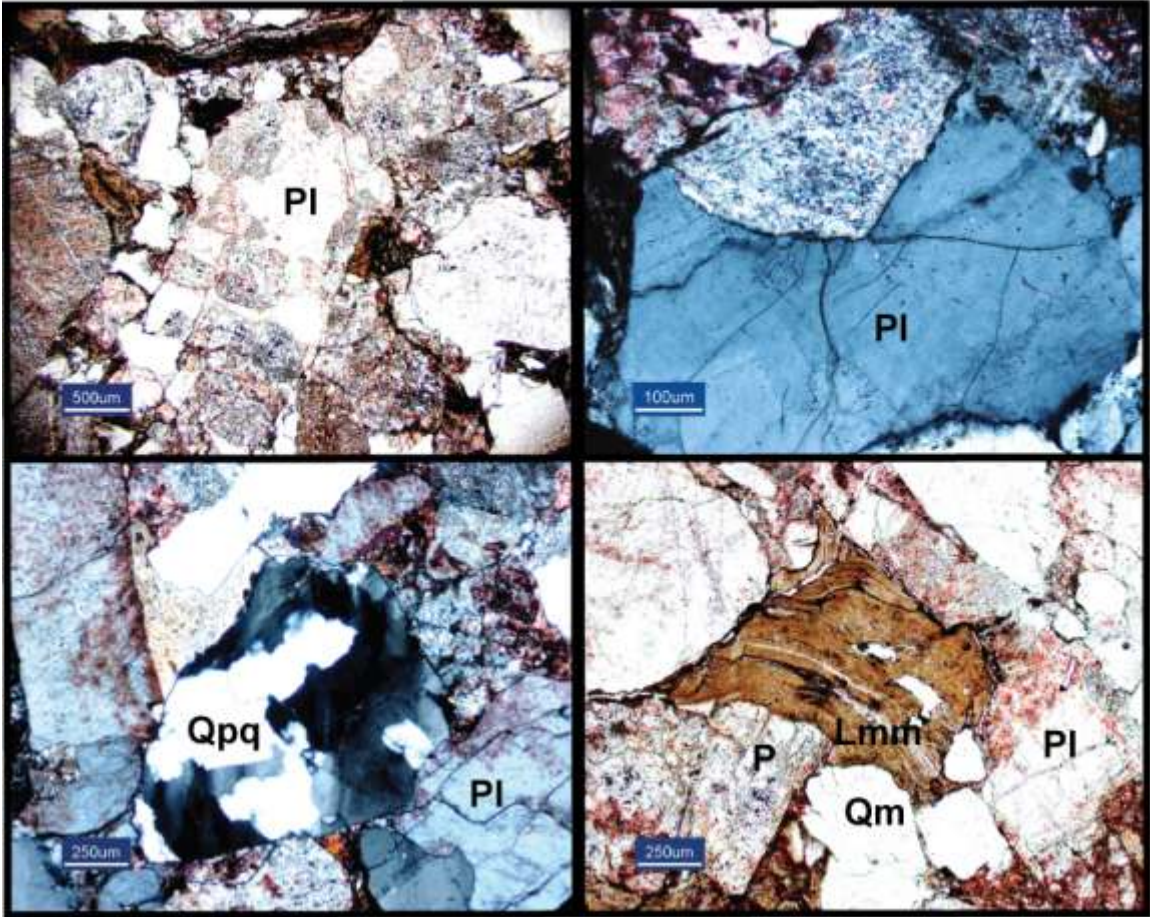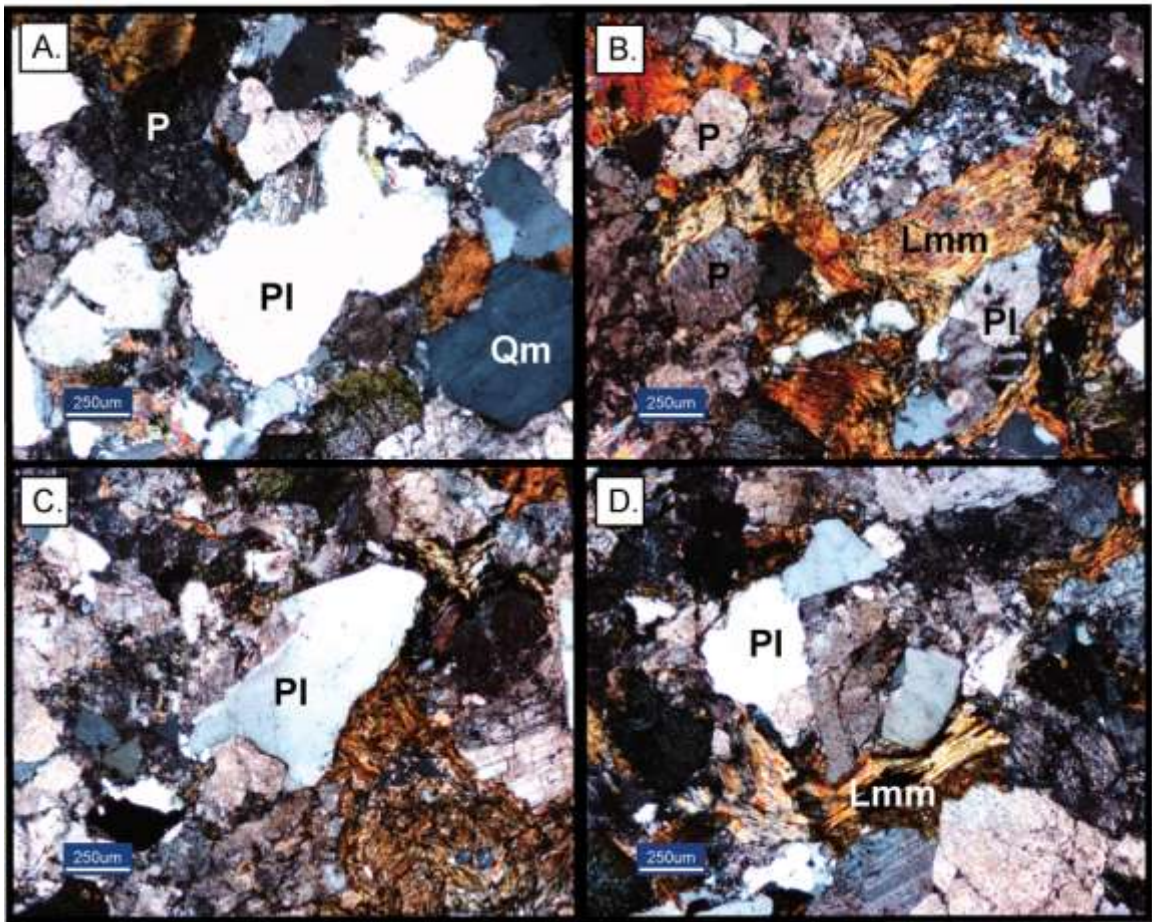
GR-78
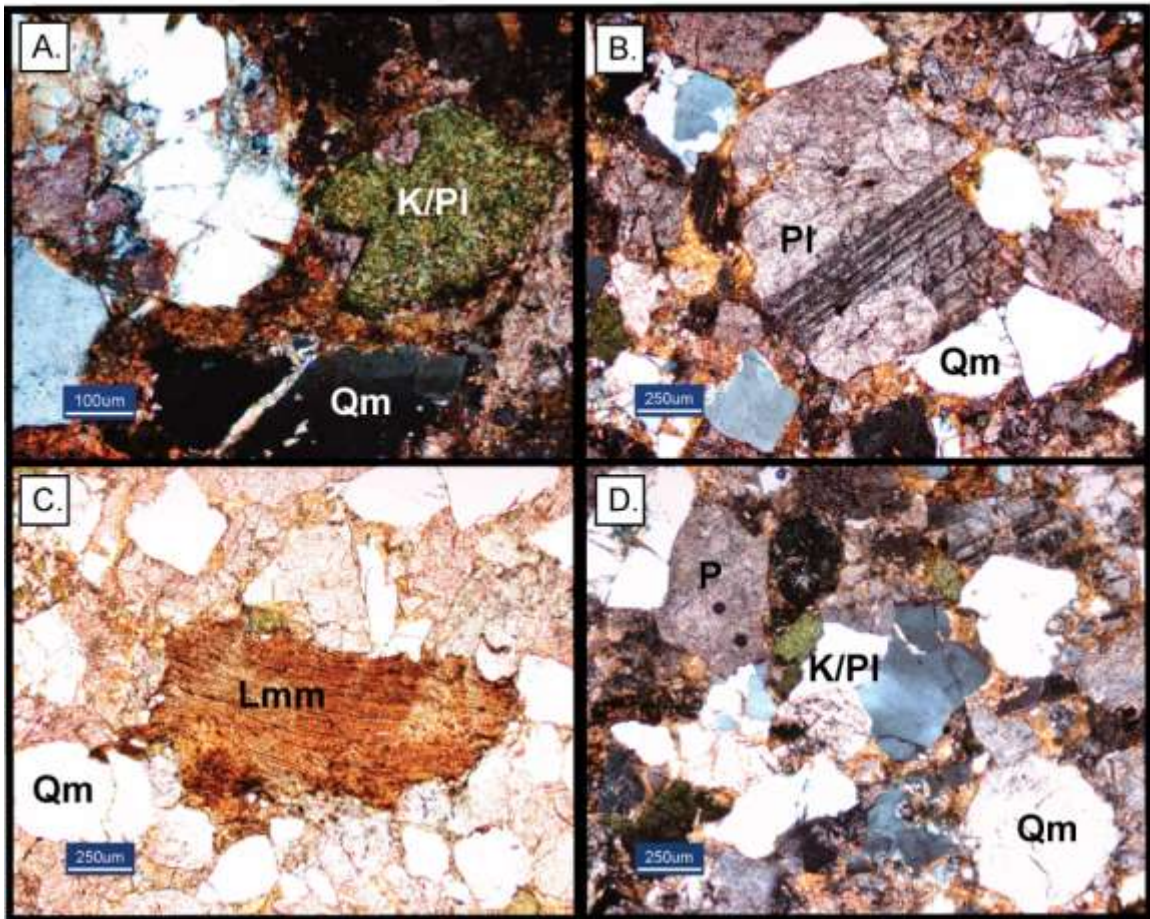
GR-105
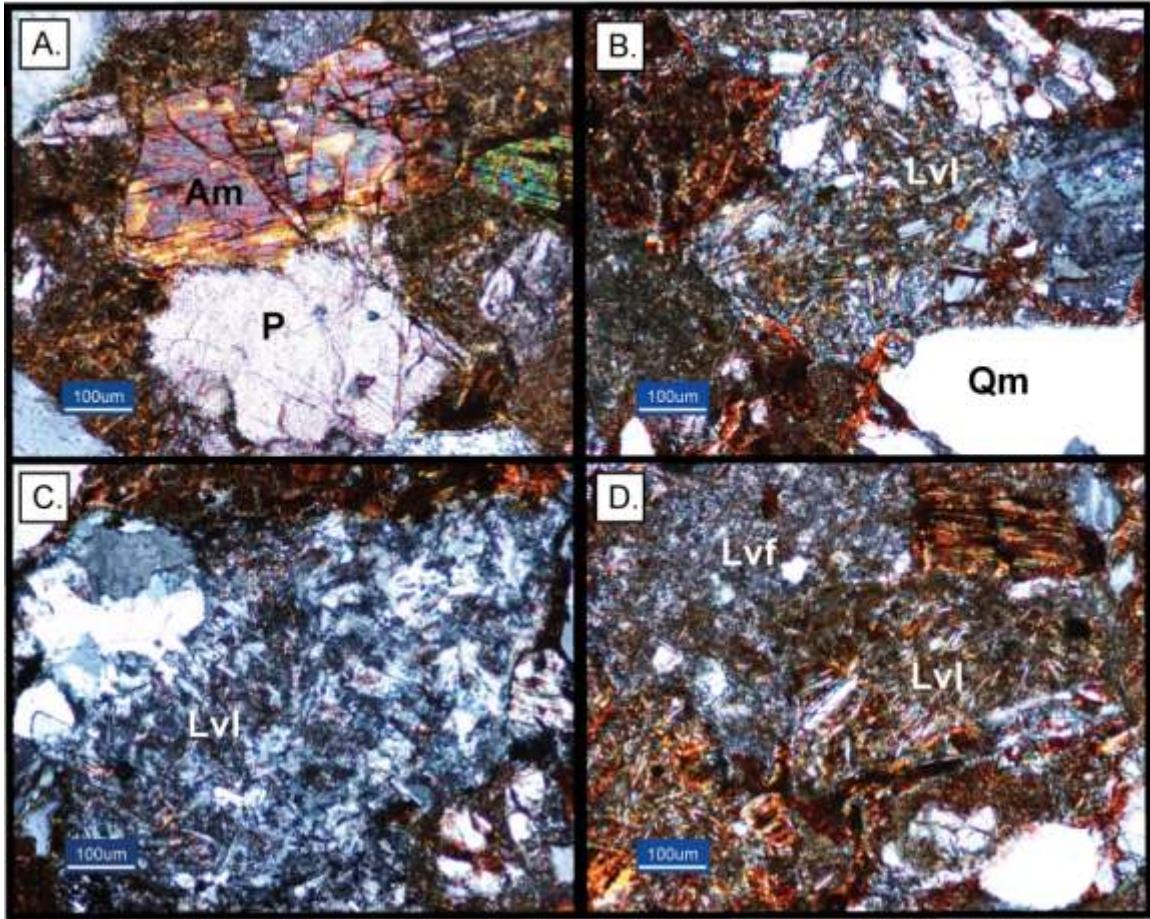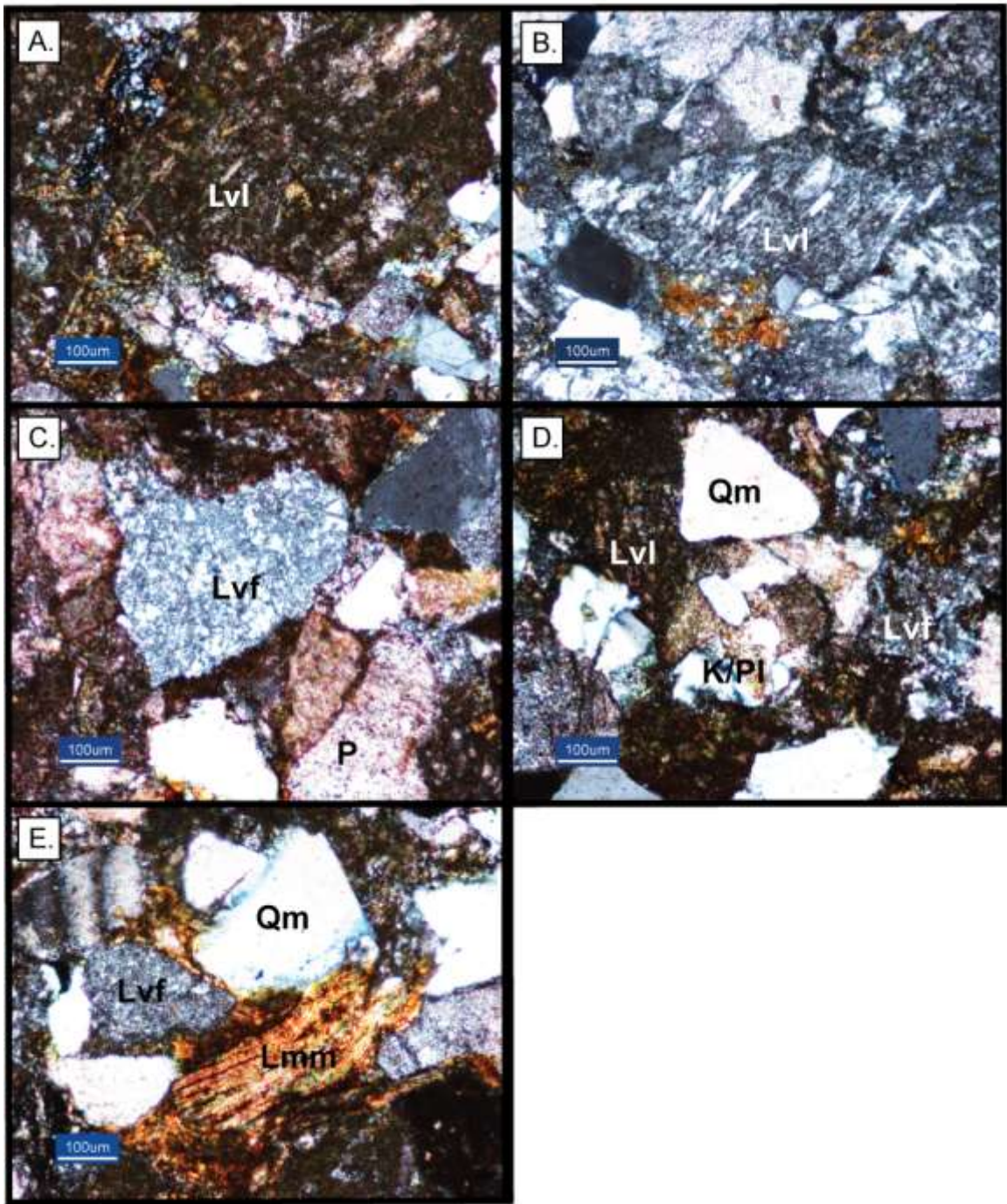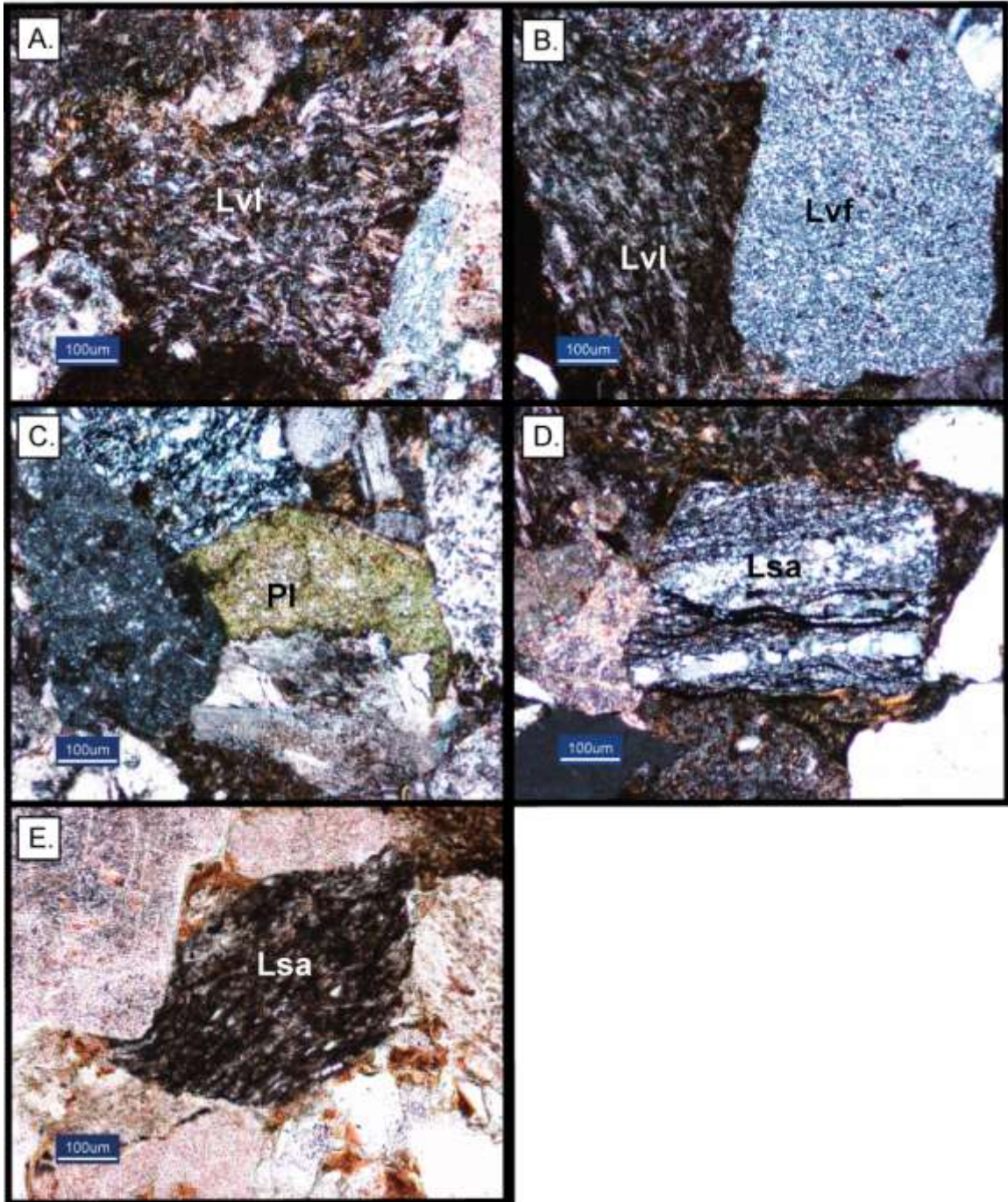
GR-282

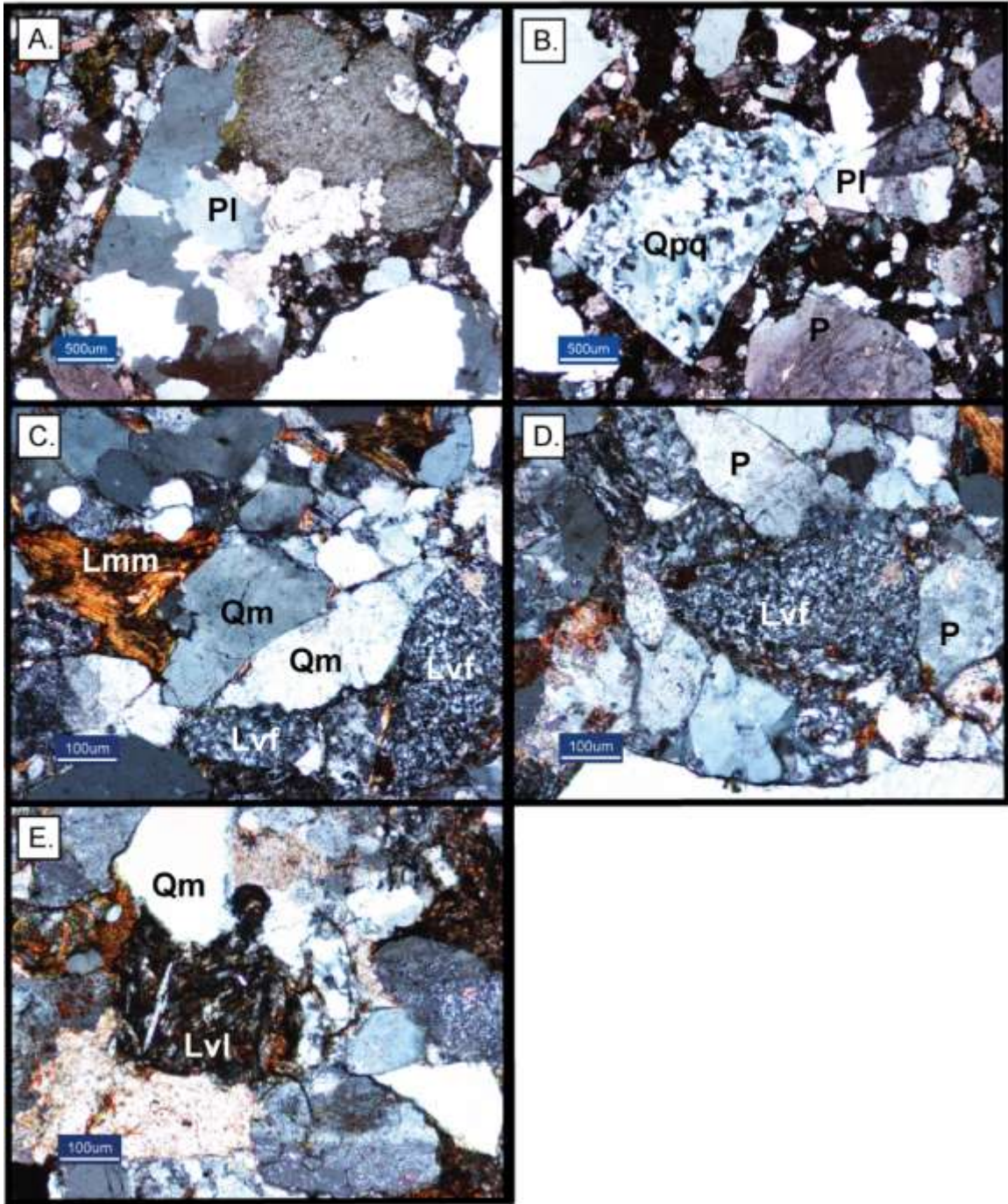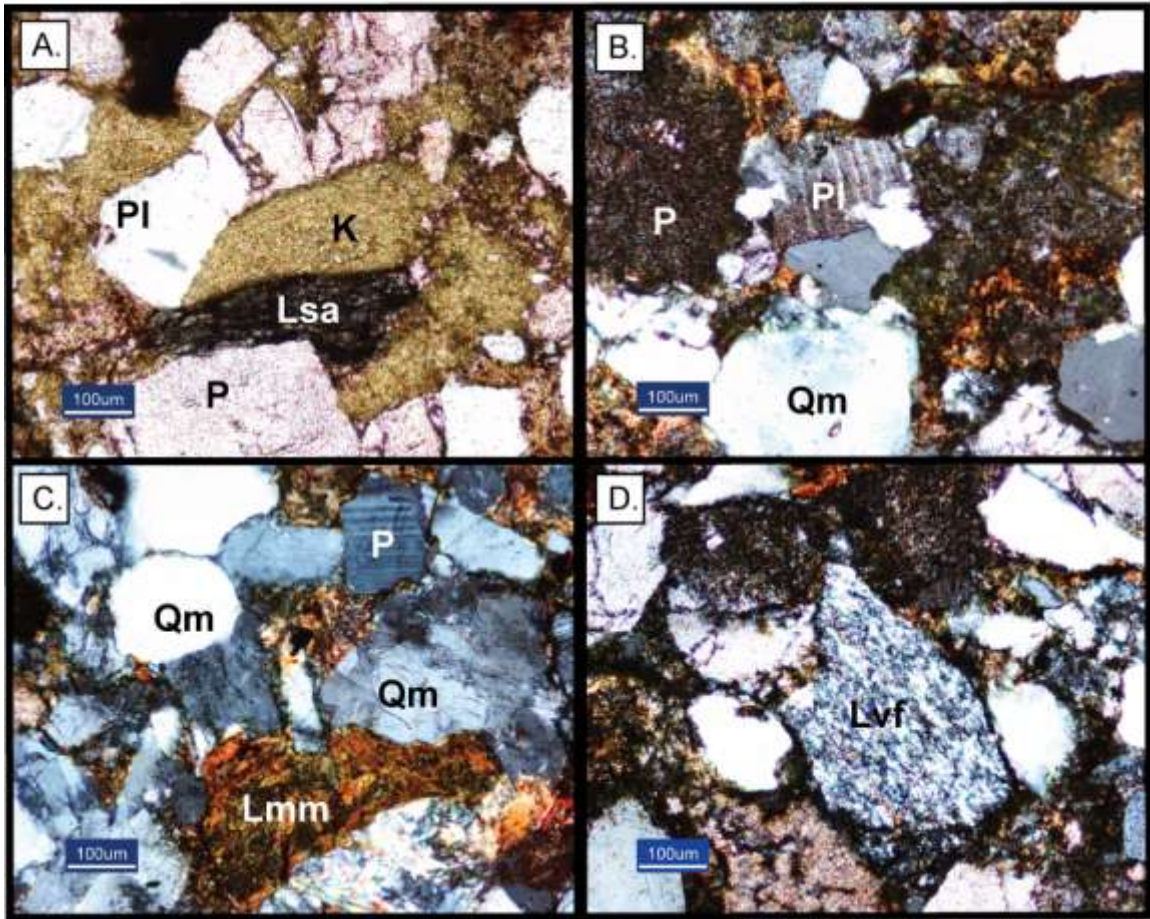GR-282
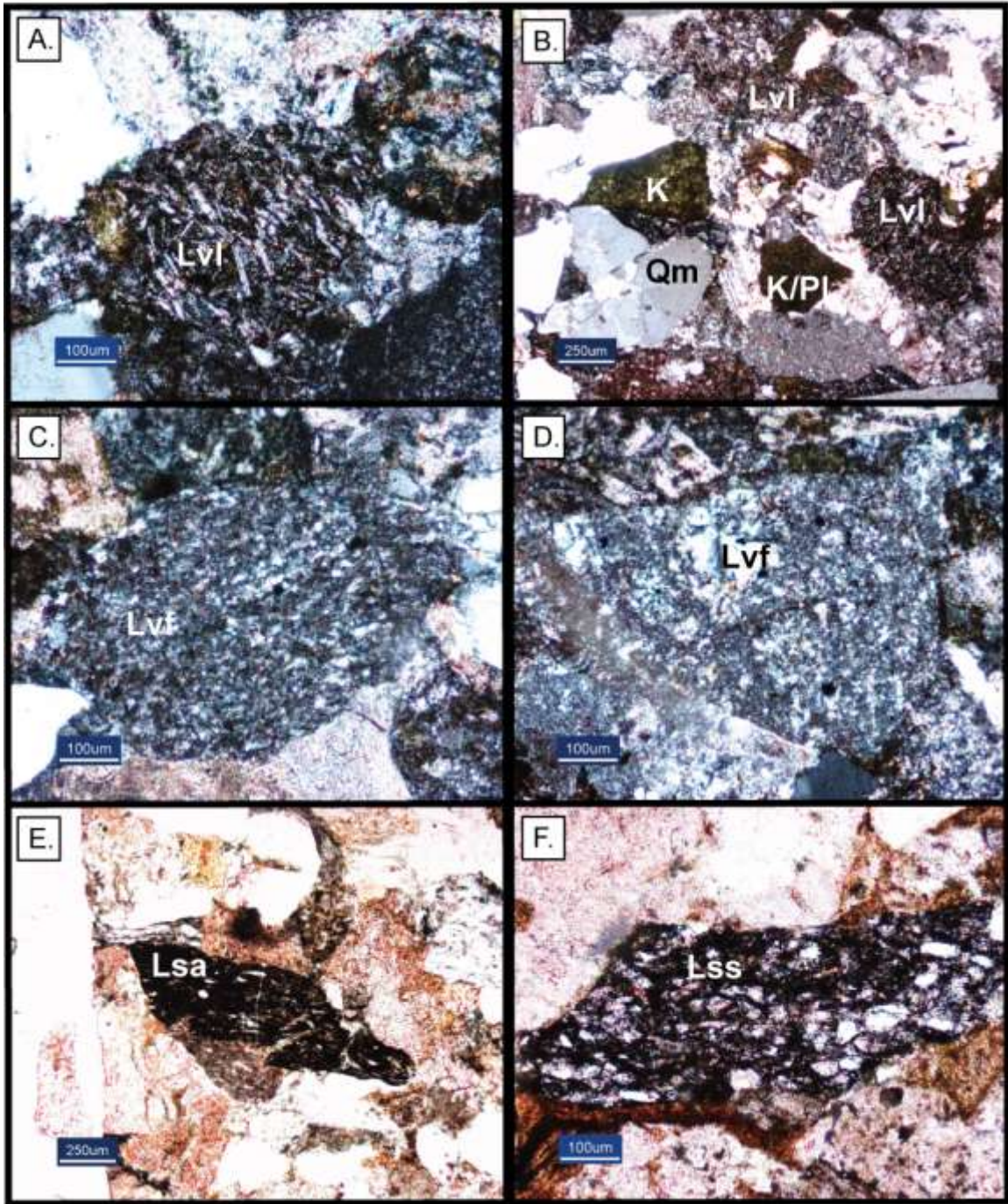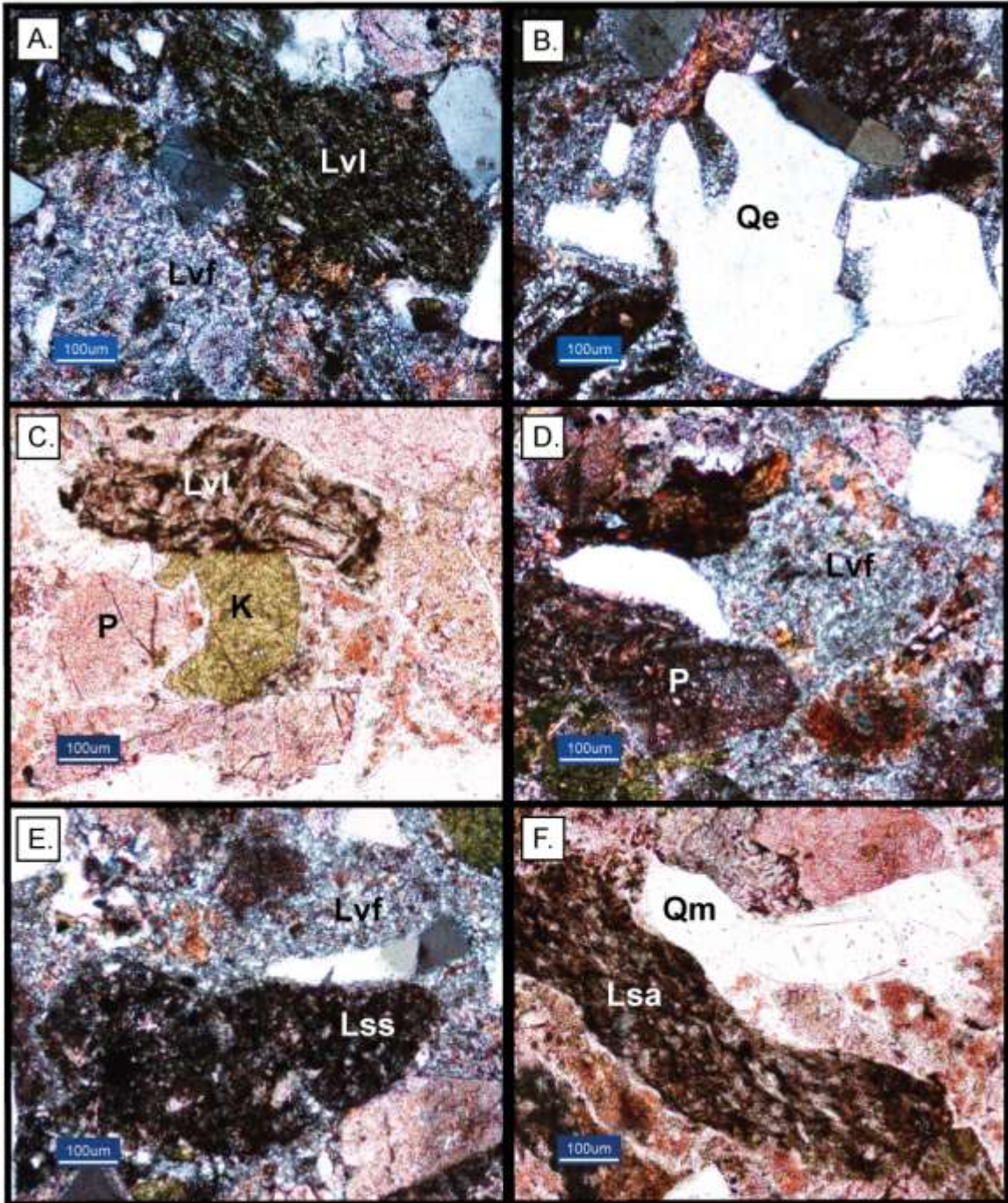
GR-404
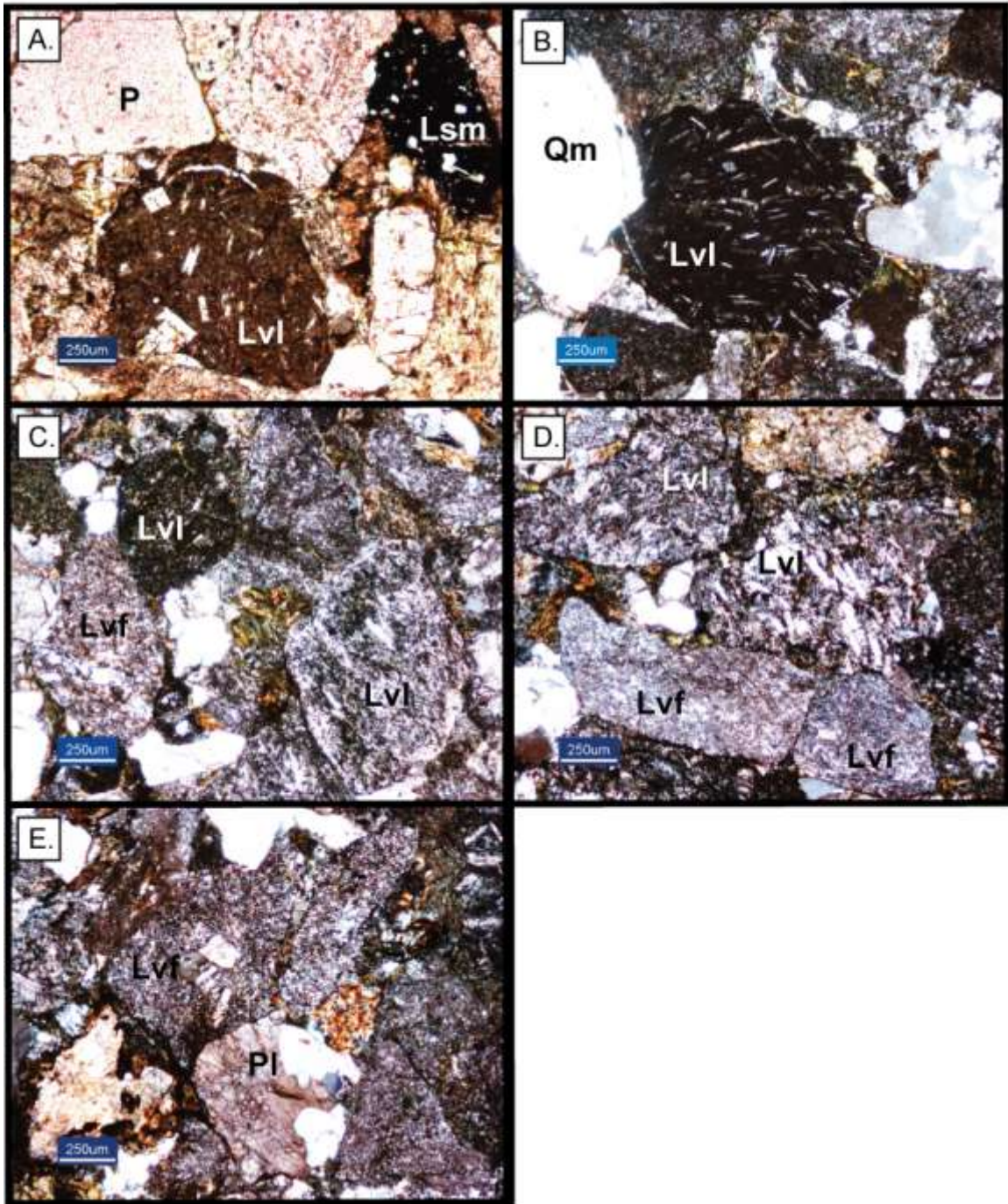
GR-406.6
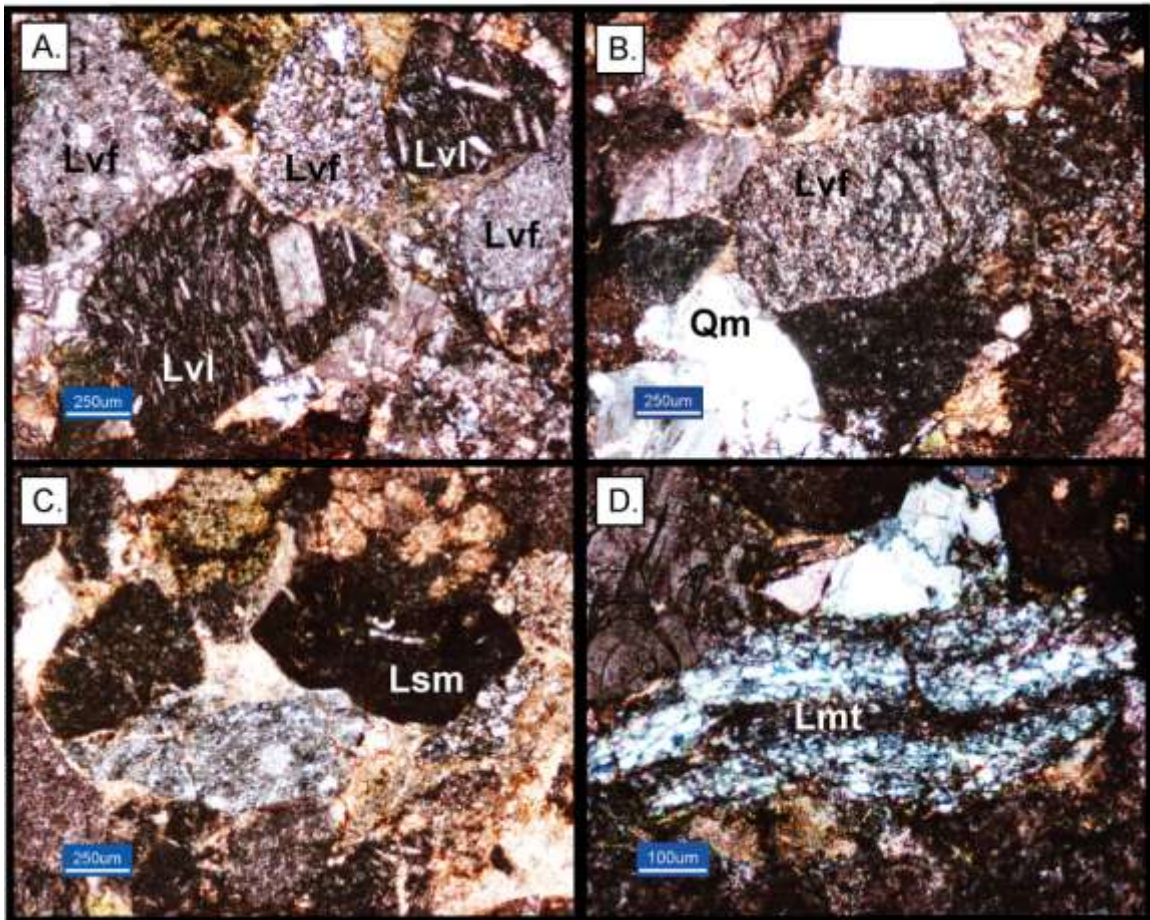
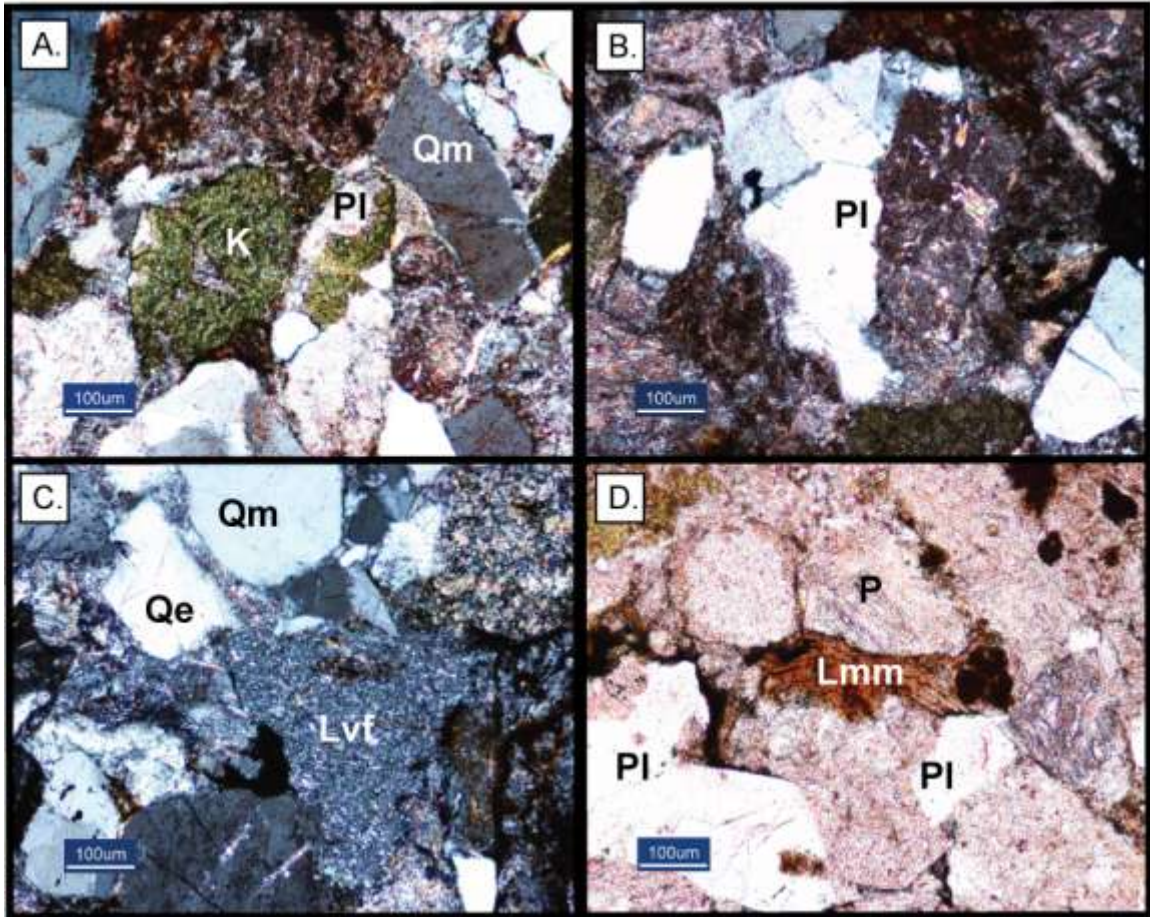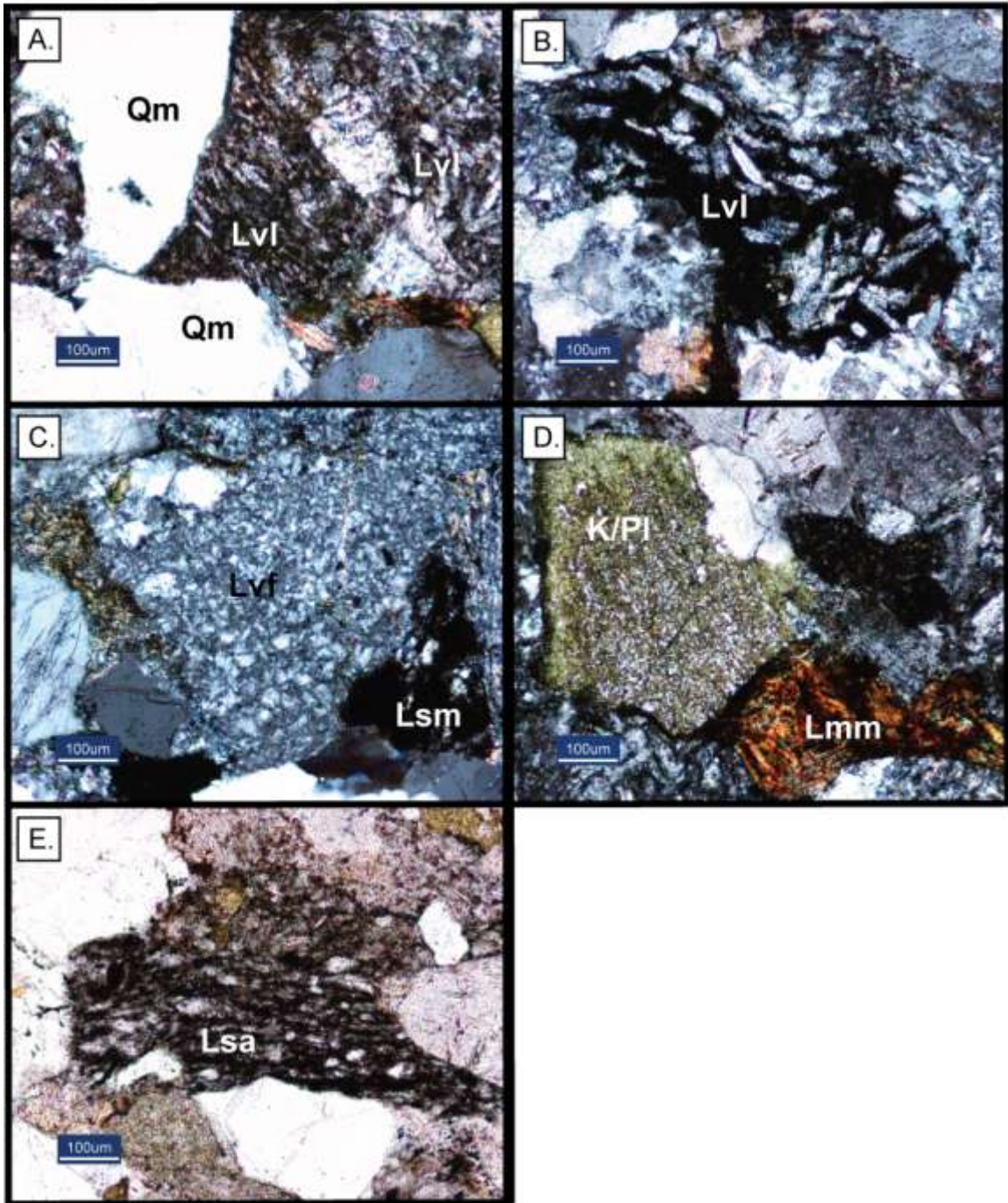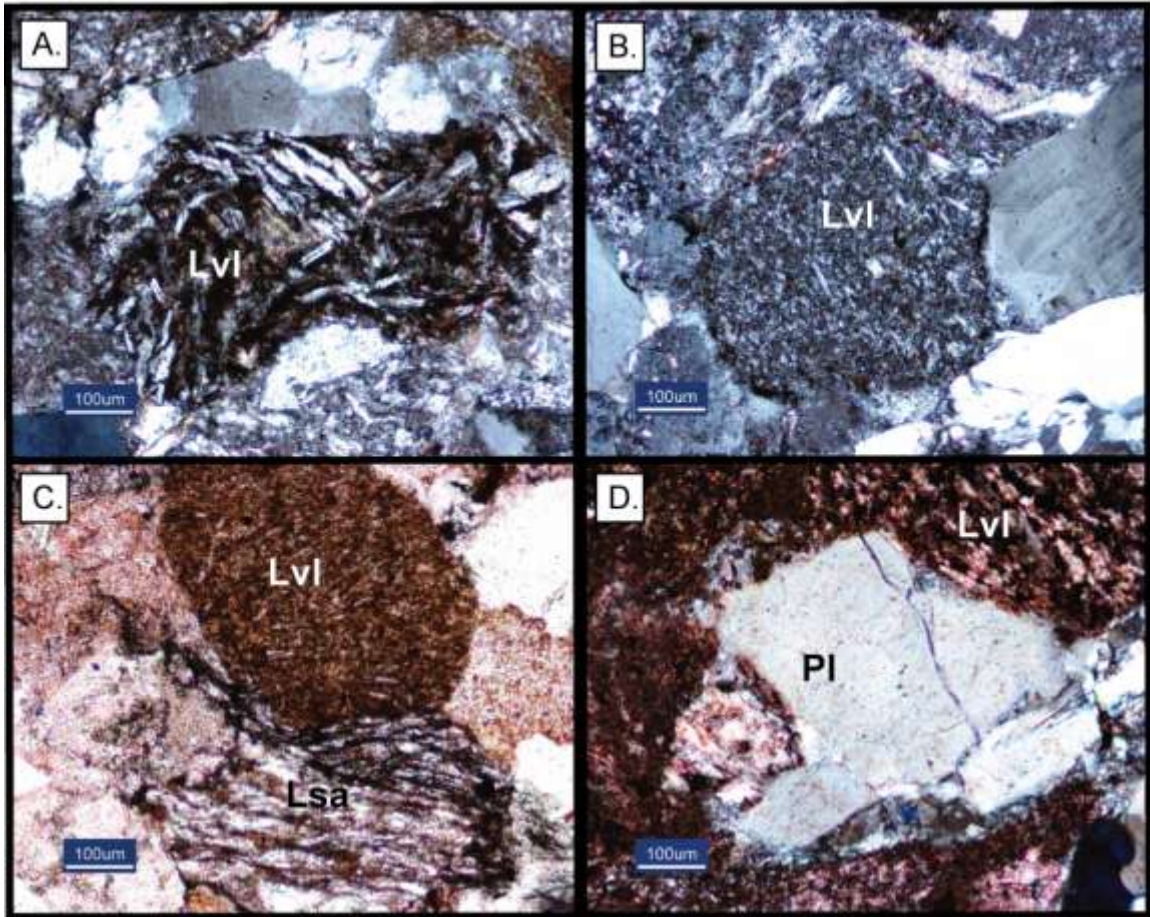GR-455.7
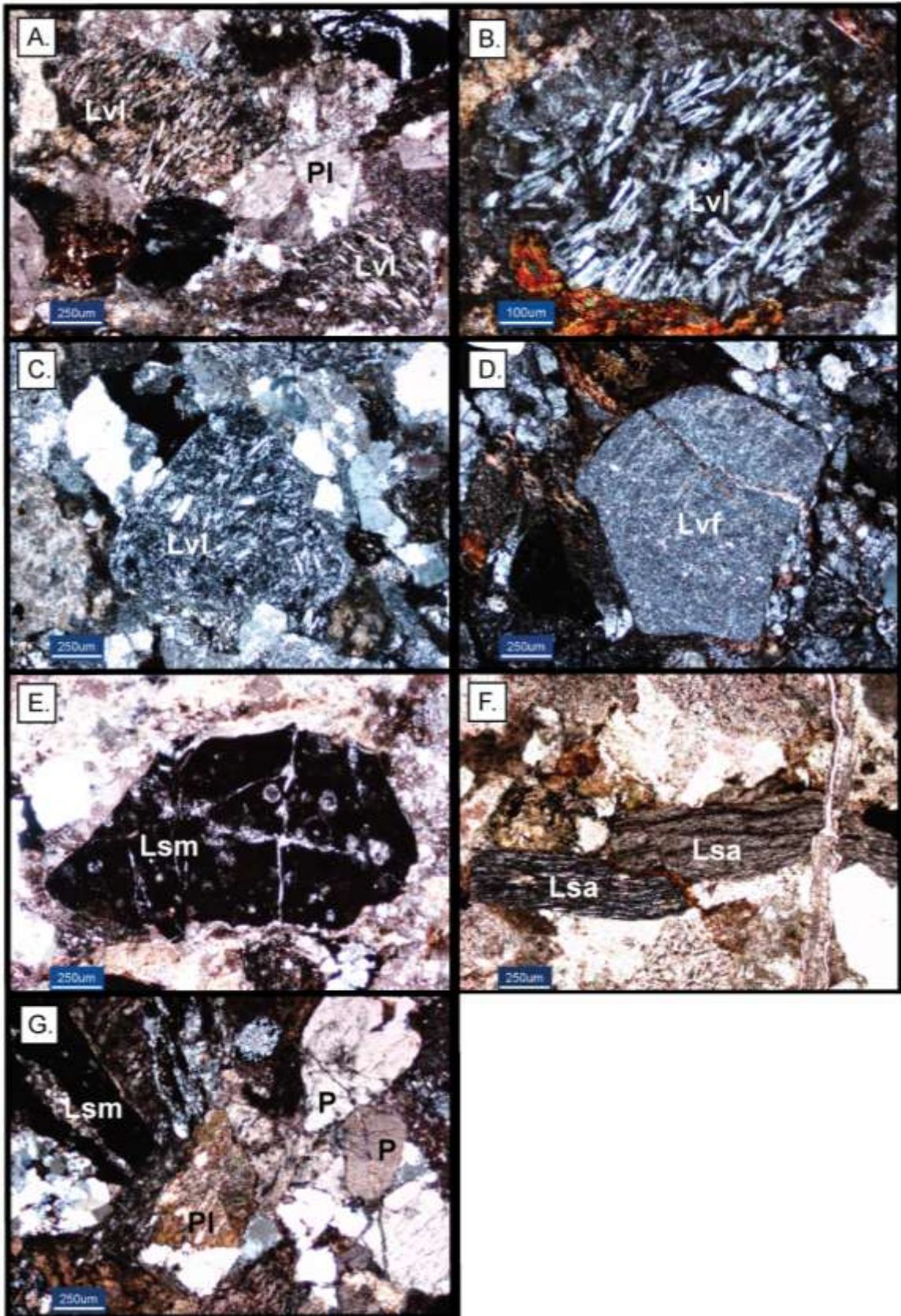
GR-471.2

GR-500.6

130
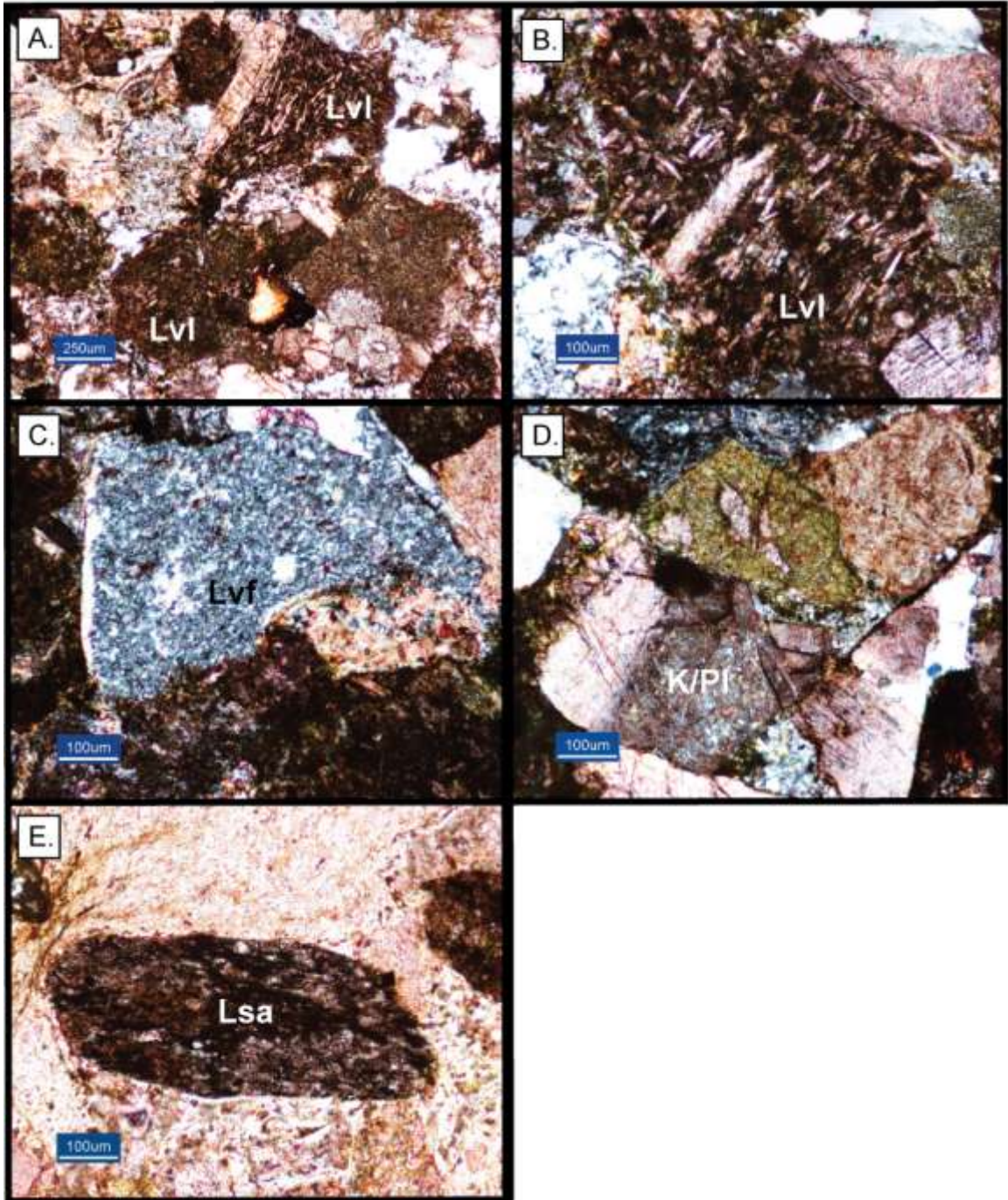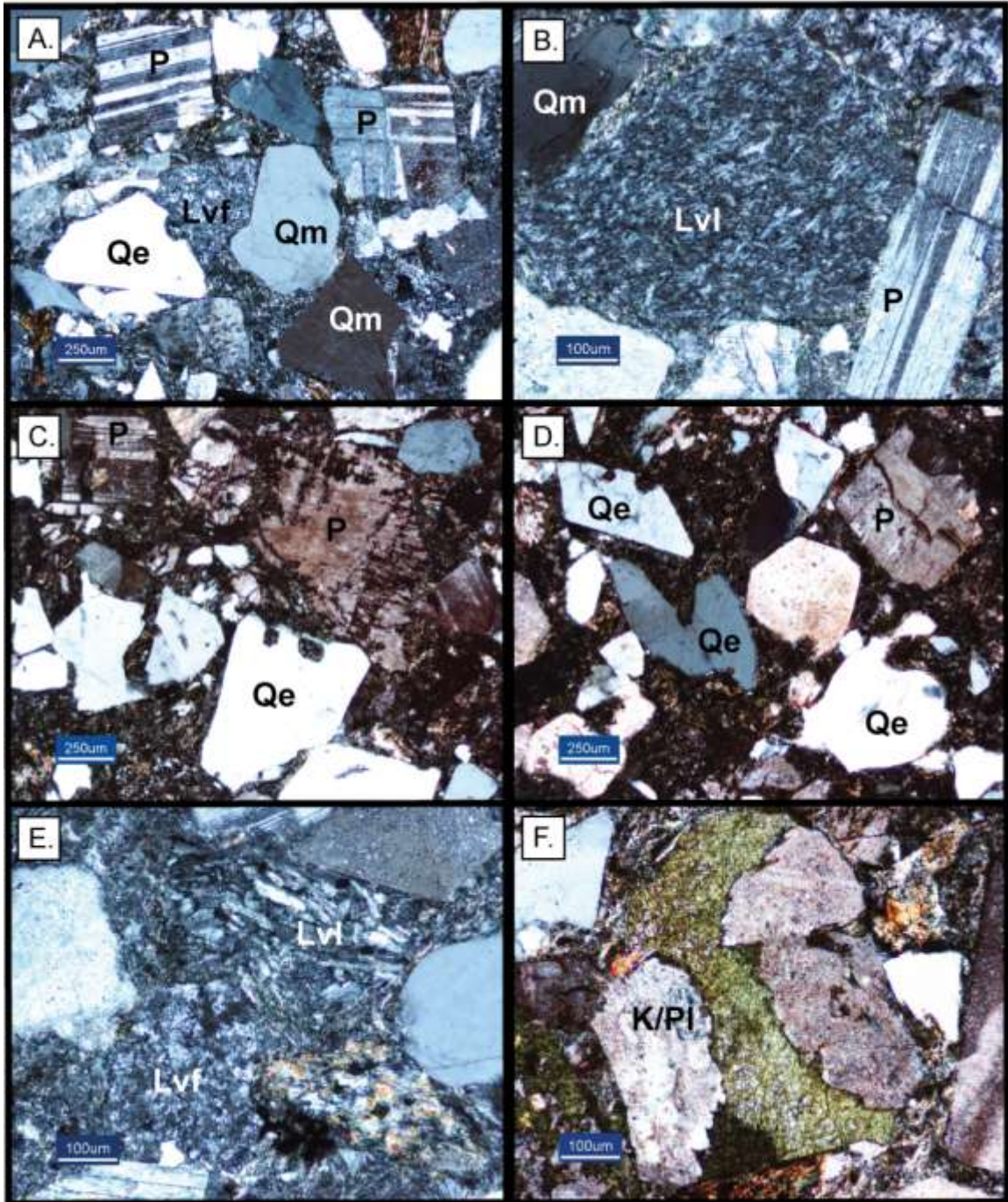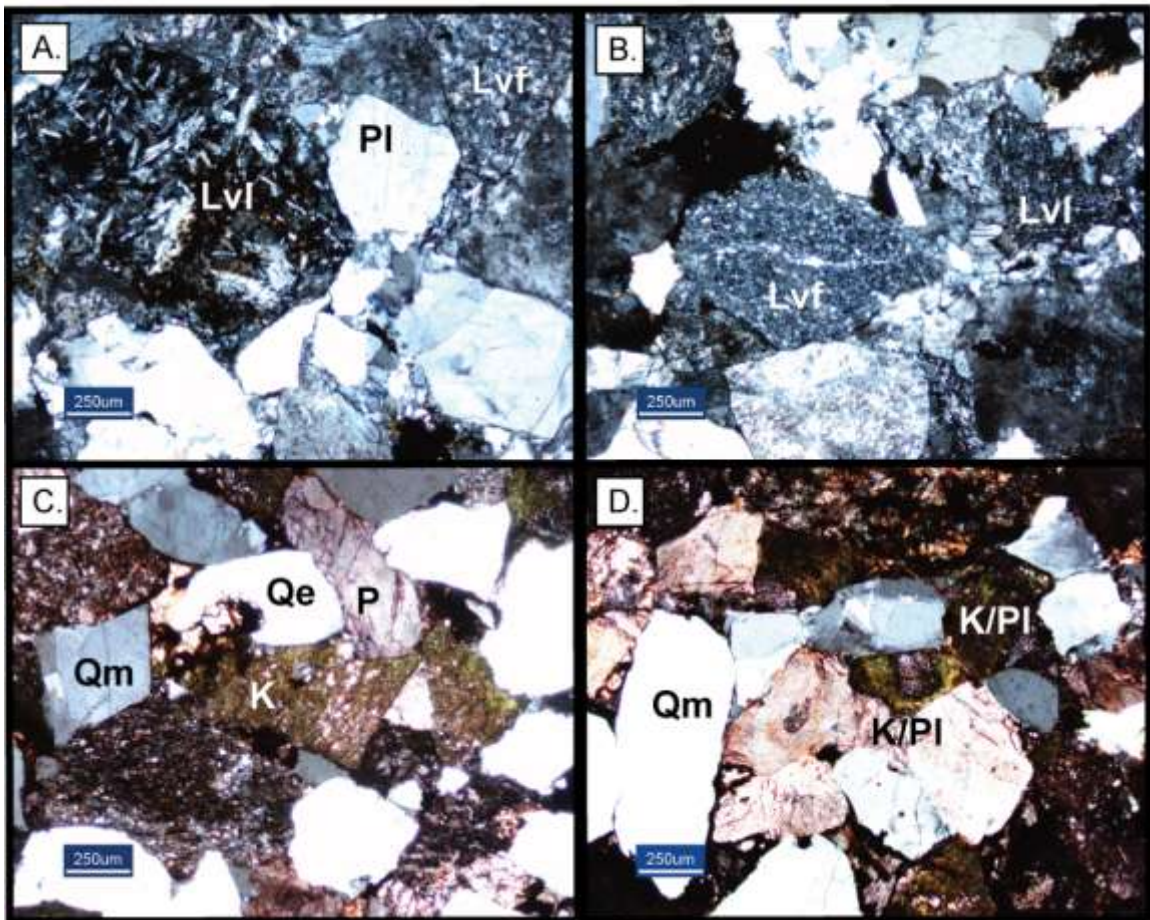
GR-592.2
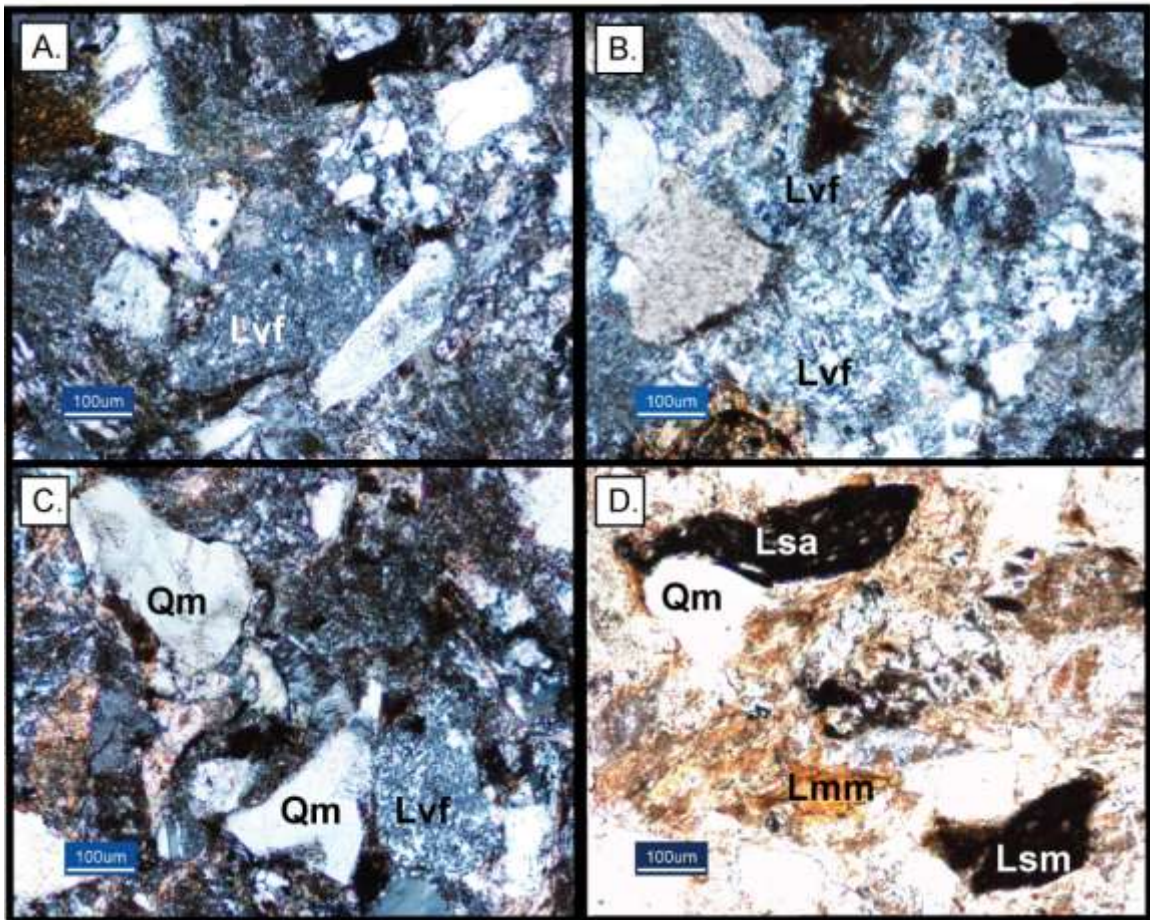
GR-656.8
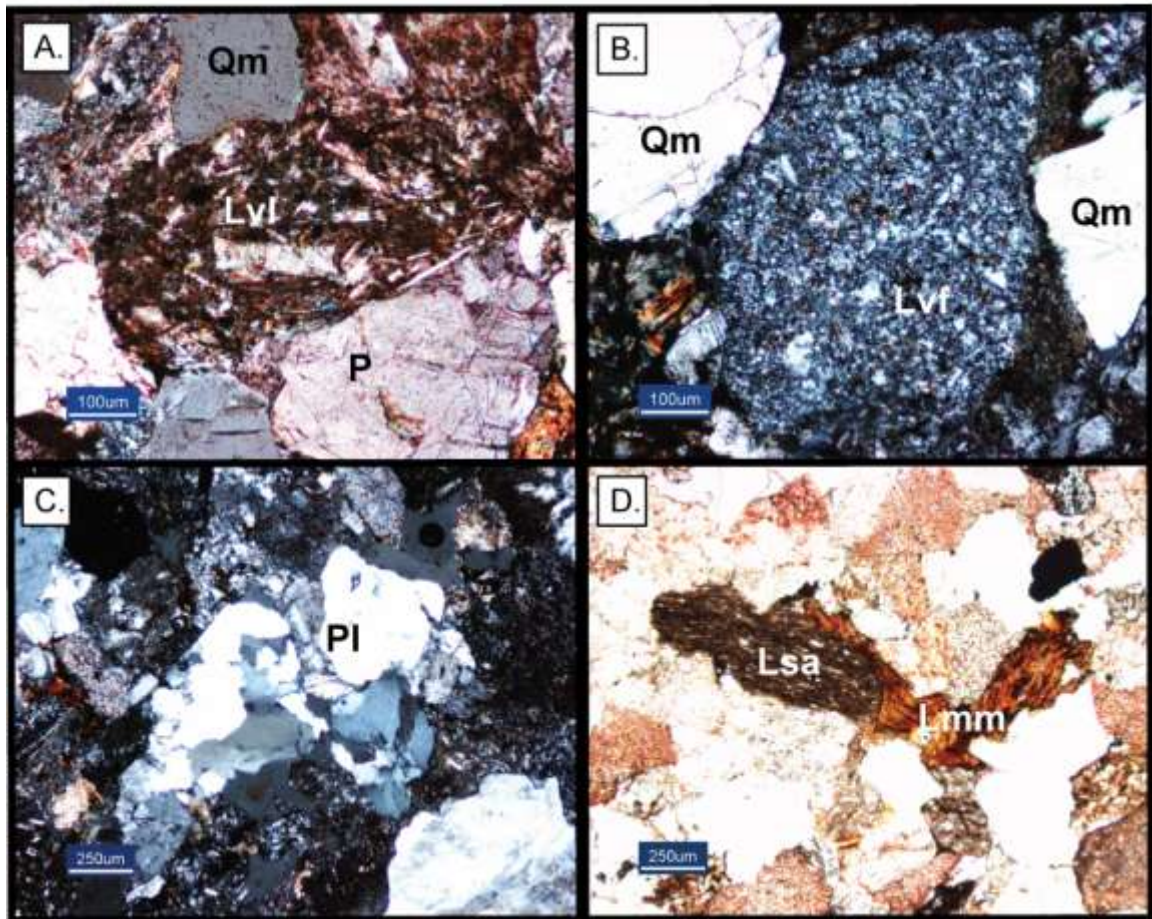
GR-678.7

GR-708.2

GR-727.2

135

GR-752.6

GR-813.8

GR-834.6

GR-861.3

GR-930.6